

EFFECT OF IMMUNOSUPPRESSIVE OLIGODEOXYNUCLEOTIDE A151 ON
INFLAMMASOME ACTIVATION PATHWAYS

A THESIS SUBMITTED TO
THE GRADUATE SCHOOL OF NATURAL AND APPLIED SCIENCES
OF
MIDDLE EAST TECHNICAL UNIVERSITY

BY

NAZ SÜRÜCÜ

IN PARTIAL FULFILLMENT OF THE REQUIREMENTS
FOR
THE DEGREE OF MASTER OF SCIENCE
IN
BIOLOGY

SEPTEMBER 2017

Approval of the Thesis

**EFFECT OF IMMUNOSUPPRESSIVE OLIGODEOXYNUCLEOTIDE A151
ON INFLAMMASOME ACTIVATION PATHWAYS**

Submitted by **NAZ SÜRÜCÜ** in partial fulfillment of the requirements for the degree
of **Master of Science in Biology Department, Middle East Technical University**
by,

Prof. Dr. Gülbin Dural Ünver
Dean, Graduate School of **Natural and Applied Sciences** _____

Prof. Dr. Orhan Adalı
Head of Department, **Biology** _____

Assoc. Prof. Dr. Mayda Gürsel
Supervisor, **Biology Dept., METU** _____

Examining Committee Members:

Prof. Dr. Dicle Güç
Basic Oncology Department, Hacettepe University _____

Prof. Dr. Mayda Gürsel
Department of Biological Sciences, METU _____

Prof. Dr. Ayşe Lale Doğan
Basic Oncology Department, Hacettepe University _____

Assoc. Prof. Dr. Çağdaş D. Son
Department of Biological Sciences, METU _____

Assist. Prof. Dr. Serkan Göktuna
Dept. of Molecular Biology and Genetics, İhsan Doğramacı Bilkent University _____

Date: 06/09/2017

I hereby declare that all information in this document has been obtained and presented in accordance with academic rules and ethical conduct. I also declare that, as required by these rules and conduct, I have fully cited and referenced all material and results that are not original to this work.

Name, Last name : Naz Sürücü

Signature :

ABSTRACT

EFFECT OF IMMUNOSUPPRESSIVE OLIGODEOXYNUCLEOTIDE A151 ON INFLAMMASOME ACTIVATION PATHWAYS

Sürücü, Naz

M.Sc., Department of Biology

Supervisor: Prof. Dr. Mayda Gürsel

September 2017, 80 pages

Inflammasome activation is triggered by pathogen associated molecular patterns (PAMPs) and/or host derived danger associated molecular patterns (DAMPs) leading to caspase-1 (canonical) or caspase-11/caspase-4/5 activation (non-canonical) pathways stimulating IL-1 β and IL-18 secretion. Excessive inflammasome activation has been associated with the pathogenesis of neurodegenerative and metabolic disorders as well as the macrophage activation syndrome (MAS) and cryopyrin associated periodic syndromes (CAPS). H syndrome, is another rare disease arising due to mutations in the genes encoding hENT3 (human equilibrative nucleoside transporter). This syndrome shares common symptoms with the inflammasome overactivation associated disorders CAPS and MAS which might suggest a common mechanistic origin of these diseases and the pathogenesis of H syndrome. The existence of these inflammasome overactivation related disorders necessitates the development of therapeutic agents targeting distinct pathways of inflammasome activation. Synthetic oligodeoxynucleotide (ODN) A151 expressing immunosuppressive TTAGGG motifs has been shown to ameliorate various inflammatory responses. In this study, we observed a significant decrease in IL-1 β secretion and percent cytotoxicity of A151-ODN treated cells in AIM2, NLRC4, non-

canonically activated, and nucleic acid induced NLRP3 inflammasomes but not in bacterial toxin stimulated NLRP3 inflammasome formation. Furthermore, we demonstrate a decrease in the release of ASC specks and inhibition of mitochondrial stress in A151 ODN treated samples. These are encouraging results for the potential therapeutic immunosuppressive effects of A151 ODN on dysregulated inflammasome complex formation. Finally, preliminary experiments using PBMC from an H syndrome patient suggested that autoinflammatory manifestations in this disease might in part be associated with over-active inflammasome formation.

Keywords: Inflammasome, A151 oligodeoxynucleotide (ODN), pyroptosis, H syndrome

ÖZ

İMMÜN BASKILAYICI SENTETİK OLİGODEOKSİNÜKLEOTİD A151'İN ENFLAMAZOM AKTİVASYON YOLAKLARINA OLAN ETKİSİ

Sürücü, Naz

Yüksek Lisans, Biyoloji Bölümü

Tez Yöneticisi: Prof. Dr. Mayda Gürsel

Eylül 2017, 80 sayfa

Enflamazom yolları patojenik tehlike oluşturabilecek moleküller ve endojen tehlike oluşturabilecek moleküller tarafından tetiklenmektedir. Bu tetiklenme NOD-benzeri reseptör, ASC proteini ve pro-kaspaz 1'in bir araya gelmesiyle enflamatuar kaspaz aktivasyonuna, piroptoz aracılı hücre ölümüne ve IL-1 β /IL-18 sitokinlerinin salınmasına sebep olur. Düzensiz enflamazom aktivasyonu nörodejeneratif ve metabolik hastalıklarla beraber makrofaj aktivasyon sendromu (MAS) ve kriyopirin ilişkili periyodik sendromu (CAPS) ile bağdaştırılmıştır. Ayrıca H sendromu adında, hENT3 (dengeleyici nükleosid taşıyıcısı 3) genindeki mutasyonlar sonucu gelişen nadir bir hastalık tanımlanmıştır. Bu sendromun MAS ve CAPS hastalıklarıyla ortak semptomlar göstermesi, patojenezinde bu hastalıklarla ortak bir temelin olabileceğine işaret etmektedir. Düzensiz enflamazom aktivasyonu ile ilişkili hastalıkların varlığı enflamazomların terapötik açıdan baskılanmasının önemini arttırmıştır. TTAGGG motifleri içeren baskılayıcı sentetik oligodeoksinükleotid (ODN) A151'in immün uyarıcı moleküllerle rekabet ederek sitozolik algılama yollarının aktivasyonunu önlediği bilinmektedir. Bu çalışmada elde edilen sonuçlara göre A151-ODN, AIM2, NLRC4, dolaylı aktivasyonu görülen, ve nükleik asit ile uyarılan NLRP3 enflamazom yollarında IL-1 β salımını ve hücre ölümünü anlamlı ölçüde baskılayabilirken bakteriyel toksin ile uyarılan NLRP3 aktivasyonunda azalmaya sebep olmamıştır.

Ayrıca, A151-ODN eklenmesi sonucunda hücre dışına verilen ASC zerreciklerinin sayısında ve mitokondrial stresde azalma olduğu görülmüştür. Bu verilere göre, A151 ODN'in AIM2, NLRC4, ve dolaylı enflamazomların kontrolsüz aktivasyonu sebebiyle meydana gelen patolojik durumlarda terapötik ajan olarak kullanım potansiyeli olduğu düşünülmektedir. Ayrıca, H sendromu hastasından elde edilen hücrelerle yapılan ön çalışmalar sonucunda bu hastalığın patojenezinde düzensiz enflamazom aktivasyonunun kısmi bir etkisi olabileceğine işaret etmektedir.

Anahtar Kelimeler: Enflamazom, Oligodeoksinükleotid A151, Piroptoz, H sendromu

ACKNOWLEDGMENTS

First of all, I would like to convey my deepest gratitude to my advisor, Prof. Mayda Gürsel for her brilliant scientific guidance, endless patience, continuous encouragement and motivation. She is a true example of pure scientific enthusiasm that I am extremely fortunate to experience and learn from. I could not think of a better mentor to begin a scientific career with.

I also want to thank the members of my thesis examining committee; Assoc. Prof. Çağdaş Devrim Son, Prof. Dicle Güç, Prof. Ayşe Lale Doğan, and Assist. Prof. Serkan Göktuna for taking the time to evaluate this thesis and their valuable contributions.

I would like to convey my thanks to Prof. Nesrin Özören of Boğaziçi University for providing us with ASC-GFP expressing THP-1 cell line and Assoc. Prof. Deniz Nazire Çağdaş Ayvaz of Hacettepe University for providing us H syndrome patient blood samples.

I would like to thank my former lab mates Bilgi Güngör, Soner Yıldız, and Ersin Gül for overseeing my first steps in the laboratory and my current lab mates Hatice Asena Şanlı, Büşranur Geçkin, Başak Kayaoğlu, and İhsan Cihan Ayanoğlu for creating a constantly supportive and friendly atmosphere in our lab. Also, I would like to thank Esin Alpdündar Bulut for always being there when a helping hand is needed, for sharing her experiences, and being a friend more than a lab mate.

My sincere thanks go to Prof. Dr. İhsan Gürsel for his invaluable instructions and lab members of I.G Group for their generous help and hospitality at all times.

Last but not the least; I would like to express my endless thanks to my mother Aysan Canver who has always put my education before anything else and has provided me with the opportunities to be where I am today.

TABLE OF CONTENTS

ABSTRACT	v
ÖZ.....	vii
ACKNOWLEDGMENTS.....	ix
TABLE OF CONTENTS	x
LIST OF TABLES	xiii
LIST OF FIGURES.....	xiv
LIST OF ABBREVIATIONS	xvi
CHAPTERS	
1. INTRODUCTION	1
1.1 The Immune System	1
1.2 Innate Immunity and Pattern Recognition Receptors(PRRs)	2
1.3 Inflammasome Complexes.....	4
1.3.1 AIM2 Inflammasome	8
1.3.2 NLRC4 Inflammasome.....	9
1.3.3 Non-canonical Inflammasome.....	10
1.3.4 NLRP3 Inflammasome	11
1.4 Suppressive ODN A151.....	12
1.5 Histiocytosis and lymphadenopathy syndrome (H Syndrome)	13
1.6 Aim of the Study	14

2. MATERIALS & METHODS.....	15
2.1. MATERIALS.....	15
2.1.1. Cell Lines and Primary Cells	15
2.1.2. Cell Culture Media, Solutions, and Buffers	15
2.1.3. Reagents	16
2.1.4 Inflammasome Activators	16
2.1.5 Oligodeoxynucleotides.....	17
2.2 METHODS	18
2.2.1 Cell Culture	18
2.2.1.1 THP-1 Cell Line Specifications and Maintenance	18
2.2.1.2 Human PBMC Isolation	18
2.2.1.3 Bone Marrow Derived Macrophage Generation	19
2.2.2 Stimulation Experiments	19
2.2.2.1 Ligand preparation	19
2.2.2.2 THP-1 and hPBMC stimulations.....	20
2.2.2.3 BMDM stimulations.....	20
2.2.3 Enzyme Linked Immunosorbent Assay (ELISA) for Cytokine Quantification.....	20
2.2.4 GFP labelled ASC Detection via Fluorescent Microscopy and Flow Cytometry from THP-1-GFP	21
2.2.5 Cytotoxicity Assays	22
2.2.5.1 Lactate dehydrogenase (LDH) Assay.....	22
2.2.5.2 Propidium iodide (PI) and SytoxOrange stainings.....	22
2.2.6 JC-1 Mitochondrial Membrane Potential Assay	22

2.2.7 LegendPlex Human Type 1/2/3 Interferon Panel.....	23
2.2.8 Percent Inhibition and Fold Induction Calculations.....	23
2.2.9 Statistical Analysis	24
2.2.10 Ethical Statement.....	24
3. RESULTS & DISCUSSION	25
3.1 A151 ODN inhibits inflammasome activation dependent IL-1 β secretion in THP-1 human monocytic cells.....	25
3.2 A151 ODN inhibits speck formation in THP-1 cells.....	29
3.3 A151 ODN modulates inflammasome activation dependent pyroptosis	40
3.4 A151 ODN inhibits inflammasome activation by reducing mitochondrial stress.....	47
3.5 A151 ODN inhibits inflammasome activation dependent IL-1 β secretion from hPBMC.....	54
3.6 Histiocytosis and lymphadenopathy syndrome (H Syndrome)	56
4. CONCLUSION	63
REFERENCES	67
APPENDICES	
A. BUFFERS, SOLUTIONS AND CULTURE MEDIA.....	73
B. PERMISSION TO THE COPYRIGHTED MATERIAL.....	75

LIST OF TABLES

TABLES

Table 2.1 Inflammasome Induction Ligands.....16

Table 2.2 Suppressive ODN and Control ODN.....17

Table 4.1 Summary of the effect of A151 ODN on investigated inflammasome pathways.....65

LIST OF FIGURES

FIGURES

Figure 1.1 DNA sensors of immune cells.....	4
Figure 1.2 Structural illustrations of broadly identified canonical and non-canonical inflammasome complexes.....	6
Figure 1.3 Brief illustration of inflammasome activation leading to cell death and cytokine secretion.....	7
Figure 1.4 Autoinflammatory disease mechanisms in relation to inflammasome complexes.....	8
Figure 1.5 5 Illustration of canonical NLRP3 activation and non-canonical inflammasome activation.....	10
Figure 3.1 IL-1 β response of inflammasome activated groups compared to suppressive A151 ODN treated or and neutral control K3-flip ODN.....	26
Figure 3.2 IL-1 β response of inflammasome activated groups compared to suppressive ODN treated groups.....	28
Figure 3.3 ASC specks released from primed and stimulated THP-1-GFP cells were counted from 40 μ l of cell-free culture media.....	30
Figure 3.4 Fluorescent microscopy images of THP1-GFP cells stimulated with indicated canonical inflammasome activators and cytosolic LPS for non-canonical inflammasome activation in the presence or absence of A151 ODN.....	33
Figure 3.5 Flow cytometry analysis of ASC-speck release from primed and dose-dependently stimulated THP-1-ASC-GFP cells.....	36
Figure 3.6 Percent cytotoxicity comparison of primed and inflammasome activated THP-1 cells (4 x 10 ⁵ /ml) with or without A151 ODN treatment.....	41
Figure 3.7 Fluorescence microscopy images of THP-1-ASC-GFP cells stained with cell impermeable nucleic acid dye SytoxOrange following dose dependent inflammasome activation.....	43
Figure 3.8 Fluorescence microscopy images of JC-1 treated BMDM's following inflammasome activation.....	48
Figure 3.9 Flow cytometric analysis of mitochondrial stress assessed by JC-1 staining of BMDM's stimulated with 3 different doses of various inflammasome activators.....	50

Figure 3.10 ELISA results for IL-1 β response of inflammasome activated hPBMC.....	55
Figure 3.11 IL-1 β , IFN α (pan-specific), and IL-29 (IFN λ 1) ELISA results of PBMC isolated from one H Syndrome patient and one healthy donor.....	57
Figure 3.12 Flow cytometry results for the fluorogenic bead based interferon panel (LegendPlex) of PBMC isolated from one H Syndrome patient and one healthy donor.....	58
Figure 3.13 Flow cytometry analysis of mitochondrial stress in PBMC isolated from one H Syndrome patient and three unrelated healthy donors.....	60

LIST OF ABBREVIATIONS

AIM2	Absent in melanoma 2
ALP	Alkaline phosphatase
AMP	Adenosine monophosphate
ASC	Apoptosis associated speck like protein containing a CARD
ATP	Adenosine triphosphate
bp	Base pairs
BMDM	Bone marrow derived macrophages
BSA	Bovine serum albumin
CAPS	Cryopyrin associated periodic syndromes
CARD	caspase activation and recruitment domain
cGAMP	cyclic GMP-AMP
cGAS	cyclic GMP-AMP synthetase
CLR	C-type lectin receptor
CpG	Unmethylated cytosine-phosphate-guanosine motifs
DAMP	Danger/damage associated molecular pattern
DC	Dendritic cell
DMEM	Dulbecco's Modified Eagle's Medium
DHR	Dihydrorhodamine
DNA	Deoxyribonucleic acid
dsRNA	Double-stranded RNA
EDTA	Ethylenediaminetetraacetic acid
ELISA	Enzyme Linked-Immunosorbent Assay

ER	Endoplasmic reticulum
FACS	Fluorescence Activated Cell Sorting
FBS	Fetal Bovine Serum
GBP	Guanylate binding protein
GFP	Green fluorescent protein
GSDMD	Gasdermin-G
GMP	Guanosine monophosphate
hENT3	Human equilibrative nucleoside transporter 3
HIV	Human Immunodeficiency Virus
HRP	Horseradish peroxidase
hPBMC	Human peripheral blood mononuclear cell
HSV	Herpes simplex virus
IAPP	Islet amyloid polypeptide
IFI16	Interferon- γ inducible protein 16
IFN	Interferon
Ig	Immunoglobulin
IL	Interleukin
IRF	Interferon-regulatory factor
IP 10	Interferon gamma-induced protein 10
IRF	Interferon-regulatory factor
ISG	Interferon stimulated genes
LDH	Lactate dehydrogenase
LPS	Lipopolysaccharide
LRR	Leucine-rich repeat
MAS	Macrophage activation syndrome
MAVS	Mitochondrial anti-viral signaling protein
MCSF	Macrophage colony stimulating factor
MDA5	Melanoma differentiation associated protein 5

MyD88	Myeloid differentiation factor-88
MS	Multiple sclerosis
NAIP	NLR family apoptosis inhibitory protein
NEK7	NIMA related kinase 7
NF- κ B	Nuclear factor- kappa B
NK	Natural killer
NLR	Nucleotide-binding oligomerization domain like receptors
NOD	Nucleotide-binding oligomerization domain
ODN	Oligodeoxynucleotide
PAMP	Pathogen-associated molecular pattern
PBS	Phosphate buffered saline
PCR	Polymerase chain reaction
pDC	Plasmacytoid dendritic cell
PGN	Peptidoglycan
PI	Propidium iodine
PMA	Phorbol 13-myristate 12-acetate
PNPP	Para-nitrophenyl pyro phosphate
PO	Phosphodiester
poly I:C	Polyriboinosinic polyribocytidylic acid
RPMI	Roswell Park Memorial Institute
PRR	Pattern recognition receptor
PS	Phosphorothioate
PYD	Pyrin domain
PYHIN	Pyrin and HIN
RIG-I	Retinoic acid-inducible gene-I
RLR	Retinoic acid-inducible gene-I like receptor
RNA	Ribonucleic acid

ROS	Reactive oxygen species
RPMI	Roswell Park Memorial Institute
SA-AP	Streptavidin-alkaline phosphatase
SLC	Solute carrier
SLE	Systemic lupus erythematosus
STAT	Signal transducer and activator of transcription
STING	Stimulator of interferon genes
T3SS	Type 3 secretion systems
TBK	TANK-binding kinase
TLR	Toll-like receptor
TNF	Tumor necrosis factor
TRIF	TIR domain containing adaptor inducing interferon- β

CHAPTER 1

INTRODUCTION

1.1 The Immune System

The immune system is a highly organized network of cells, tissues and organs, constituting a host defense system to ensure that organisms are rarely infected by disease causing microorganisms even though they are surrounded by them. The immune system is shaped by the cooperation of innate and adaptive immunity. The innate immune system provides first-line defense against foreign invaders. The adaptive immune system, on the other hand, takes the lead in defense in case the innate system fails to overcome the invasion. The reason for the difference in response time of the innate and adaptive system lies in their diversity of their pathogen recognition process. While the innate immune system recognizes evolutionary conserved pathogen associated molecular patterns (PAMPs) through its germline encoded receptors and is able to respond immediately, the adaptive immune system is equipped with a repertoire of highly specific antigen recognition receptors, generated by somatic gene rearrangements. Antigen recognition through these receptors activates signaling pathways, leading to clonal expansion and unleashes the effector functions of activated T- and B- lymphocytes.

Although an immune response to pathogenic invaders is paramount to protect the host, sustained or unchecked immune activation may otherwise cause severe damage to the host. It is critical to note that while the immune system is well-organized and effective in combating foreign infectious invaders, without immunomodulatory mechanisms or in case of dysregulated immune activation, autoimmune or autoinflammatory conditions may arise. Herein, we will focus on the major innate immune activation pathways with a special emphasis on inflammasome activation.

1.2 Innate Immunity and Pattern Recognition Receptors(PRRs)

The innate immune system has evolved to differentiate between non-self infectious microbial patterns and self-derived molecules (Janeway & Medzhitov, 2002). It consists of a physical barrier made up of epithelial cells that form tight junctions and secrete mucus as well as antimicrobial peptides, the microbiota that covers non-sterile surfaces and competes with pathogens for nutrients and habitation, the complement system that accumulates on pathogen surfaces to initiate cell lysis and/or phagocytosis, and immune cells capable of phagocytosis and initiation of an immediate inflammatory response. When physical and chemical first line barriers are breached by a pathogen, an inflammatory response is initiated through the activation of the complement system and recruitment innate immune cells. These cells include macrophages, dendritic cells (DCs), neutrophils, mast cells, eosinophils, and natural killer (NK) cells (Janeway & Medzhitov, 2002). An inflammatory response is initiated through the recognition of pathogen associated molecular patterns (PAMPs) that are conserved throughout the microbial species (Takeuchi & Akira, 2010). PAMPs are recognized by special pattern recognition receptors (PRRs) expressed by immune cells. In addition to PAMPs, PRRs can also recognize endogenous molecules known as damage associated molecular patterns (DAMPs) that were released from injured cells. The PRR family of receptors consist of Toll-like receptors (TLRs), C-type lectin receptors (CLRs), retinoic acid-inducible gene (RIG)-I-like receptors (RLRs), NOD-like receptors (NLRs), PYHIN (Pyrin and HIN) receptors and cytosolic dsDNA/cyclic di-nucleotide sensors. TLRs and CLRs are transmembrane proteins whereas RLRs, NLRs and dsDNA/cyclic di-nucleotide sensors are cytoplasmic. TLRs are classified under two groups depending on their cellular localization. TLR1, TLR2, TLR4, TLR5, TLR6, TLR11 (only in mice) reside on the cell surface whereas TLR3, TLR7, TLR8, and TLR9 are found in endolysosomal compartments such as the endoplasmic reticulum (ER), lysosomes, and endosomes (Kawai & Akira, 2010). TLRs are able to recognize a wide variety of PAMPs including nucleic acids, lipids, and proteins that belong to bacteria, viruses, fungi, and parasites. CLRs, on the other hand, are able to recognize carbohydrate motifs on bacteria, viruses, and fungi. Functionally they are involved in the

polarization of T-cells, activation of the transcription factor NF- κ B, and have influence on TLR signaling pathways (Geijtenbeek & Gringhuis, 2009; Takeuchi & Akira, 2010). Major members of the cytosolic RLR family are RIG-I and MDA5 which detect short dsRNA containing 5'triphosphate caps and long genomic dsRNA, respectively (Reikine, Nguyen, & Modis, 2014). Recognition of dsRNA through these receptors activates a signaling pathway that involves the oligomerization of the adaptor protein MAVS (mitochondrial anti-viral signaling protein) and subsequent IRF3-IRF7 phosphorylation and nuclear translocation, which results in type I interferon production and secretion. Additionally, transmembrane TLRs like TLR3, TLR7, and TLR8 are responsible for endosomal RNA sensing through the adaptor proteins MyD88 (myeloid differentiation primary response protein 88) and TRIF (TIR domain containing adaptor inducing IFN- β) that subsequently lead to the production of type I interferons through IRF3-IRF7 transcription factor activation (Schlee & Hartmann, 2016). Endosomal DNA recognition, on the other hand, is detected by TLR9 which recognizes CpG-motifs and continues signaling through MyD88-IRF7 and results in type I interferon production. Cytosolic DNA is recognized through various sensors. These include AIM2 (absent in melanoma 2) and IFI16 (IFN- γ inducible protein 16) which are members of the PYHIN family and lead to inflammasome activation. Another sensor is RNA polymerase III that transcribes DNA into 5' triphosphorylated RNA, thereby activating the RIG-I pathway. Another major sensor is the cyclic GMP-AMP synthetase (cGAS) (Hornung, Roers, Carus, & Universita, 2016; Schlee & Hartmann, 2016). cGAS binds to dsDNA and generates the secondary messenger cyclic dinucleotide cGAMP (cyclic GMP-AMP) which binds to and activates the adaptor protein STING (stimulator of interferon genes). STING activation through cGAMP binding recruits TBK1 and IRF3. Following phosphorylation, IRF3 translocates to the nucleus where it activates NF- κ B dependent type I interferon production (Shu, Li, & Li, 2014). NOD1 and NOD2 (nucleotide binding oligomerization domain containing protein) are best identified members of another cytoplasmic receptor family, the NLRs. This large family of receptors are made up of protein binding N-terminal, a NACHT domain, and C-terminal leucine rich repeats (Takeuchi & Akira, 2010). NLRs recognize peptidoglycans and initiate IFN- β

production through NF- κ B activation. Moreover, they were shown to activate inflammasome complexes as a result of DAMP or PAMP induced signaling (Broz & Monack, 2013). The major DNA sensing receptors are summarized in Figure 1.1.

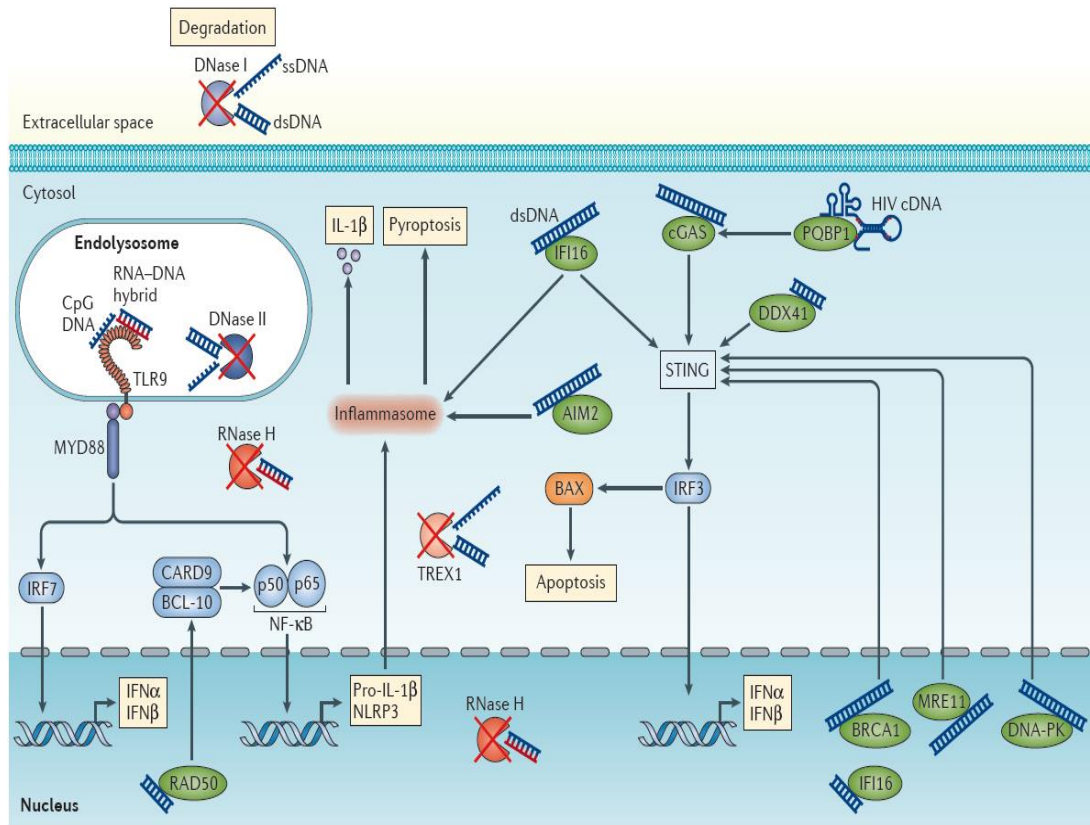


Figure 1.1 DNA sensors of immune cells. (Adapted from Schlee & Hartmann, 2016)

1.3 Inflammasome Complexes

Inflammasomes are multiprotein platforms that are assembled for the recruitment of inflammatory response elements, triggered by PAMPs and/or DAMPs. These elements include ASC specks (apoptosis associated speck like protein containing a CARD), inflammatory caspases 1 and 11 (caspase 4/5 instead of 11 in humans). Once activated, NLR proteins/ASC multimeric complexes recruit and activate pro-caspase 1 (or pro-caspase 11 depending on the activated pathway) which in turn cleave pro-IL-1 β and pro-IL18 into their active forms. In general, the pro-caspases and the pro-IL-1 β and pro-IL18 production is transcriptionally upregulated following a priming step wherein a signaling event (usually a TLR-dependent signaling) leads to NF- κ B transcription

factor activation (priming ligand for NF- κ B activation depends on the cell type). Upon priming and activation of inflammasome complexes, autoproteolytic cleavage of caspases 1 or 11 is followed by the maturation of IL-1 β and IL-18 via the cleavage of activated caspase-1 (Broz & Dixit, 2016; Lamkanfi & Dixit, 2014). Active caspase-1/4-5-11 also cleaves a pore-forming effector protein GSDMD (gasdermin-D; GsdmD) to its N- terminal pore-forming domain (PFD) separated from its C-terminal repressor. The PFD, known as GsdmD p30 forms oligomers on the plasma membrane, leading to pore formation, whereby the cellular contents, including the activated inflammatory cytokines IL-1 β and IL-18, active caspases and ASC specks are leaked into the extracellular space (Shi et al., 2015). This process is termed as pyroptosis, a pyrogenic, highly inflammatory type of programmed cell death.

Inflammasome activation contributes to immune activation through pyroptosis where pro-inflammatory cytokines are released. These cytokines then contribute to further activation of helper T cells, macrophages and neutrophils (Broz & Dixit, 2016). Furthermore, ASC specks can stably remain in the extracellular space where they are taken up by macrophages and further promote the maturation of IL-1 β (Franklin et al., 2014).

Depending on the type of caspase involved, two general inflammasome pathways have been described: The canonical inflammasome pathway involves the activation of caspase-1 whereas the non-canonical inflammasome formation requires caspase-11 (caspase-4/5 in humans) activation. However, non-canonical inflammasome initiation and progression has not yet been extensively studied whereas some canonical inflammasome pathways have been more clearly identified. These pathways include NLRP1, NLRP3, NLRC4, and AIM2 inflammasomes.

NLRs are proteins that consist of either a pyrin domain (PYD) and/or a caspase activation and recruitment domain (CARD) (Figure 1.2).

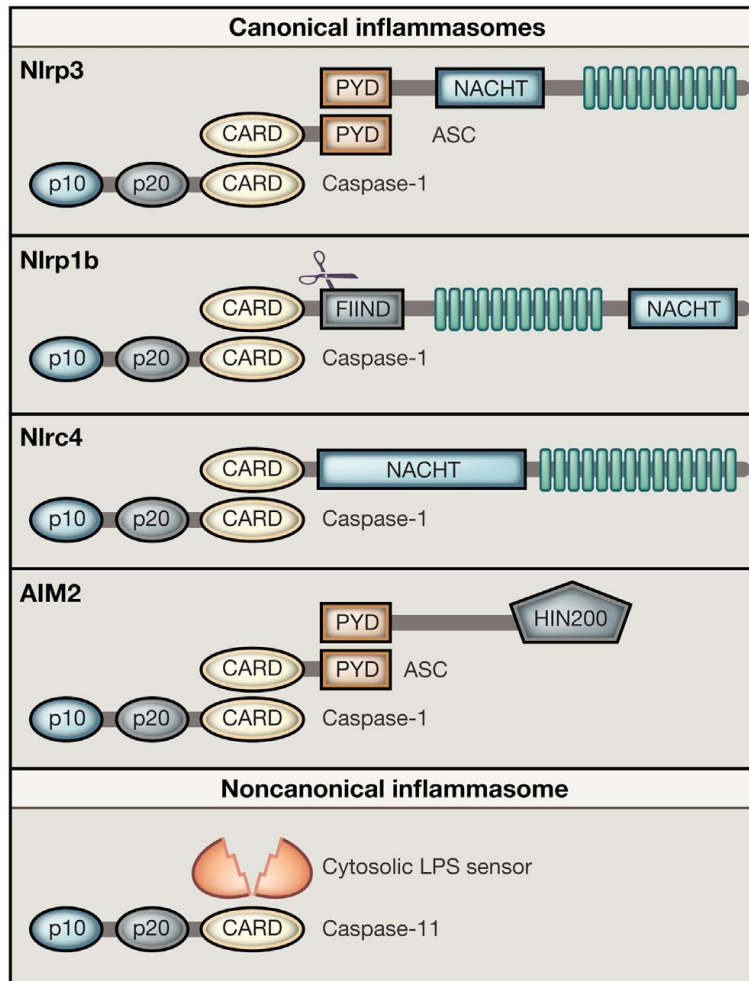


Figure 1.2 Structural illustrations of broadly identified canonical and non-canonical inflammasome complexes. (Adapted from Lamkanfi & Dixit, 2014)

As the name suggests, the zymogen caspase-1 interacts with the CARD. If the NLR contains PYD instead of CARD, ASC proteins multimerize into a speck through PYD/PYD interactions. Thereby, the ASC speck will act as an adaptor since its PYD interacts with the NLR's PYD and its CARD interacts with caspase-1's CARD, completing the formation of the inflammasome complex. Following the recruitment of pro-caspase-1, autoproteolytic cleavage through proximity interactions activates caspase-1, which then carries out the cleavage of pro-IL-1 β and pro-IL-18 (Figure 1.3).

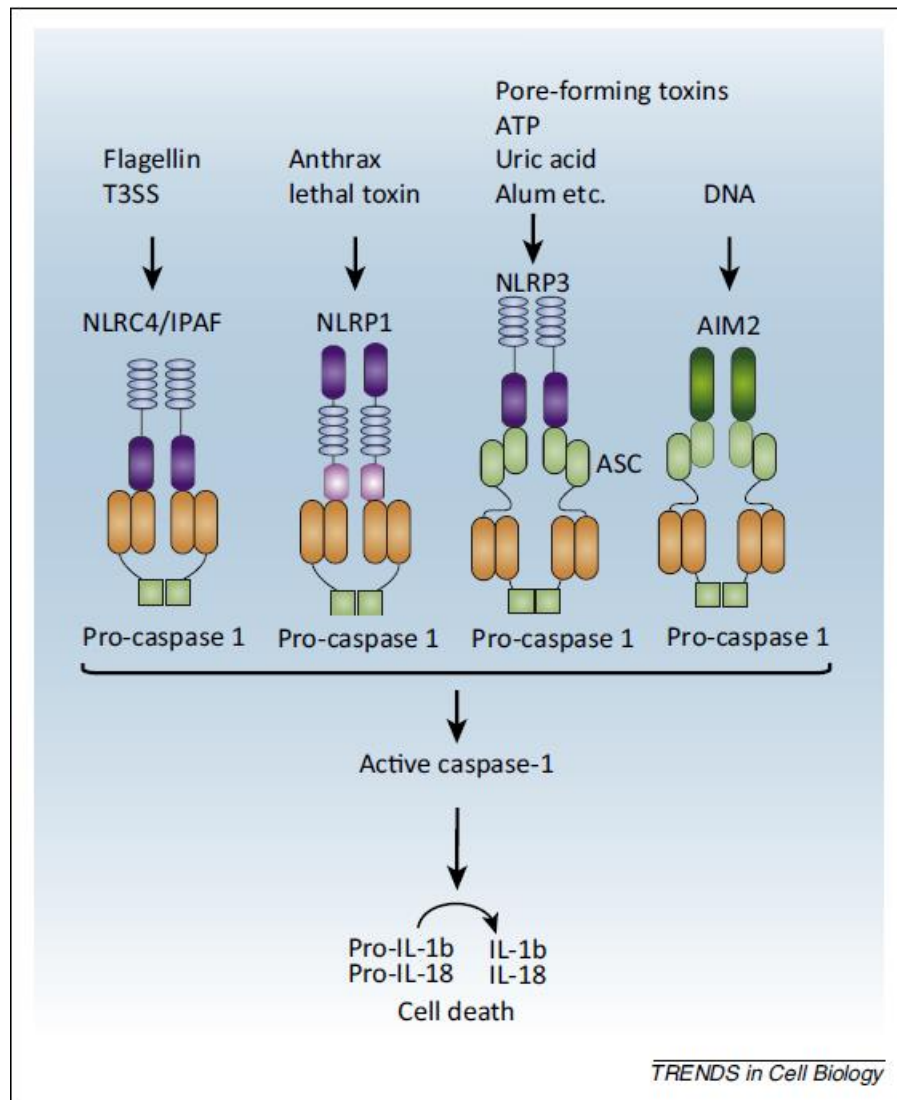


Figure 1.3 Brief illustration of inflammasome activation pathways leading to cell death and cytokine secretion (Adapted from Vanaja, Rathinam, & Fitzgerald, 2015).

Dysregulated inflammasome activation has been indirectly associated with a number of metabolic disorders that include type-2 diabetes, obesity, and atherosclerosis as well as neurodegenerative disorders such as Alzheimer’s disease, Parkinson’s disease, and MS (multiple sclerosis) (Guo, Callaway, & Ting, 2015). Moreover, there are diseases directly linked to constitutive inflammasome activation. For example, cryopyrin associated periodic syndromes (CAPS) is caused by a gain-of-function mutation on *NLRP3* which results in spontaneous activation of the NLRP3 inflammasome. Macrophage activation syndrome (MAS) is another disease that has been linked to

spontaneous NLRC4 activation due to a missense mutation at its nucleotide binding domain (Canna et al., 2014). Current knowledge on autoinflammatory diseases associated with inflammasome activation is summarized in Figure 1.4.

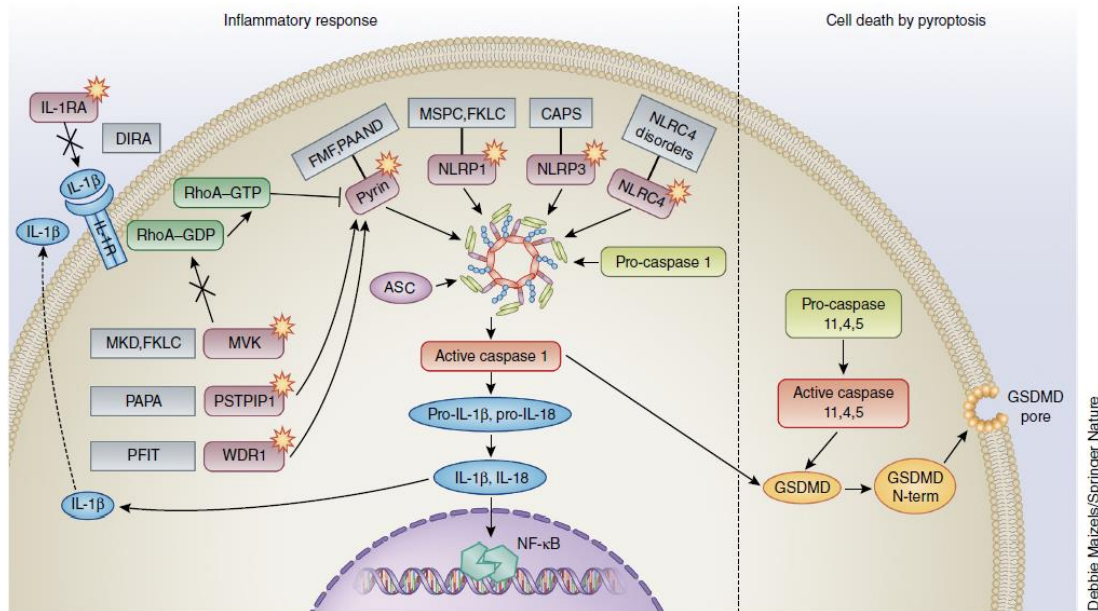


Figure 1.4 Autoinflammatory disease mechanisms in relation to inflammasome complexes (Adapted from Manthiram, Zhou, Aksentijevich, & Kastner, 2017)

1.3.1 AIM2 Inflammasome

Absent in melanoma 2, or the AIM2 protein is a cytosolic DNA sensor and a member of the PYHIN (Pyrin and HIN) protein family. It is composed of a PYD and HIN-200C domain. HIN 200 domains contain oligonucleotide/oligosaccharide folds and therefore can bind ssDNA and dsDNA (Schattgen & Fitzgerald, 2011). Hence, AIM2 plays a crucial role in detection of and protection from DNA viruses. The function of AIM2 is not only restricted to viral DNA detection. For example, intracellular bacterial infections lead to the production of guanylate binding proteins (GBPs) that destabilize vacuoles and bacterial outer membranes, causing the release of bacterial DNA into the cytosol, where it is detected by AIM2 (Man et al., 2015). Structurally, AIM2 does not

contain a CARD and therefore requires the assistance of the adaptor ASC for the recruitment of caspase-1. Of note, AIM2 recognizes cytosolic DNA indiscriminately and cannot differentiate host-derived nucleic acids from pathogen-derived ones. Therefore, it is suggested that AIM2 plays a role in certain autoinflammatory diseases such as systemic lupus erythematosus (SLE) where host DNA can escape into the cytoplasm. It is suggested that effective AIM2 activation requires the presence of a minimum of 80 bp of DNA in the cytosol (Vanaja et al., 2015).

1.3.2 NLRC4 Inflammasome

The NLRC4 inflammasome contains a CARD instead of a PYD and therefore the recruitment of ASC is not essential for NLRC4 mediated pyroptosis. However, ASC is still indispensable for caspase-1 cleavage and IL-1 β maturation (Broz, Moltke, Jones, Vance, & Monack, 2010; Opdenbosch et al., 2014). Unlike AIM2, NLRC4 does not directly bind to its activating ligand but rather requires NAIP, another NLR protein. Upon binding to a ligand, NAIP oligomerizes with NLRC4 and forms the NAIP-NLRC4 inflammasome complex. This inflammasome pathway is activated in response to the detection of cytosolic bacterial flagellin and/or bacteria with type-3 secretion systems (T3SS) in mice. In humans, on the other hand, only T3SS rather than flagellin has been observed to activate the NLRC4 complex. Spontaneous activation of the NLRC4 inflammasome due to a missense mutation that alters its nucleotide binding domain has been directly linked to macrophage activation syndrome (MAS). This leads to continuous active caspase-1 formation and subsequent IL-1 β and IL-18 maturation and secretion (Canna et al., 2014). As the name suggests, MAS is the extreme proliferation and overactivation of macrophages and is clinically observed to present with fever, hepatosplenomegaly and lymphadenopathy (Sawhney, Woo, & Murray, 2001).

1.3.3 Non-canonical Inflammasome

Non-canonical inflammasome activation remains a poorly understood process among the inflammasome field. Its activation occurs through the detection of cytosolic gram-negative bacterial endotoxin LPS by caspase-11 rather than caspase-1. (Guo et al., 2015). Since caspase-11 is only expressed in mice, caspase-4 and caspase-5 were shown to reciprocate its function in humans (Vanaja et al., 2015). The recognition of LPS by caspase-11 is independent of the TLR4 pathway. Hence, it has become clear that non-canonical inflammasome activation is essential for intracellular gram-negative bacteria surveillance. In addition, it is suggested that caspase-11 processes GSDMD (gasdermin-D) and that GSDMD not only promotes pyroptosis but also stimulates the activation of NLRP3 and caspase-1 that is followed by IL-1 β maturation and secretion (Kayagaki et al., 2015). So, it seems pyroptotic cell death upon cytosolic LPS detection is caspase-1 independent and mediated by caspase-11 activity. IL-1 β maturation, on the other hand, still requires cleavage by caspase-1. The differences in canonical and non-canonical inflammasome pathways are summarized in Figure 1.5.

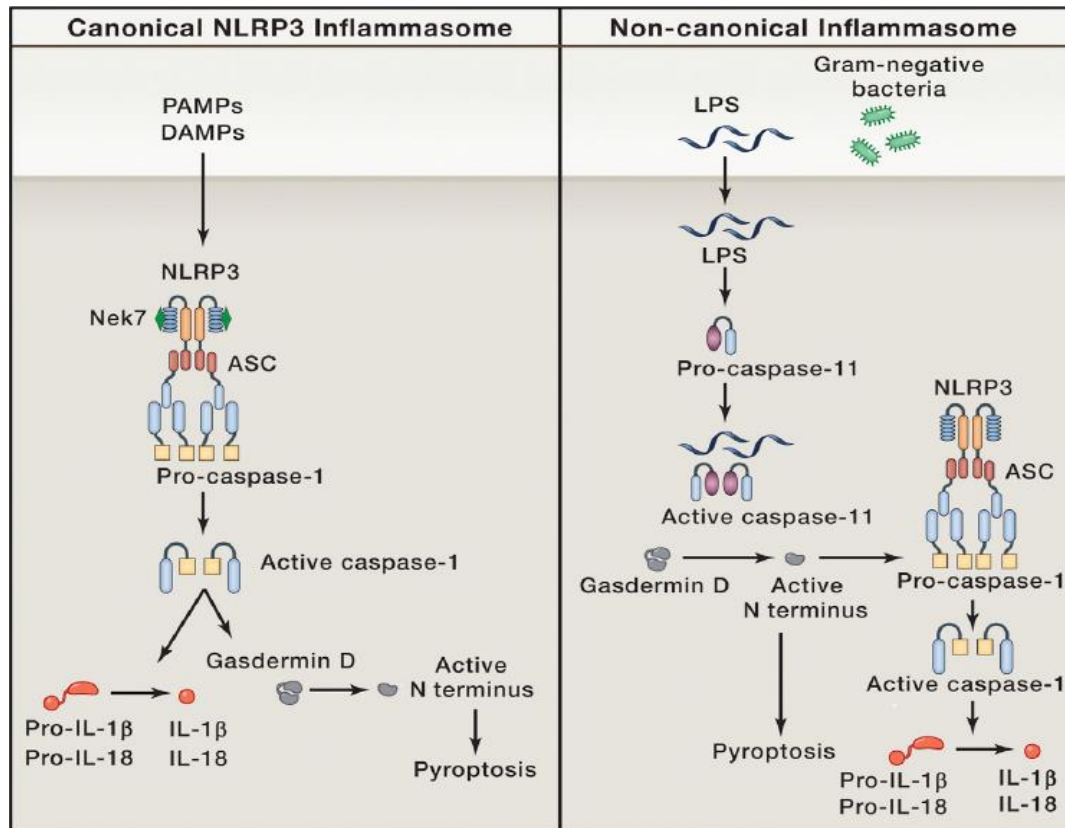


Figure 1.5 Illustration of canonical NLRP3 activation and non-canonical inflammasome activation (Adapted from Rathinam & Fitzgerald, 2016).

1.3.4 NLRP3 Inflammasome

The NLRP3 inflammasome is the most widely studied inflammasome complex due to its broadly varied stimuli. NLRP3 contains a PYD and requires ASC speck recruitment to engage and activate pro-caspase-1 and subsequently IL-1 β and IL-18. The fact that NLRP3 is initiated by a number of ligands, it is likely that all of those ligands induce common downstream events that lead to the same outcome (Guo et al., 2015). These events include NLRP3 translocation to mitochondria, production of ROS (reactive oxygen species), cathepsin release following loss of lysosomal integrity, K⁺ (potassium) efflux. In addition, RNA viruses and RNA:DNA hybrids were shown to indirectly cause NLRP3 activation by causing mitochondrial destabilization. Another recent finding was the serine-threonine kinase NEK7 interacting with NLRP3 (He et al., 2016). Normally known to be involved in mitosis, NEK7 aids NLRP3 in the

oligomerization with ASC in response to nigericin or ATP stimulation. NLRP3 has been associated with a number of diseases, one of which is type-2 diabetes, where pancreatic islet amyloid polypeptides (IAPP) oligomers stimulate NLRP3 activation (Vanaja et al., 2015). Another directly linked disorder is the cryopyrin associated periodic syndromes (CAPS), originating due to a gain-of-function mutation in *NLRP3* (Manthiram et al., 2017). CAPS have been reported to present with fever, rash, joint abnormalities, and deafness (Shinkai, Mccalmon, & Leslie, 2007).

1.4 Suppressive ODN A151

Immune suppressive motifs rich in polyG or GC content were shown to down-modulate immune stimulatory effects of unmethylated bacterial CpG motifs (Yamada et al., 2002; Krieg et al., 1998). Telomeric repeats that are frequent in mammals but absent in bacteria are an example for immune suppressive motifs. TTAGGG repeats, an example for telomeric sequences later termed as A151, was observed to block CpG colocalization with TLR9 in endosomal vesicles (Gursel et al., 2003). This suppressive effect was associated with the ability of TTAGGG motifs to form G-tetrads (Gursel et al., 2003). In addition, TTAGGG was demonstrated to prevent STAT1 and STAT4 phosphorylation, thereby inhibiting the release of proinflammatory and Th1 cytokines upon LPS stimulation (Shirota et al., 2017). Moreover, synthetic ODN-A151, containing four repeats of TTAGGG, was found to down modulate the effect of cytosolic DNA by inhibiting interferon stimulated gene transcription and TNF- α , and type-1 interferon production (Kaminski et al., 2013). Furthermore, the same group demonstrated that ODN-A151 abrogates AIM2 dependent inflammasome activation and subsequent IL-1 β and IL-18 maturation and secretion via competing with the stimulatory DNA.

Furthermore, this group also demonstrated that the phosphorothioate backbone of ODN-A151 was critical to carry out its inhibitory effect. However, ODN-A151 did not display the same effects on nigericin induced NLRP3 inflammasome initiation and whether or not it suppressed other inflammasome pathways was not investigated.

1.5 Histiocytosis and lymphadenopathy syndrome (H Syndrome)

The autosomal recessive disorder H syndrome is characterized by cutaneous hyperpigmentation, the accumulation of excess melanin, hypertrichosis, abnormal growth of body hair, hepatosplenomegaly, enlargement of liver and spleen, cardiac anomalies, hearing loss, hypogonadism, short stature and in rare cases hyperglycemia. The term H syndrome refers to these major clinical manifestations. Three mutations in the SLC29A3 gene, coding for the equilibrative nucleoside transporter hENT3, were identified in 11 families of Bulgarian and Arab descent that showed clinical symptoms (Molho-pessach et al., 2008).

The human equilibrative nucleoside transporter 3 (hENT3), is part of the solute carrier (SLC) transporters known as ENT or SLC29 family. The transporter was shown to be localized in late endosomes/lysosomes as well as in the mitochondria. Its subcellular position and low working pH range (5.5-6.5) implies that hENT3 carries nucleosides from late endosomes/lysosomes into the cytosol and through the mitochondrial membrane (Kang et al., 2010). However, the functional mechanisms for its role in nucleoside transportation remain unresolved.

Interestingly, H syndrome shows similar clinical features to the inflammasome associated autoinflammatory disorders macrophage activating syndrome (MAS) and cryopyrin associated periodic syndromes (CAPS). Febrile attacks and hearing loss that are seen in H syndrome patients are also symptoms of CAPS (Molho-pessach et al., 2008; Shinkai et al., 2007). Additionally; depending on the severity of disease onset some MAS patients demonstrate lymphadenopathy and hepatosplenomegaly, both of which are observed in H syndrome patients as well (Canna et al., 2014; Sawhney et al., 2001). Putting these clinical manifestations together with the functional properties of hENT3 where its dysregulation could potentially destabilize the endolysosomal compartment, it is plausible that the underlying cause of the above mentioned unexplained inflammatory manifestations could be due to inflammasome overactivation and presentation of the H syndrome phenotype.

1.6 Aim of the Study

Several inflammasome activation mechanisms have been described, including NLRP1, NLRP3, NLRC4 and AIM-2-dependent pathways. Excessive inflammasome activation is associated with the pathogenesis of Alzheimer's disease, gout disease, type-2 diabetes, atherosclerosis, MAS (macrophage activation syndrome) and obesity, necessitating development of therapeutic agents targeting distinct pathways of activation. Synthetic oligodeoxynucleotides containing TTAGGG suppressive motifs has been shown to exhibit immune modulatory effects. In this study, we aimed to study the effects of suppressive ODN A151 on the above mentioned inflammasome activation pathways. In order to do so, we stimulated THP-1 cells, human peripheral blood mononucleated cells (hPBMC), bone marrow derived macrophages (BMDM) with specific inflammasome activating ligands in the absence or presence of A151-ODN addition. As a readout of inflammasome activation and pyroptosis, we determined IL-1 β levels and percent cytotoxicity, respectively. Moreover, we used GFP labelled ASC expressing THP-1 cells and counted ASC specks that were released in the extracellular environment via flow cytometry or fluorescence microscopy. Furthermore, we analyzed mitochondrial membrane integrity with the fluorogenic JC-1 assay. Apart from these studies, we initiated a preliminary study in which we attempted to clarify whether inflammasome overactivation played a pathological role in development of autoinflammatory symptoms in a patient with H syndrome.

CHAPTER 2

MATERIALS & METHODS

2.1. MATERIALS

2.1.1. Cell Lines and Primary Cells

Human acute monocytic leukemia cell line THP1, was obtained from ATCC (American Type Culture Collection, USA). Interferon signaling reporter cell line THP1-Blue ISG was purchased from Invivogen (USA). GFP tagged ASC (apoptosis associated speck-like protein containing a CARD) expressing THP1 (THP1-GFP) cells were a kind gift from Prof. Dr. Nesrin Özören of Boğaziçi University.

Healthy donor blood for human peripheral blood mononucleated cells (PBMC) isolation was obtained at METU Medical Center.

Bone marrow derived macrophages (BMDM) were obtained from bone marrow precursors isolated from healthy 8-12 weeks old BALB/c mice of the Animal Center at Bilkent University.

2.1.2. Cell Culture Media, Solutions, and Buffers

Gibco RPMI 1640 growth medium appended with L-Glutamine and Opti-MEM serum reduced medium was purchased from Thermo Fisher Scientific (USA). Fetal Bovine Serum (FBS), Penicillin/Streptomycin, non-essential amino acids, sodium pyruvate, and HEPES buffer were procured from Lonza(Switzerland) or Biological Industries (BI, USA). Molecular biology grade water and phosphate buffered saline (PBS) were purchased from Lonza(Switzerland) and Biological Industries (USA). Gradient cell separation medium Lympho-Paque for human PBMC isolation was from Genaxxon (Germany). Recipes for various buffers (ELISA wash buffer, T-cell buffer, FACS buffer, blocking buffer) and culture media are listed in Appendix A.

2.1.3. Reagents

Monoclonal unlabeled capture antibodies, biotinylated detection antibodies, and alkaline phosphatase conjugated streptavidin (Strep-AP) for Enzyme Linked Immunosorbent Assay (ELISA) were procured from BioLegend (USA) or Mabtech (Sweden). PNPP (*p*-nitrophenyl phosphate disodium salt) was obtained from Thermo Fisher Scientific (USA). Propidium iodide solution for dead cell staining was obtained from BioLegend (cat# 421301, USA). Lactate dehydrogenase (LDH) cytotoxicity detection kit was from Roche (cat # 11644793001, Switzerland). JC-1 mitochondrial membrane potential assay kit and dihydrorhodamine123(DHR123) reactive oxygen intermediate detection reagent was purchased from Cayman Chemical (USA). MitoSOX Red mitochondrial superoxide indicator was procured from Thermo Fisher Scientific (USA). LegendPlex Human Type 1/2/3 Interferon Panel (5-plex) with V-bottom plate was obtained from BioLegend (USA).

2.1.4 Inflammasome Activators

Identity, company of origin and concentration of each ligands used for inflammasome activation is listed in **Table 2.1**

Table 2.1 Inflammasome induction ligands.

Ligand	Description	Pathway	Working concentration	Company	Catalog #
PMA (TPA)	phorbol 12-myristate 13-acetate	NF-KB	50µg/ml	Invivogen (USA)	tlrl-pma
poly (dA:dT)*	dsDNA analog	AIM2 inflammasome	5µg/ml	Invivogen (USA)	tlrl-patn-1
poly (I:C)*	dsRNA analog	NLRP3 inflammasome	5µg/ml	Invivogen (USA)	tlrl-pic-5
flagellin *	bacterial flagella component	NLRC4 inflammasome	1µg/ml	Invivogen (USA)	tlrl-epstfla-5

Table 2.1 continued

LPS* from E.coli	gram-neg bacterial outer membrane component	non-cannonical inflammasome	1µg/ml	Sigma-Aldrich	L2630-10MG
nigericin	microbial toxin	NLRP3 inflammasome	2µM	Invivogen (USA)	tlrl-nig
alum crystals*	aluminum hydroxide and potassium salts	NLRP3 inflammasome	200µg/ml	Invivogen (USA)	tlrl-alk

*Denotes ligands transfected using Lipofectamine2000 from Thermo Fisher Scientific (USA). Working concentration was optimized as 0.3ul/200µl well of 96-well flat bottom tissue culture plate.

2.1.5 Oligodeoxynucleotides

The sequence and concentration of the immunosuppressive A151 ODN and the control non-suppressive K3-flip ODN used in experiments is summarized in **Table 2.2**.

Table 2.2 Suppressive ODN and control ODN

ODN	Sequence	BB	work. conc.	company
A151	5`-TTAGGGTTAGGGTTAGGGTTAGGG-3`	PS	8µg/ml (1µM)	Alpha DNA
K3 flip	5`-ATG CACTCTGCAGGCTTCTC-3`	PS	4µg/ml (1µM)	Alpha DNA

BB: backbone; PS: phosphorothioate

2.2 METHODS

2.2.1 Cell Culture

2.2.1.1 THP-1 Cell Line Specifications and Maintenance

THP-1 monocytic cell line has been established from a 1year old male infant with acute monocytic leukemia. THP-1 cells are a model cell line commonly used for the study of vitro inflammasome activation. They become receptive to inflammasome ligands after priming with PMA (phorbol 12-myristate 13-acetate) or LPS (lipopolysaccharide) which induces the upregulation of pro-IL1 β , pro-caspase1, ASC (apoptosis associated speck-like protein containing a CARD), and the inflammasome protein complexes. Caspase-1 cleavage and IL-1 β maturation and secretion occurs upon subsequent stimulation with inflammasome inducers. THP-1 cells were maintained in T25 or T75 tissue culture flasks in RPMI 1640 medium enriched with 10 % FBS and normocin (100 μ g/ml). Cells were passaged every 2-3 days at 2-4 x10⁵ cells/ml confluency and discarded after 20th passage.

2.2.1.2 Human PBMC Isolation

Blood samples from healthy donors were drawn into 10 ml vacutainers coated with EDTA or heparin at METU medical center. Whole blood was diluted 1:1 with PBS and slowly layered onto gradient cell separation medium at a 1:1.5 ratio. Samples were centrifuged at 400g for 30 minutes at room temperature with disabled break setting. The cloudy buffy coat layer sandwiched between the upper plasma layer and the separation medium contained mononuclear cells and was removed into a fresh 50ml tube using plastic Pasteur pipettes. RPMI 1640 supplemented with 2% FBS was used as wash medium and was added onto the cells which were then centrifuged at 400g for 10 minutes at room temperature. This step was repeated twice. Wash medium was aspirated and cells were resuspended in RPMI 1640 with 10% FBS and counted using a flow cytometer. Afterwards, cells were layered onto 96-well tissue culture flat bottom plates at 400,000 cells/well confluency in 200 μ l medium.

2.2.1.3 Bone Marrow Derived Macrophage Generation

Stem cells were isolated from femur and tibia of BALB/c mice that were procured from Bilkent University Department of Molecular Biology and Genetics Animal Housing Facility. Animals were under controlled environmental conditions where they have access to food and water and are under 12 hour day and night cycles. Mice were sacrificed via cervical dislocation. Their femur and tibia were removed with sterilized surgical equipment and put into 75% ethanol, followed by RPMI 1640 with 2% FBS as wash medium. The ends of the bones were cut and 1ml insulin syringes were filled with wash medium. Syringes were used to flush stem cells out of the bones from each end. Isolated cells were run through a cell strainer to obtain a pure single cell suspension. Wash medium was added onto the acquired cell suspension and centrifuged at 300g for 10 minutes at room temperature. Next, cells were resuspended in 20% FBS containing RPMI 1640 and counted using a flow cytometer. Cells were layered at 150,000 cells/well confluency in 400 μ l/well in 48-well plates with 20 ng/ml M-CSF (macrophage colony stimulating factor) on day 0. Another 20 ng/ml M-CSF was added in 100 μ l/well medium on day 3 so that the final well volume was 500 μ l. Progress of differentiation and attachment was monitored daily. On day 6, culture medium was aspirated and cells were incubated at +4°C for 15 minutes for their detachment. Cells were pooled, centrifuged in wash medium (RPMI 1640 with 2% FBS) and counted via flow cytometry.

2.2.2 Stimulation Experiments

2.2.2.1 Ligand preparation

Extracellular ligands like nigericin were prepared directly in cell culture media (RPMI 1640 with 10% FBS) and added into relevant wells. Ligands that needed to be delivered to the cytosol were transfected using the lipid-based transfection reagent Lipofectamine2000. The stimulant and Lipofectamine2000 (0.3 μ l/200 μ l final well volume) were mixed in serum deprived Opti-MEM medium to increase efficiency and incubated 5 minutes at room temperature to allow complexation. Next, the ligands were diluted in cell culture media and added onto cells.

2.2.2.2 THP-1 and hPBMC stimulations

THP-1 cells were layered onto 96-well tissue culture flat bottom wells at 80,000 cells/well confluency in RPMI 1640 medium enriched with 10% FBS. 50 ng/ml PMA was added at a final well volume of 200 μ l. Cells were incubated overnight (16-18hr) at 37°C with 5% CO₂ in a humidified incubator. Next, cell attachment to wells was observed and cells were spun at 250g for 5 minutes at room temperature. Medium was aspirated and cells were observed again to make sure they were attached. Wash medium (RPMI 1640 with 2% FBS) was added in order to remove residual PMA and cells were centrifuged at 250g for 5 minutes at room temperature. Inflammasome activating ligands were prepared and added at a final volume of 200 μ l/well. Groups were designed in duplicates. Cells were incubated at 37°C with 5% CO₂ for 24 hours. Afterwards, cell media was collected into a new 96-well flat bottom tissue culture plate and stored at -20°C for later use. PBMC do not require a priming step with PMA or another ligand, otherwise the stimulation steps were similar to the protocol used with THP-1 stimulations.

2.2.2.3 BMDM stimulations

Cells were layered at 80,000 cells/well (200 μ l) confluency in culture medium (RPMI 1640 with 10% FBS) in a 96-well flat bottom tissue culture plate and primed using 1 μ g/ml LPS for 3 hours at 37°C with 5% CO₂. Next, LPS containing media was aspirated and cells were centrifuged in wash media at 300g for 5 minutes at room temperature. Stimulations for inflammasome activation were carried out as described for THP-1 and hPBMC stimulations.

2.2.3 Enzyme Linked Immunosorbent Assay (ELISA) for Cytokine

Quantification

Collected cell culture media of stimulated cells was stored at -20°C and used for cytokine detection. Semi-hydrophobic immunoplates of SPL Life Sciences were coated with 50 μ l/well PBS containing 2 μ g/ml human IL-1 β monoclonal capture antibody (Mabtech) or bicarbonate buffer (pH: 9.5) with 1:200 diluted mouse IL-1 β (BioLegend) monoclonal antibody. Plates were incubated overnight (16-18 hours) at +4°C. Afterwards, contents were discarded via plate inversion. Plates were incubated

at room temperature for 2 hours with 200 μ l/well blocking buffer (1% BSA in PBS). Next, blocking buffer was removed and plates were soaked in wash buffer (0.05% Tween in PBS) 5 times, 2 minutes incubation for each wash. Following air drying, 50 μ l/well thawed culture media was added. Simultaneously, 50 μ l/well recombinant human or mouse IL-1 β were added in duplicates with 1:1 serial dilutions from 20 ng/ml for human and 10 ng/ml for mouse initial concentrations. Plates were incubated 2 hours at room temperature and washed as described above. After air drying, 1 μ g/ml human biotin conjugated detection antibody and 1:200 diluted mouse biotin conjugated detection antibody in 50 μ l/well T-cell buffer (Appendix A) were incubated overnight at +4°C. Alkaline phosphatase (ALP) conjugated streptavidin was diluted at a 1:1000 ratio in T-cell buffer and incubated overnight at +4°C as well for human IL-1 β detection. Following incubation, plates were washed, air dried and incubated with 50 μ l/well streptavidin-ALP solution for 1 hour at room temperature. Next, plates were washed again and 50 μ l of PNPP substrate for alkaline phosphatase was added. Optical density measurements at 405nm were performed with Multiskan FC Microplate Photometer (Thermo Fisher Scientific, USA) at 1 hour time intervals until color development saturation was reached. Horseradish peroxidase (HRP) conjugated streptavidin was used for mouse IL-1 β detection. After overnight incubation of biotin conjugated detection antibody strep-HRP was added and incubated at room temperature for 1 hour. Plates were washed and 50 μ l TMB, substrate for HRP, was added. Color development was observed within 20-30 minutes and enzymatic reaction was stopped using sulfuric acid solution (2N H₂SO₄). Optical density was measured at 450 nm and 570nm, where 570 nm values represent a background signal and are subtracted from 450nm results. Quantitative results are obtained through the calculations of the photometer software using the standard curve of serially diluted recombinant samples.

2.2.4 GFP labelled ASC Detection via Fluorescent Microscopy and Flow Cytometry from THP-1-GFP

THP-1 cells expressing GFP tagged ASC were primed and stimulated as previously described. Following overnight incubation at 37°C, images were taken via EVOS Flويد Cell Imaging Station (Thermo Fisher Scientific, USA) for GFP fluorescence with a

20X objective at 460X magnification. Then, culture media was collected and centrifuged at 300g for 5 minutes to rid the media of remnant cells and analyzed via NovoCyt flow cytometer for ASC specks. Event number in 40 µl of media below a 50,000 threshold was counted and particles with a positive GFP signal were gated for counting.

2.2.5 Cytotoxicity Assays

2.2.5.1 Lactate dehydrogenase (LDH) Assay

Cytotoxicity detection solution was prepared according to manufacturer's instructions. 50 µl of collected cell culture media was mixed with 50 µl detection solution and incubated 25 minutes at room temperature protected from light. Optical density at 490 nm was measured at the end of incubation. Triton X-100 was used as a positive control to represent 100 % cytotoxicity (high control) while the untreated group was used as the negative control (low control). Percent cytotoxicity calculations were as follows:

$$\text{Cytotoxicity} = [(\text{experimental value} - \text{low cntrl}) - (\text{high cntrl} - \text{low cntrl})] * 100$$

2.2.5.2 Propidium iodide (PI) and SytoxOrange stainings

After media was collected from BMDM, 1µl PI (BioLegend) containing 50µl/well PBS was added onto cells. Plate was incubated for 15 minutes at +4°C and images were captured via fluorescence microscopy. 5 µM sytox orange in PBS was added onto THP-1-GFP cells after culture media removal. Plate was incubated at 37°C for 15 minutes and images were captured for green and red signals via fluorescence microscopy. Representative images were taken after thorough examination of whole wells.

2.2.6 JC-1 Mitochondrial Membrane Potential Assay

JC-1 mitochondrial stain was added onto cells at a 1:300 dilution (50µl/well) and change in fluorescence intensity of the green and red channels were monitored under fluorescence microscopy using the EVOS Flouid Cell Imaging Station (Thermo Fisher Scientific, USA) following 15-30 minutes incubation at 37°C. Accumulation of the monomeric or aggregate form of JC-1, indicative of perturbed mitochondrial

membrane potential was also followed using flow cytometry by assessing the mean fluorescence intensity of the green or the red signs.

2.2.7 LegendPlex Human Type 1/2/3 Interferon Panel

Seven reconstituted panel standards were prepared in microfuge tubes at 1:4 dilutions using the assay buffer provided in the kit, starting from top standards of 10,000pg/ml or 50,000pg/ml so that the last standard only contained the assay buffer. The assay was performed in a U-bottom plate. Following 25 µl assay buffer distribution to all wells, 25 µl of standards and samples were introduced into standard wells and sample wells, respectively. Antibody conjugated capture beads were vortexed for 30 seconds and added into each well at 25µl/well so that the final volume in each well was 75 µl at the end of this step. Plate was sealed, wrapped in aluminum foil and incubated at room temperature for 2 hours on a shaker at 800 rpm. Following centrifugation of the plate at 250 g for 5 minutes, Supernatants were discarded with caution in order not to disrupt the bead pellet. 25 µl of detection antibody was then added into each well and the plate was incubated at room temperature for 1 hour on a shaker at 800rpm as described above. At the end of this incubation period, 25µl SA-PE (streptavidin-phycoerythrin) was added into all wells, followed by incubation at room temperature for 30 minutes on a plate shaker at 800 rpm. Plate was centrifuged at 250 g for 5 minutes, supernatants were carefully aspirated and beads were washed in 150 µl of 1X wash buffer. Samples were acquired on a flow cytometer using an autosampler and results were analyzed using the LegendPlex Software according to manufacturer's instructions.

2.2.8 Percent Inhibition and Fold Induction Calculations

Percent inhibitions indicated on the bar graphs are calculated as following;

$$\text{Percent inhibition} = \frac{((\text{treated-untreated}) - (\text{A151 treated-untreated}))}{(\text{treated-untreated})} \times 100$$

Fold inductions are calculated as **treated/untreated** or **patient/healthy**.

2.2.9 Statistical Analysis

Student's t-test (one tailed, unpaired comparison) was used for data analysis using GraphPad prism 6 software.

2.2.10 Ethical Statement

Blood samples were obtained according to ethical conduct with informed consent of the patient's family through collaboration with Deniz Nazire Çağdaş Ayvaz of Hacettepe University.

CHAPTER 3

RESULTS & DISCUSSION

3.1 A151 ODN inhibits inflammasome activation dependent IL-1 β secretion in THP-1 human monocytic cells

Various studies have verified the immunomodulatory effects of A151 ODN on CpG ODN-induced stimulation and consequently pro-inflammatory cytokine production (Refs). We further explored A151 ODN's immune suppressive potential on different inflammasome activation pathways; namely AIM2, NLRC4, NLRP3 and the non-canonical inflammasomes. In this context, we first analyzed the secretion of the pro-inflammatory cytokine IL-1 β into the extracellular environment as a major indicator of inflammasome activation. In the case of AIM2 inflammasome activation, it has been suggested that, A151 ODN competes with the cytosolic AIM2 agonist DNA and binds AIM2, thereby preventing its activation. Published results also suggest that this ODN does not suppress NLRP3 inflammasome formation (Kaminski et al., 2013). Whether or not A151 ODN suppresses other inflammasome pathways has not been investigated. To verify the previous findings and to address the unanswered questions, we transfected a synthetic dsDNA analog poly(dA:dT) [poly(deoxyadenylic-deoxythymidylic)], the bacterial flagellar protein flagellin and LPS into the cytosol of THP-1 cells for AIM2, NLRC4 and non-canonical inflammasome activation, respectively. NLRP3 inflammasome activator nigericin and an indirect activator, poly(I:C) was also tested. IL-1 β release into cell culture media was measured by ELISA after 24 hours in samples stimulated as such in the absence or presence of the immune suppressor A151 ODN or its neutral control (K3-flip ODN) (Fig 3.1).

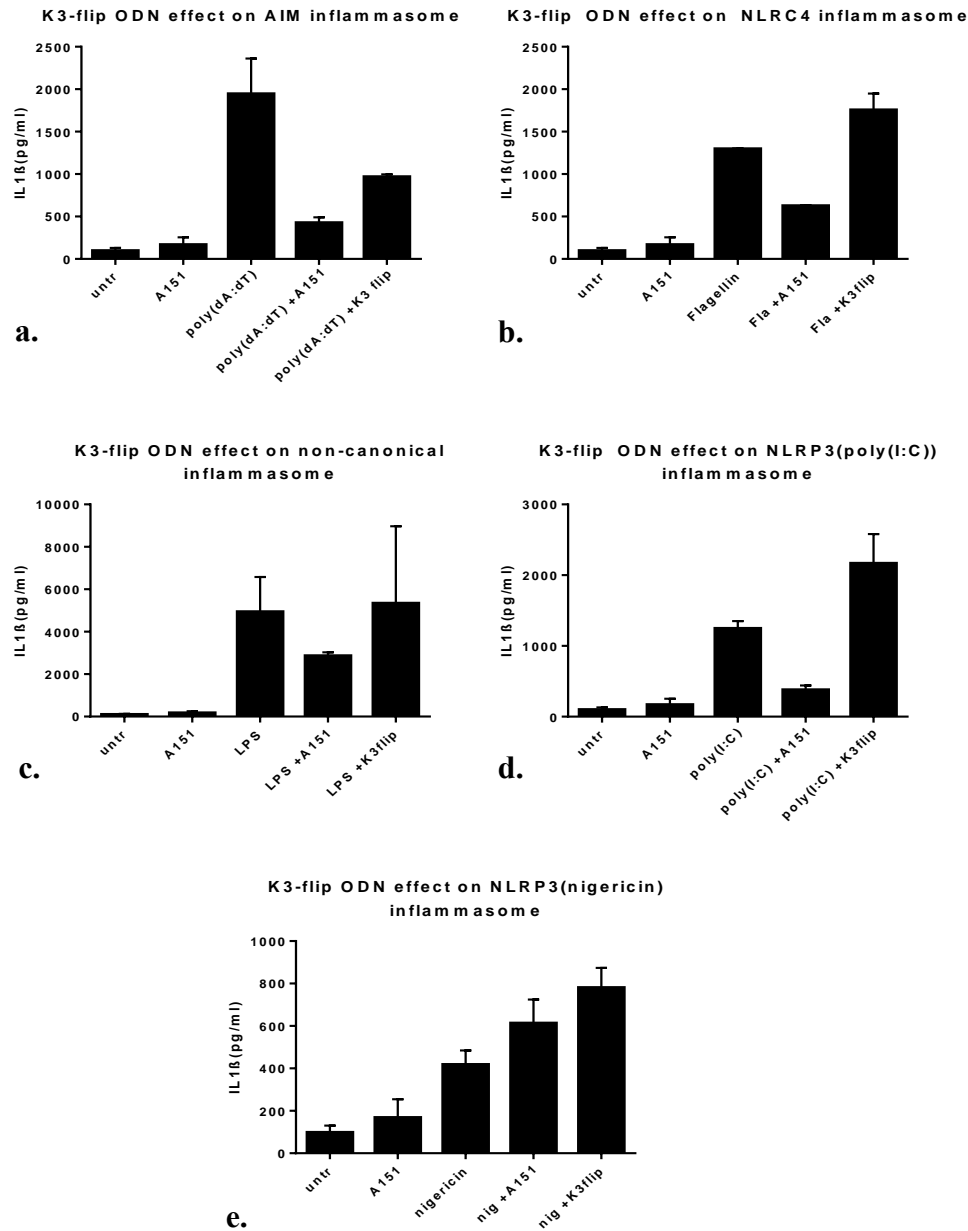


Figure 3.1 IL-1 β response of inflammasome activated groups compared to suppressive A151 ODN treated or and neutral control K3-flip ODN. THP-1 cells (4×10^5 /ml) were primed with 20 ng/ml PMA overnight (16-18 hours) and subsequently treated with the indicated inflammasome ligands. Cell culture media were collected after 24h incubation at 37°C. (a) AIM2; (b) NLRC4; (c) non-canonical; (d,e) poly(I:C), and nigericin induced NLRP3 inflammasomes, respectively.

After verifying that A151 ODN but not its neutral control (K3-flip) specifically suppressed certain types of inflammasome-dependent IL-1 β release, more in-depth experiments were performed. Specifically, various inducers of NLRP3 inflammasome were employed since these ligands display differences in the kinetics and mechanism through which they activate the NLRP3 inflammasome. For example, aluminum hydroxide (alum), which is routinely used as a vaccine adjuvant in human and animal vaccines, activates the NLRP3 inflammasome through destabilization and rupture of endolysosomal compartment (Franchi & Núñez, 2009). In contrast, cytosolic dsRNA stimulates NLRP3 inflammasome formation through a cytosolic dsRNA sensor, DHX33 (Allen et al., 2009; Mitoma et al., 2013). In order to assess the effect of A151 ODN on the NLRP3 inflammasome induced by both of these ligands, we transfected alum crystals and a synthetic dsRNA analog poly(I:C) [(poly(inosinic – cytidylic)] into the cytosol in the presence or absence of A151 ODN and evaluated the amount of IL-1 β secretion into the extracellular environment. Another well-known strong ligand for NLRP3 inflammasome activation is the bacterial toxin nigericin, derived from *Streptomyces hygroscopicus*. We included nigericin in our experiments as a positive control for NLRP3 activation and subsequent IL-1 β release. Our results showed that A151 ODN significantly inhibited AIM2, NLRC4, alum/poly(I:C) induced NLRP3 and cytosolic LPS induced non-canonical inflammasome-mediated IL-1 β release (Fig 3.2 a,b,c,d,e). However, the ODN was ineffective in inhibiting IL-1 β release following nigericin induced NLRP3 activation (Fig 3.2 f).

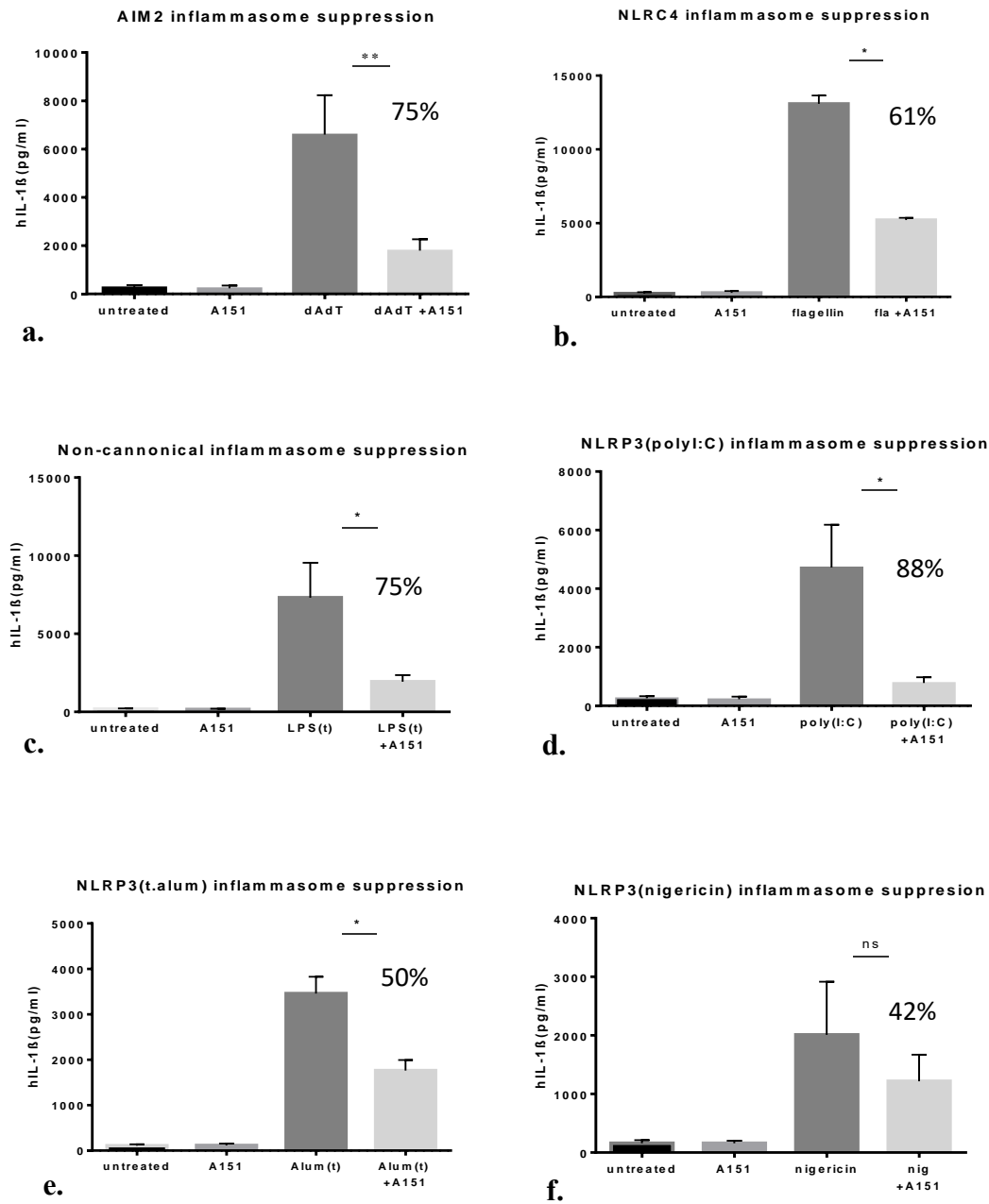
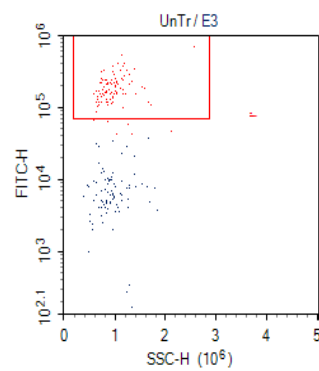


Figure 3.2 IL-1 β response of inflammasome activated groups compared to suppressive ODN treated groups. THP-1 cells (4×10^5 /ml) were primed with 20 ng/ml PMA overnight (16-18 hours) and subsequently treated with the indicated inflammasome ligands. Cell culture media were collected after 24 h incubation at 37°C. (a) AIM2; (b) NLRC4; (c) non-canonical; (d,e,f) poly(I:C), alum, and nigericin induced NLRP3 inflammasomes, respectively. Data shows mean \pm SEM of multiple experiments

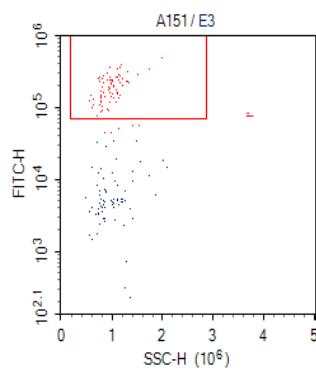
(average of 2-8 independent experiments). Student t-test was used for significance calculations (* $p < 0.05$, ** $p < 0.01$). Inhibition percentage is indicated on bar graphs.

3.2 A151 ODN inhibits speck formation in THP-1 cells

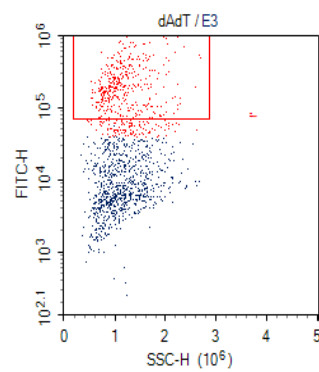
Another upstream requirement for the formation of an inflammasome complex is the recruitment of the apoptosis associated speck-like protein containing a CARD (ASC speck). In general, upon inflammasome activation, ASC proteins oligomerize to form one ASC speck/cell that is around 1 μm in size. ASC specks are then released into the extracellular environment and accumulate alongside IL-1 β and caspase-1 (Stutz, Horvath, Monks & Latz, 2013). Since A151 ODN demonstrated an inhibitory effect on IL-1 β release following inflammasome activation, we reasoned that the suppressive ODN might interfere with ASC speck formation and therefore with recruitment of the inflammasome-associated proteins. In order to test this hypothesis, we counted and compared the number of ASC specks that were released into the extracellular space from inflammasome activated cells that were treated or untreated with A151 ODN. To facilitate ASC speck quantitation, THP-1-GFP cells that stably expressed GFP tagged ASC monomers were used. Following inflammasome activation, GFP-ASC monomers oligomerize into specks that emit bright green fluorescence upon excitation at 488 nm. Released specks were collected from cell culture media after an overnight (16-18 hours) incubation which was previously determined in a time-dependent experiment to be sufficient for the release of ASC specks into extracellular space. ASC specks that were present in 40 μl volume of cell-free media was quantitated using flow cytometry (Figure 3.3). Prior to collection, speck release was verified qualitatively using fluorescent microscopy (Fig 3.4). Both quantitative and qualitative evaluation displayed a reduction in ASC speck count in the case of A151 ODN treated AIM2, NLRC4, intracellular LPS induced non-canonical inflammasomes (Fig 3.3 and 3.4, respectively). In contrast, A151 had no effect on poly(I:C), alum, and nigericin-induced ASC-speck formation (Fig 3.3).



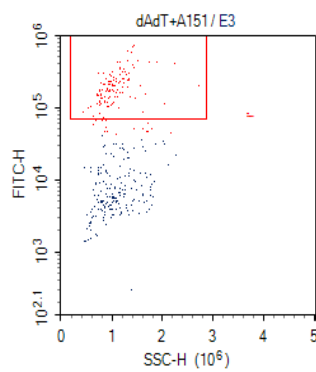
Gate	Count
E3	177
R2	86



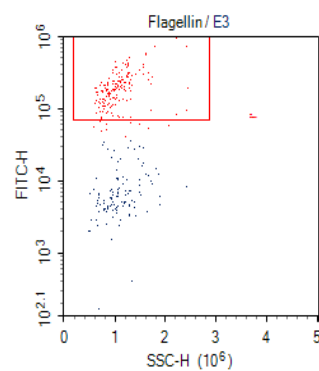
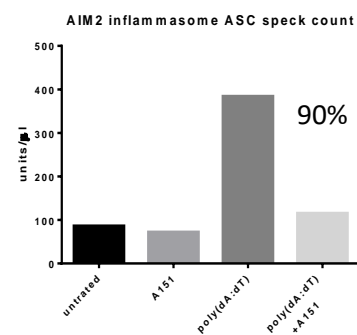
Gate	Count
E3	149
R2	72



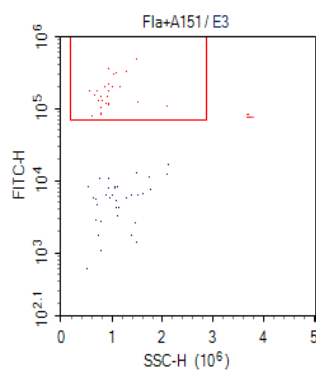
Gate	Count
E3	1,326
R2	384



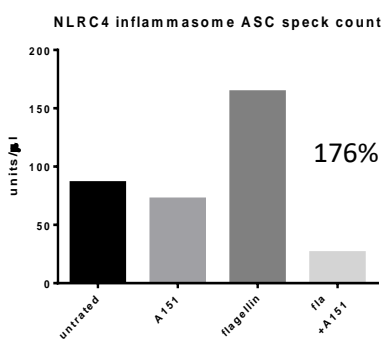
Gate	Count
E3	314
R2	115



Gate	Count
E3	288
R2	164

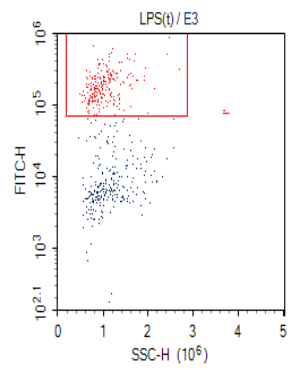


Gate	Count
E3	60
R2	26

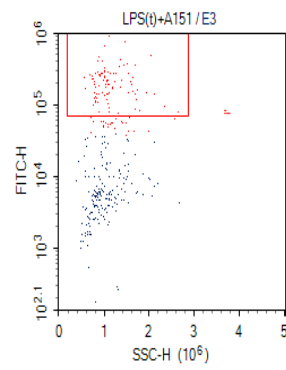


a.

b.

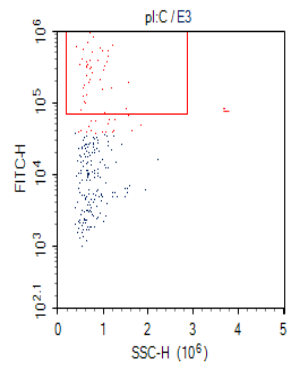
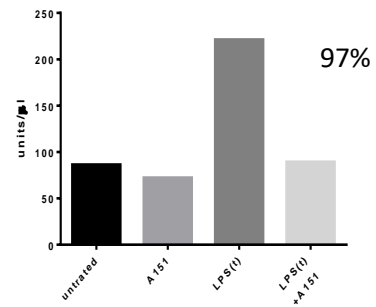


Gate	Count
E3	473
R2	221

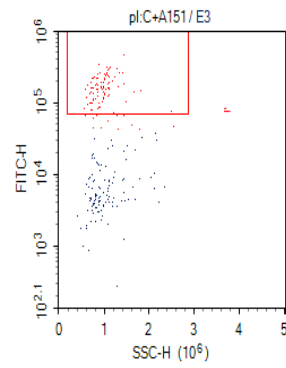


Gate	Count
E3	286
R2	89

Non-canonical inflammasome ASC speck count

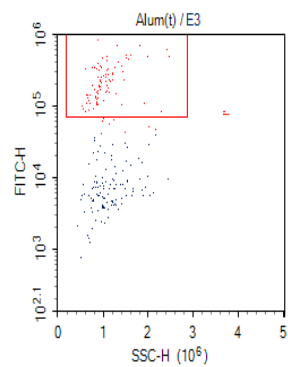
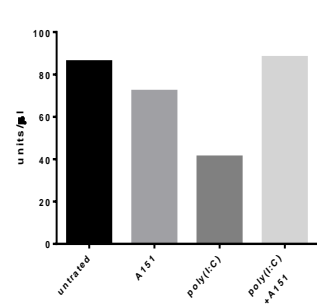


Gate	Count
E3	230
R2	41

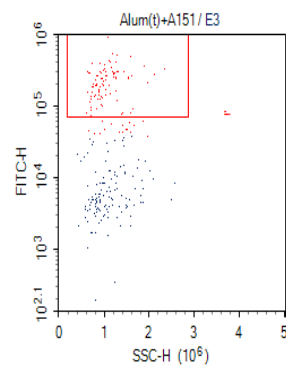


Gate	Count
E3	217
R2	88

NLRP3(poly(I:C)) inflammasome ASC speck count

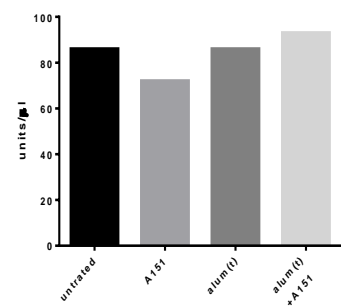


Gate	Count
E3	211
R2	86



Gate	Count
E3	237
R2	93

NLRP3(alum(t)) inflammasome ASC speck count



a.

b.

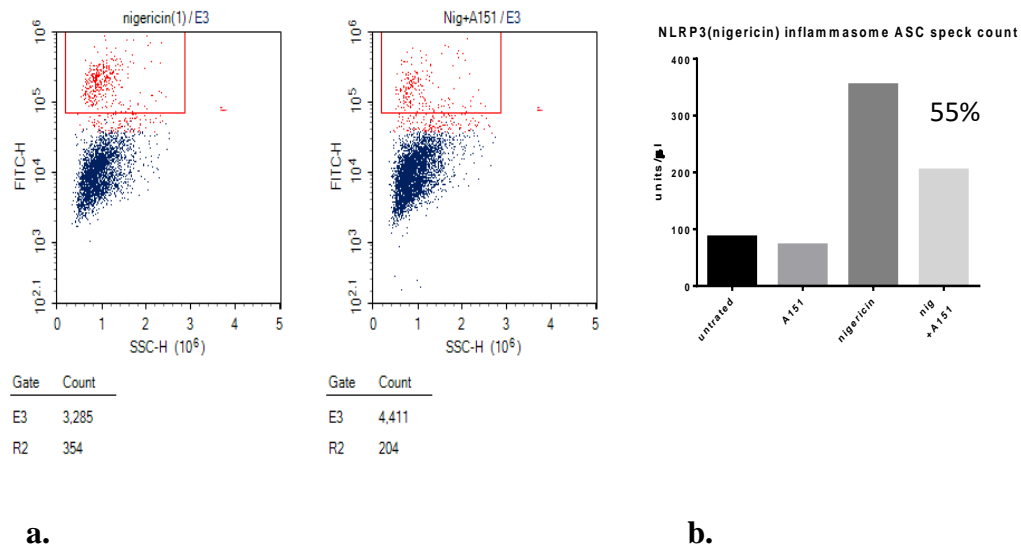
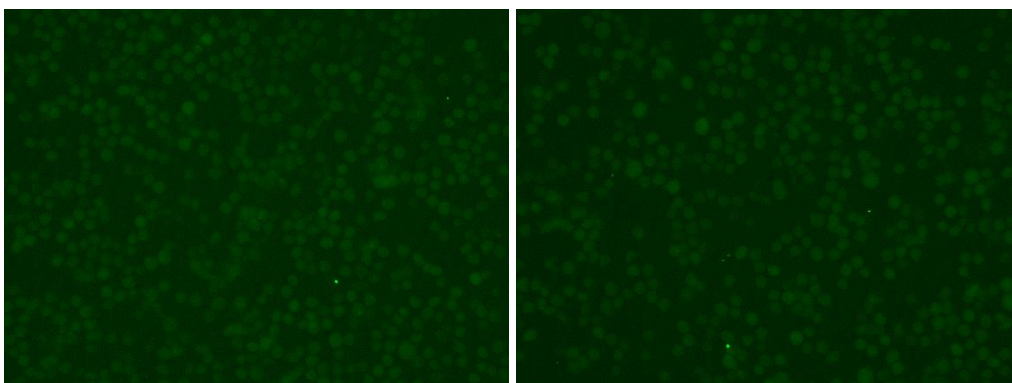


Figure 3.3 ASC specks released from primed and inflammasome stimulated THP-1-GFP cells were counted from 40 μ l of cell-free culture media. (a) Flow cytometric analysis of indicated groups of stimulated THP1-GFP cells after overnight incubation (16-18 hours). (b) Bar graph illustrations of ASC speck counts from (a). Graphs are representative of two independent experiments. Inhibition percentage is indicated on bar graphs.

Untreated

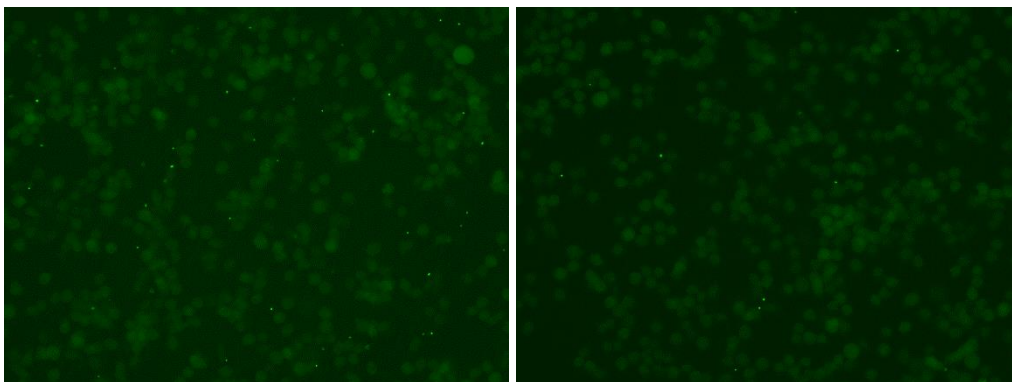
A151



a.

poly(dA:dT)

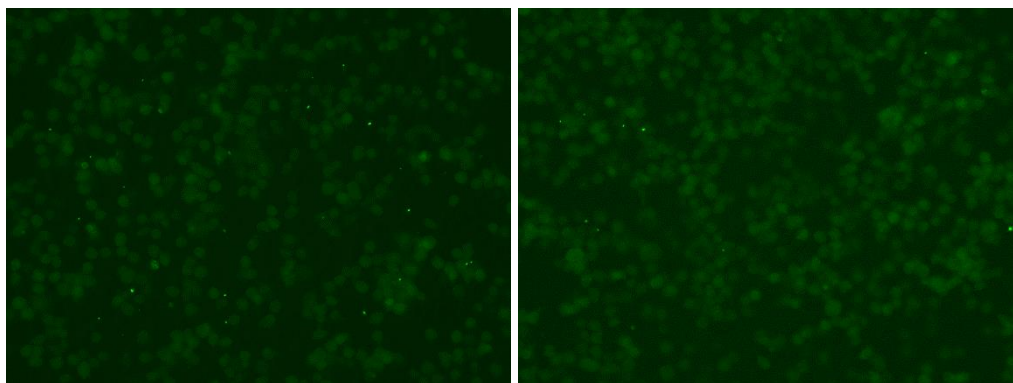
poly(dA:dT) +A151



b.

flagellin

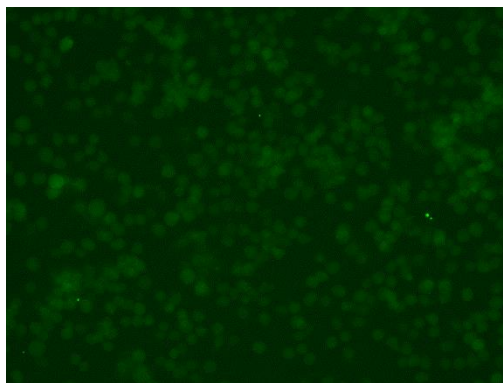
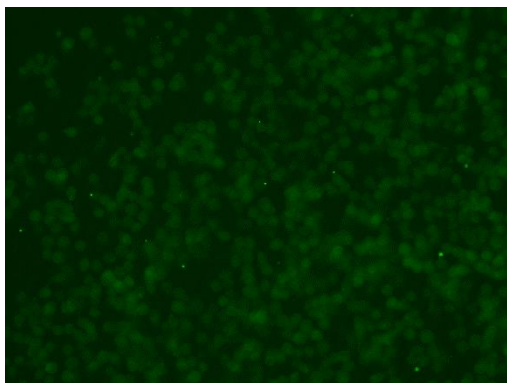
flagellin +A151



c.

LPS(t)

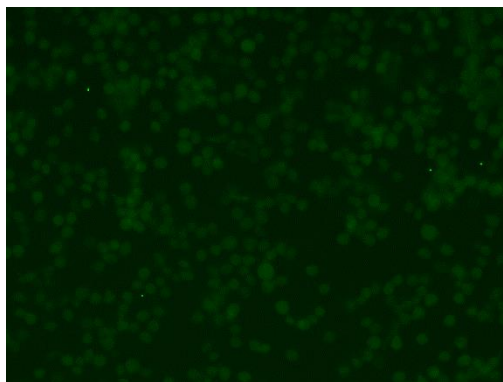
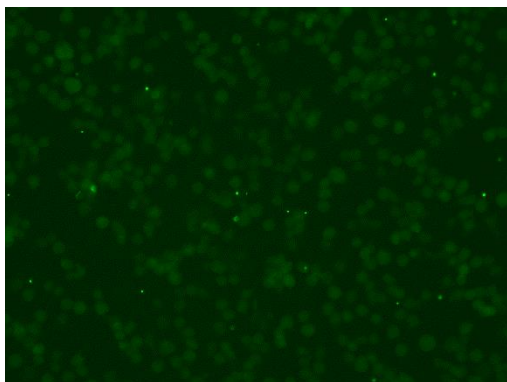
LPS(t)+A151



d.

poly(I:C)

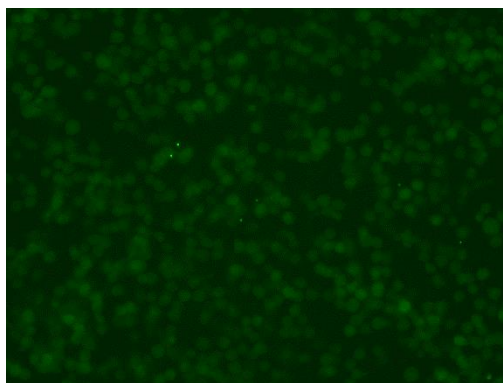
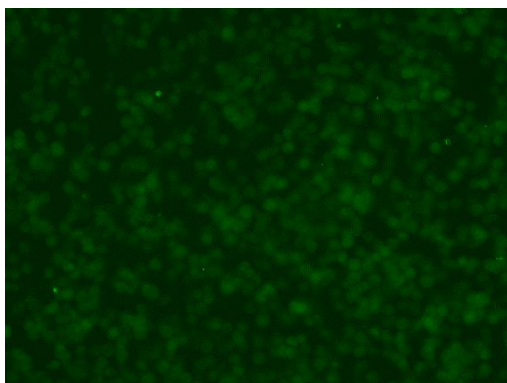
poly(I:C) +A151



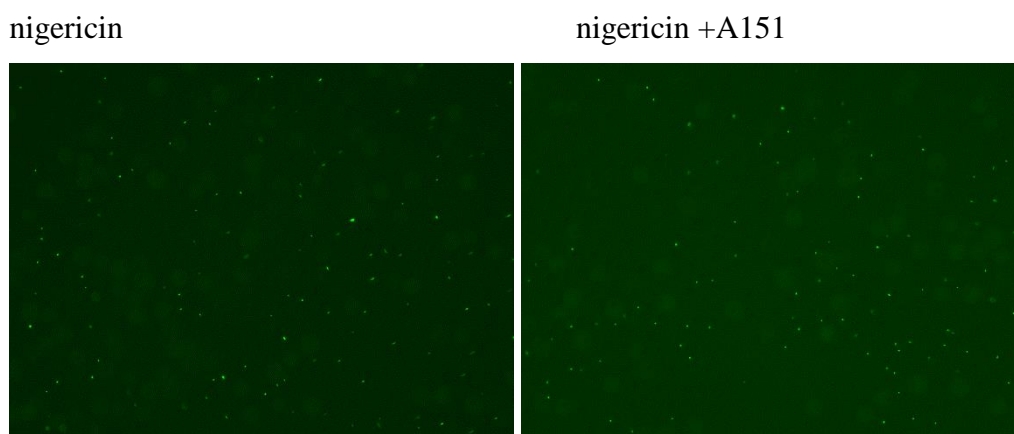
e.

Alum

Alum +A151



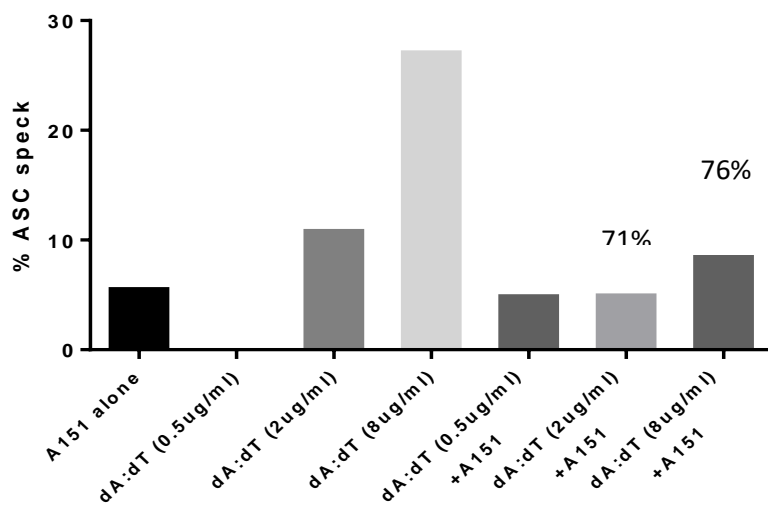
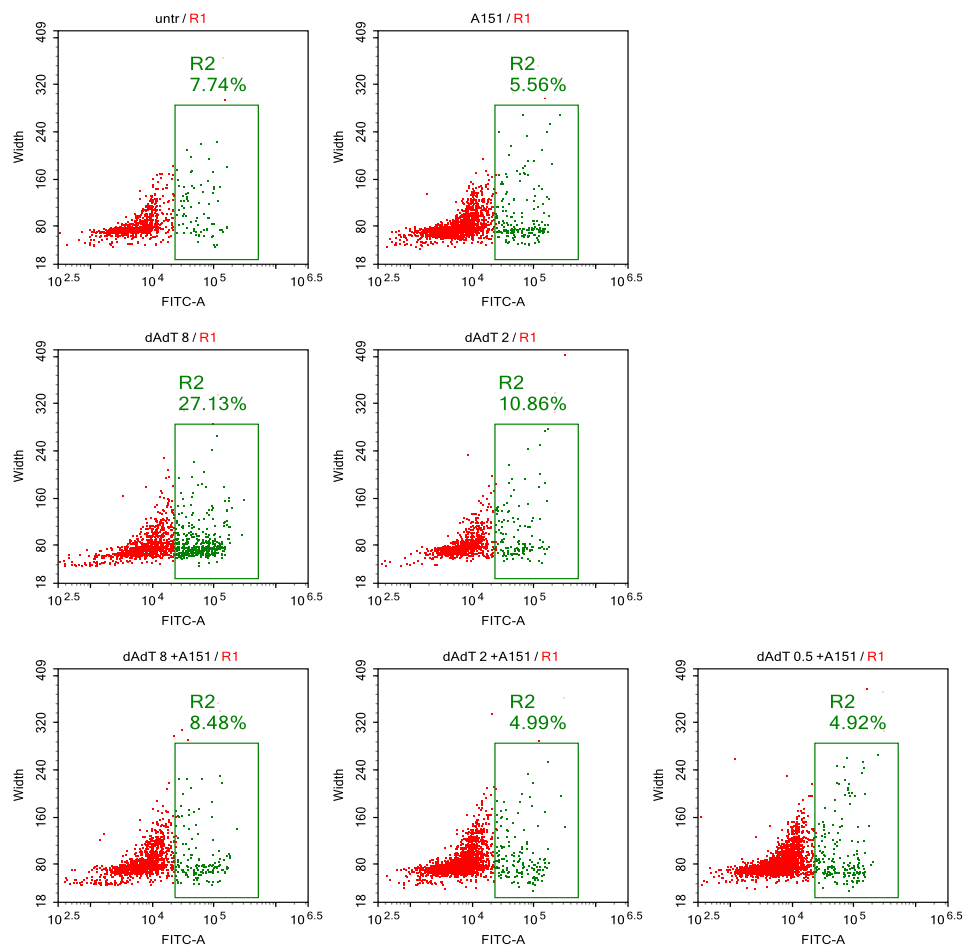
f.



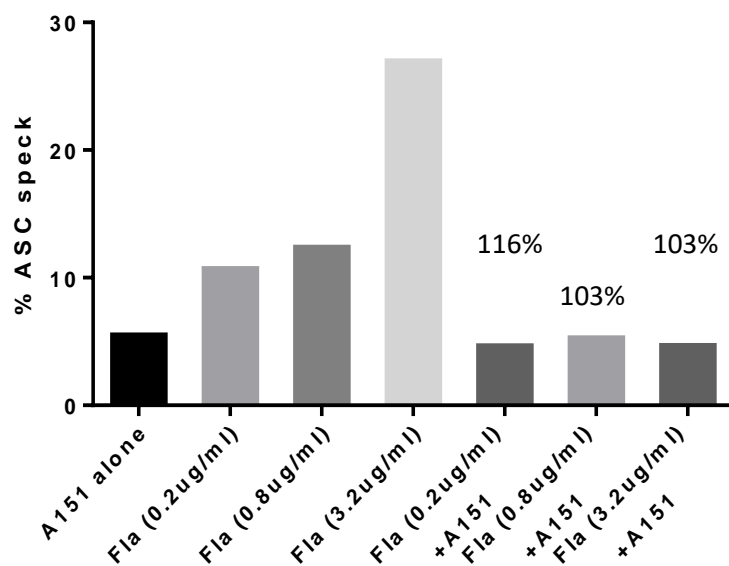
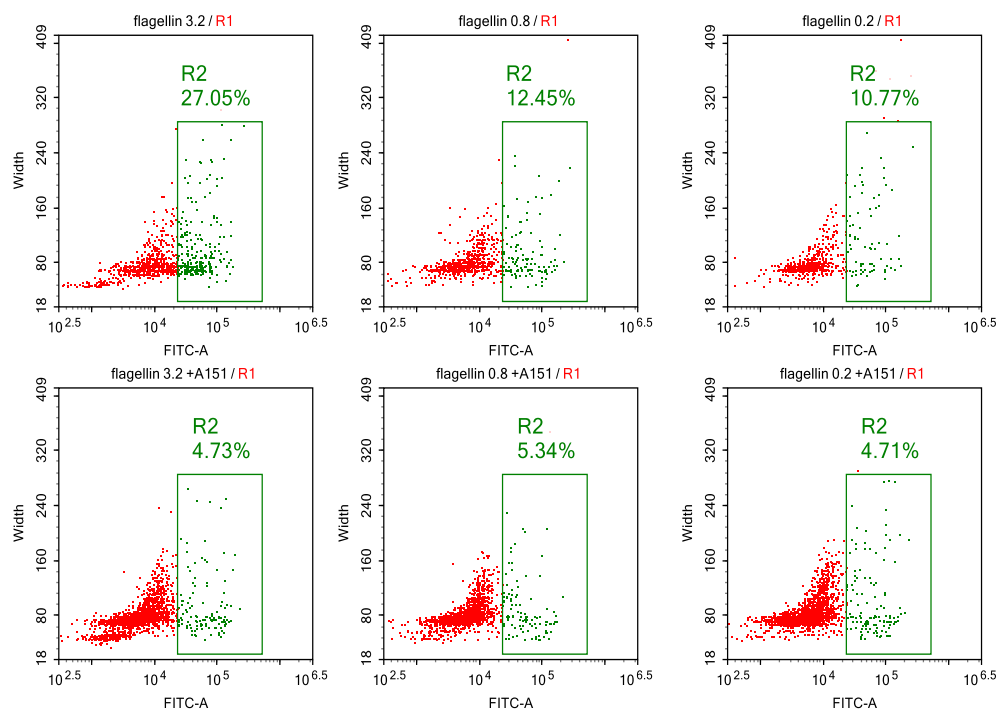
g.

Figure 3.4 Fluorescent microscopy images of THP1-GFP cells stimulated with indicated canonical inflammasome activators (a,b,c,e,f,g) and cytosolic LPS for non-canonical inflammasome activation (d) in the presence or absence of A151 ODN. Images were taken after overnight (16-18 hours) incubation at 37°C and are representative of four independent experiments.

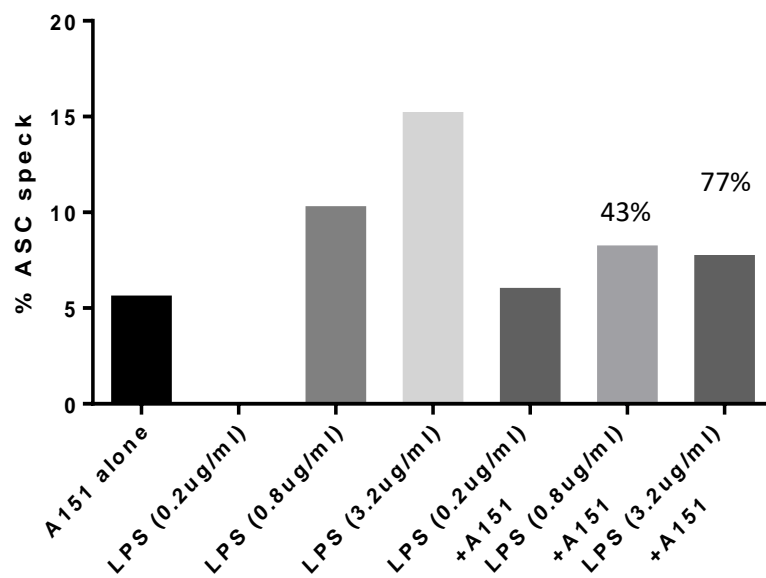
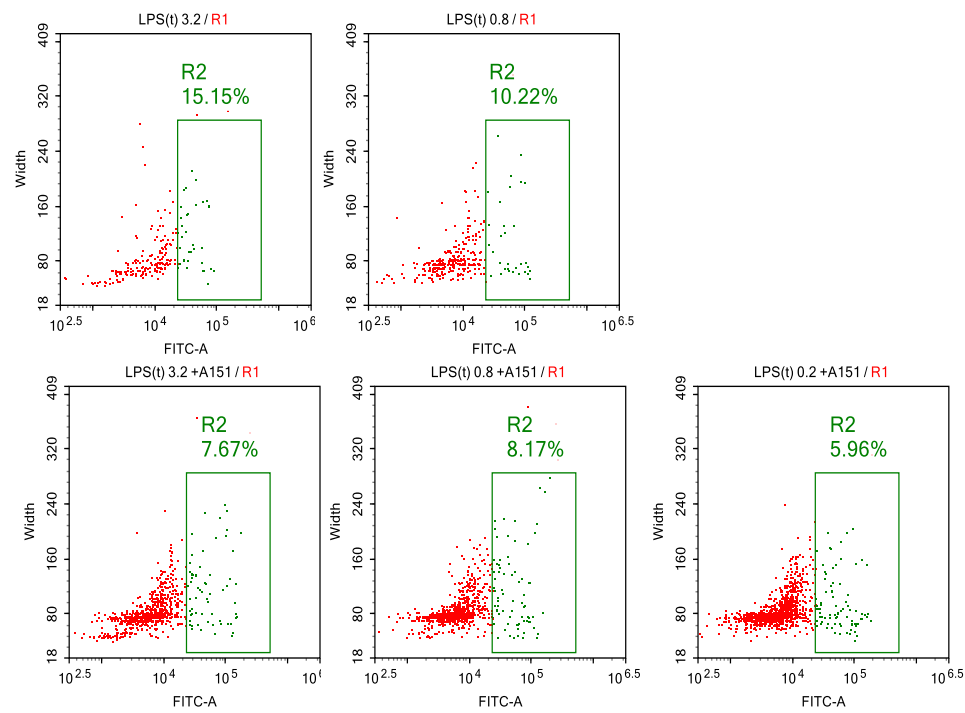
The fact that A151 ODN inhibits IL-1 β but not ASC speck release suggests an alternate mechanism of action of the suppressive ODN in poly(I:C) and alum induced NLRP3 inflammasome activation pathways, independent of ASC oligomerization. Since ASC specks are released but not IL-1 β , it is possible that A151 ODN might interfere with caspase-1 recruitment, IL-1 β maturation and/or pyroptosis. Another possibility is that the dose of the ligands used for inflammasome activation might be too concentrated for A151 to show its inhibitory effect. To address such an eventuality, we decided to use three different doses of various activators in the absence and presence of A151 ODN (Figure 3.5). Results of this experiment showed that A151 ODN failed to inhibit nigericin-dependent ASC speck formation even when a very low dose of the activator was used (i.e 0.2 μ g/ml).



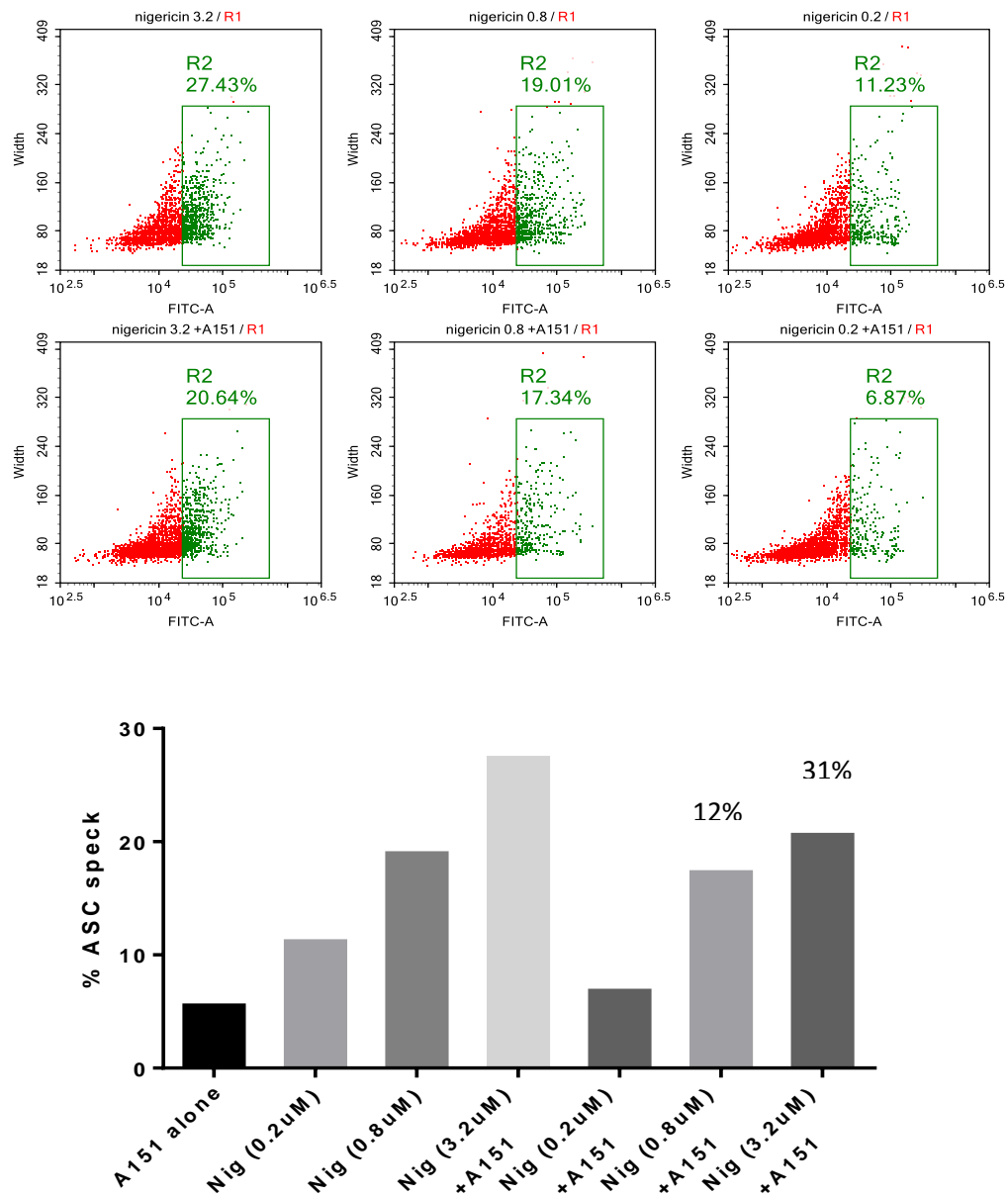
a.



b.



c.



d.

Figure 3.5 Flow cytometry analysis of ASC-speck release from primed and dose-dependently stimulated THP-1-ASC-GFP cells. Cell culture media were analysed for ASC specks after overnight (16-18 hours) incubation at 37°C. Stimulations were performed in 4-fold dilutions for (a) AIM2 with poly(dA:dT), (b) NLRC4 with cytosolic flagellin, (c) non-canonical with intracellular LPS, and (d) nigericin induced NLRP3 inflammasomes.

3.3 A151 ODN modulates inflammasome activation dependent pyroptosis

Pyroptosis is an inflammatory form of programmed cell death and the inevitable outcome of healthy inflammasome activation. It includes cell swelling and membrane rupture via pore formation on the plasma membrane (Shi et al., 2015). Pyroptosis greatly contributes to pathological inflammation by the release of pro-inflammatory cytokines and DAMPs (danger associated molecular patterns) into extracellular space. Furthermore, Shi et al. demonstrated in 2015 by inhibiting gasdermin-D (GSDMD), one of the key proteins in the process of pyroptosis, that IL-1 β secretion occurs through this type of inflammatory programmed cell death.

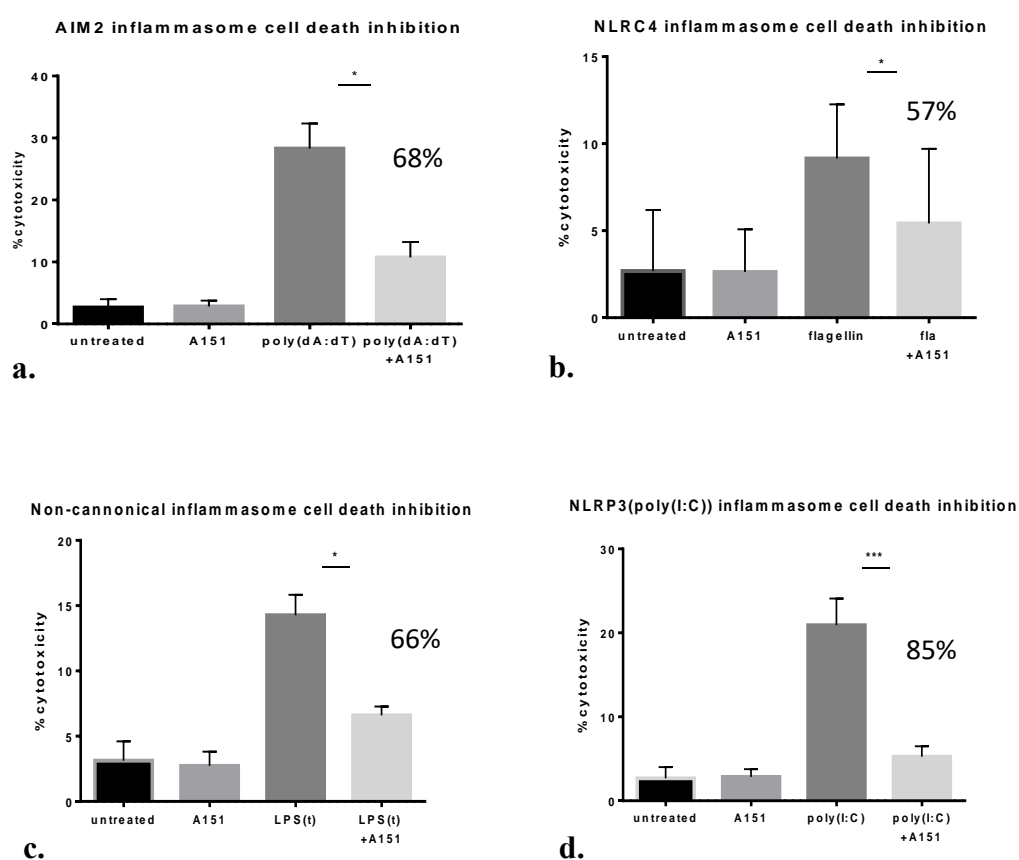
We previously demonstrated a significant reduction in IL-1 β secretion in AIM2, NLRC4, non-canonical activated, poly(I:C) and alum induced NLRP3 inflammasomes. In addition; we showed that A151 ODN also inhibits ASC speck release in AIM2, NLRC4, and cytosolic LPS activated non-canonical inflammasomes but not poly(I:C) and alum induced NLRP3. In order to further examine the mechanism of action for A151 ODN, we investigated its suppressive impact on percent cytotoxicity via lactate dehydrogenase (LDH) release assay as an indicator for pyroptosis. The LDH assay is widely used to evaluate cell death and lysis. Loss of cellular membrane integrity results in the leakage of the enzyme LDH into the extracellular environment. This assay utilizes the enzymatic activity of LDH which results in a strong-colored product absorbing at ~490-520nm. This enables LDH to be used quantitatively as an indicator of cytotoxicity.

In parallel experiments, we also used SytoxOrange, a fluorescent cell impermeant nucleic acid dye to assess cell death in THP-1-ASC-GFP causing fluorescence microscopy (Fig 3.7). Following removal of cell culture media at the indicated time point, SytoxOrange was added onto cells in fresh medium and dead cells were imaged based on their dye positivity.

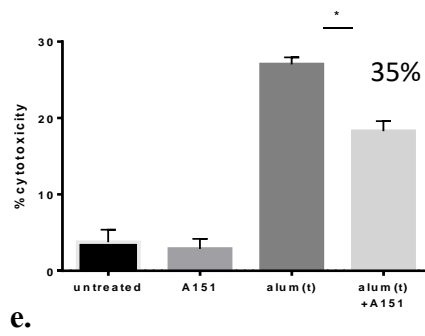
We detected a significant decrease in cell death in comparing samples of suppressive ODN treated and non-treated AIM2, NLRC4, poly(I:C), alum induced NLRP3, and non-canonically activated inflammasomes (Fig 3.6 a,b,c,d,e). However, nigericin induced NLRP3-dependent cell death was not affected in A151 ODN treated samples

(Fig 3.6 f), suggesting that the ODN had no effect on potassium efflux-dependent processes.

Collectively, our data indicate that A151 ODN acts as a general inflammasome inhibitor (except for nigericin-activated pathway), suppressing IL-1 β release, ASC-speck formation and cell death, suggesting that the inhibitory activity occurs upstream of gasdermin D-mediated pore formation.



NLRP3(alum (t)) inflammasome cell death inhibition



NLRP3(nigericin) inflammasome cell death inhibition

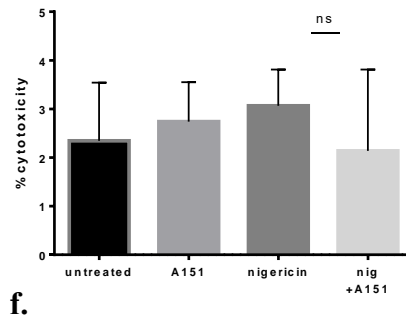
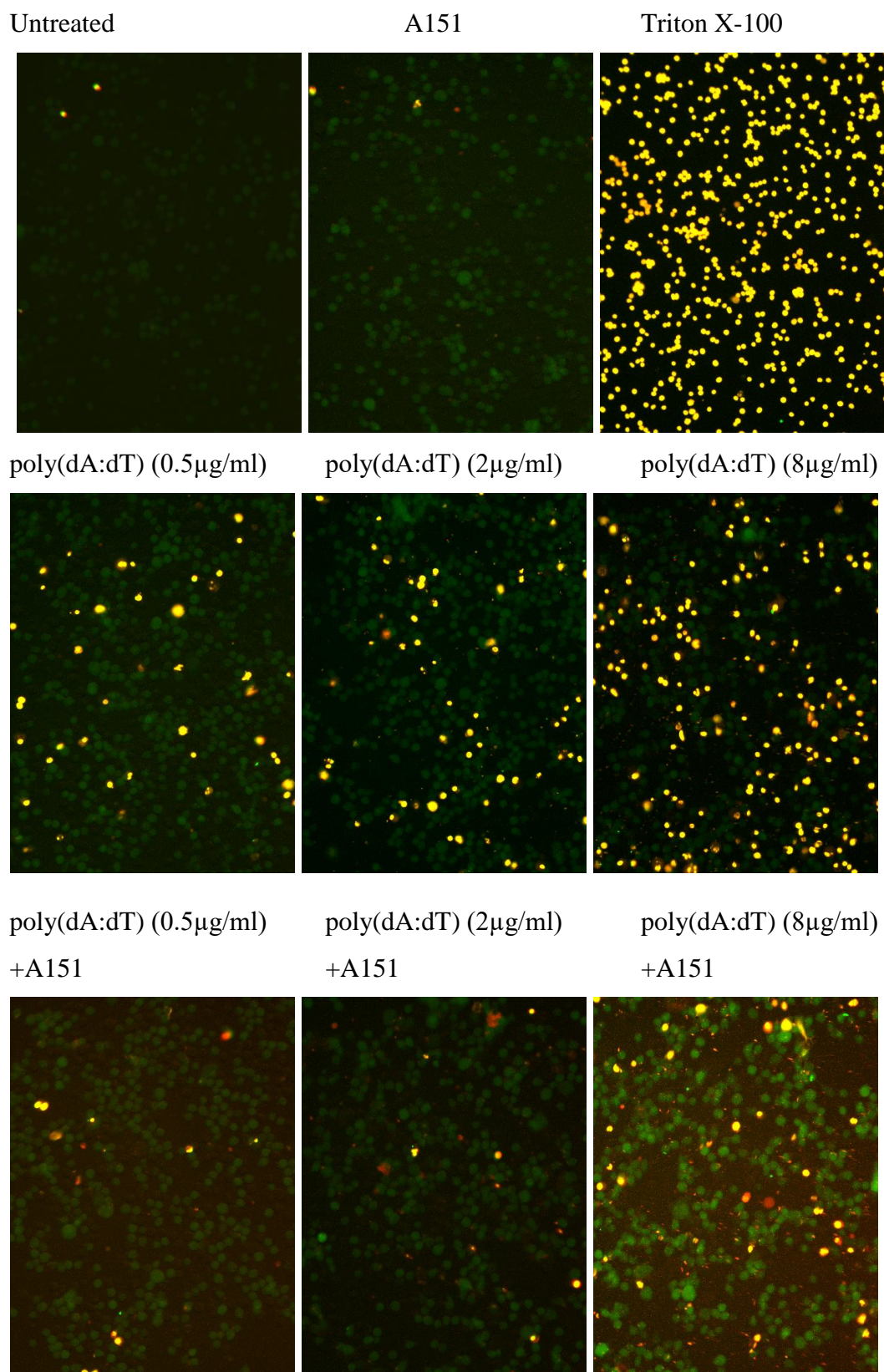
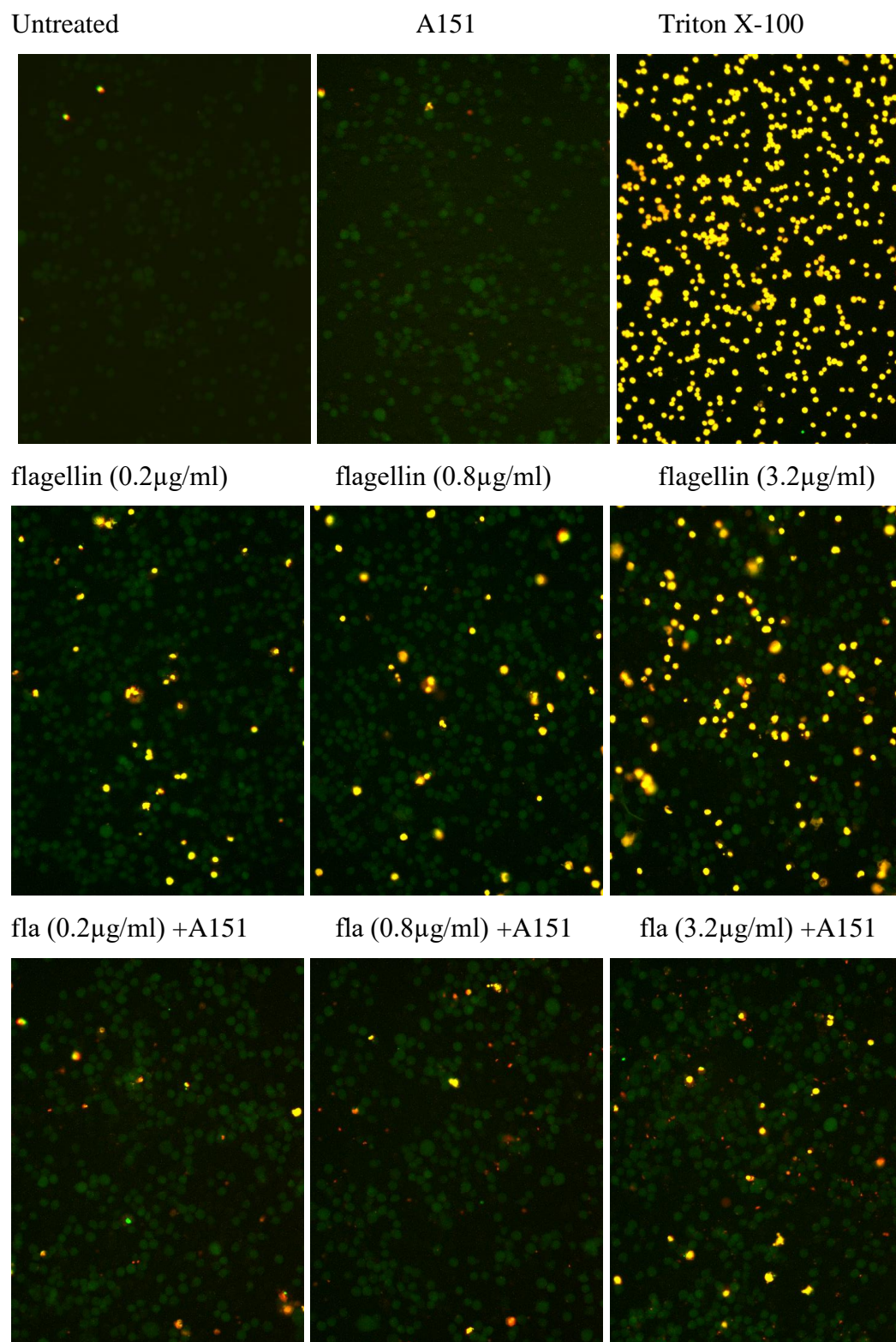


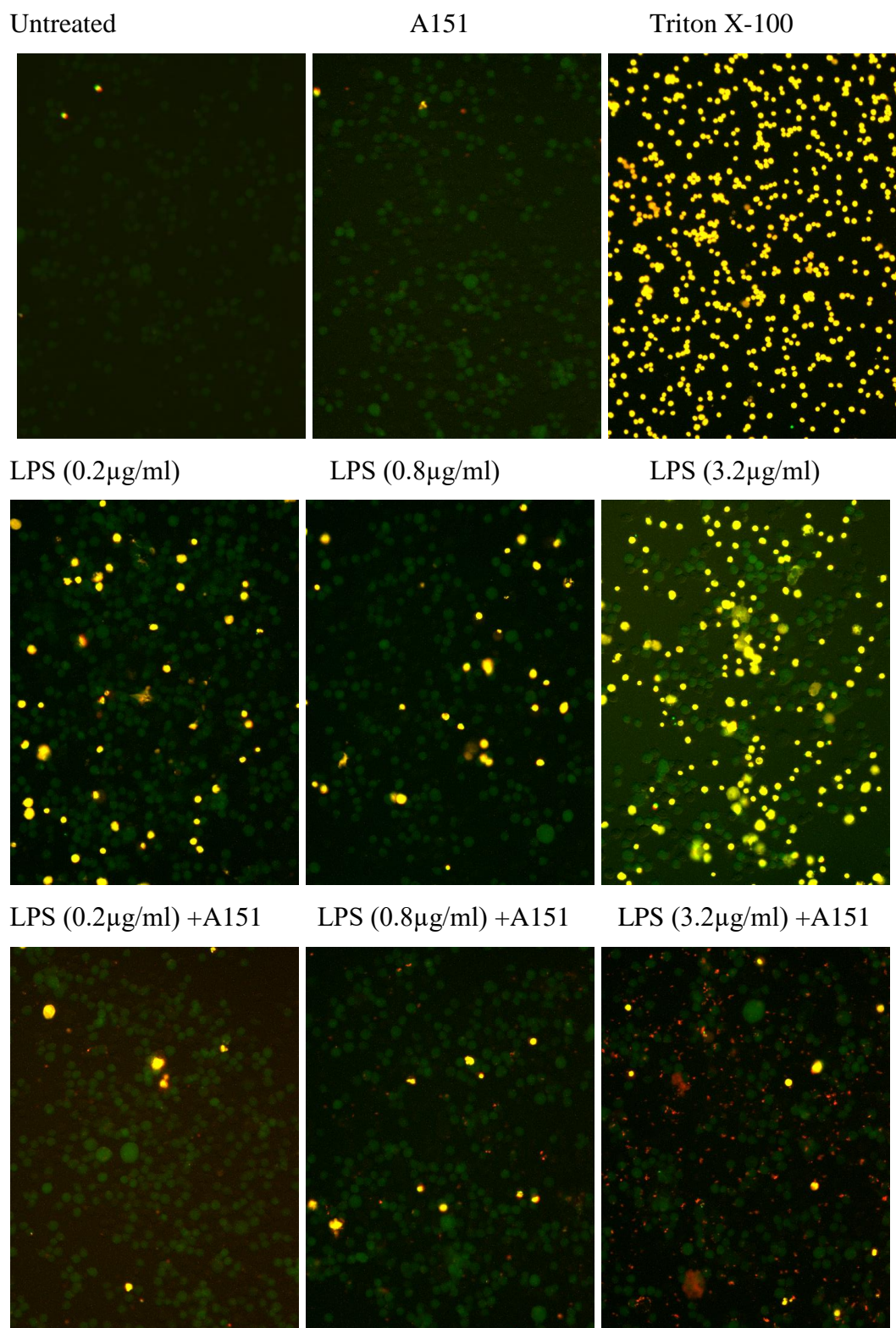
Figure 3.6 Percent cytotoxicity comparison of primed and inflammasome activated THP-1 cells ($4 \times 10^5/\text{ml}$) with or without A151 ODN treatment. LDH assay was performed with cell culture media collected after 24h incubation. (a) AIM2; (b) NLRC4; (c) non-canonical; (d,e,f) poly(I:C), alum, and nigericin induced NLRP3 inflammasomes, respectively. Data shows mean \pm SEM of 5-9 independent experiments. Student t-test was used for significance calculations (* $p < 0.05$, ** $p < 0.01$, *** $p < 0.001$). Inhibition percentage is indicated on bar graphs.



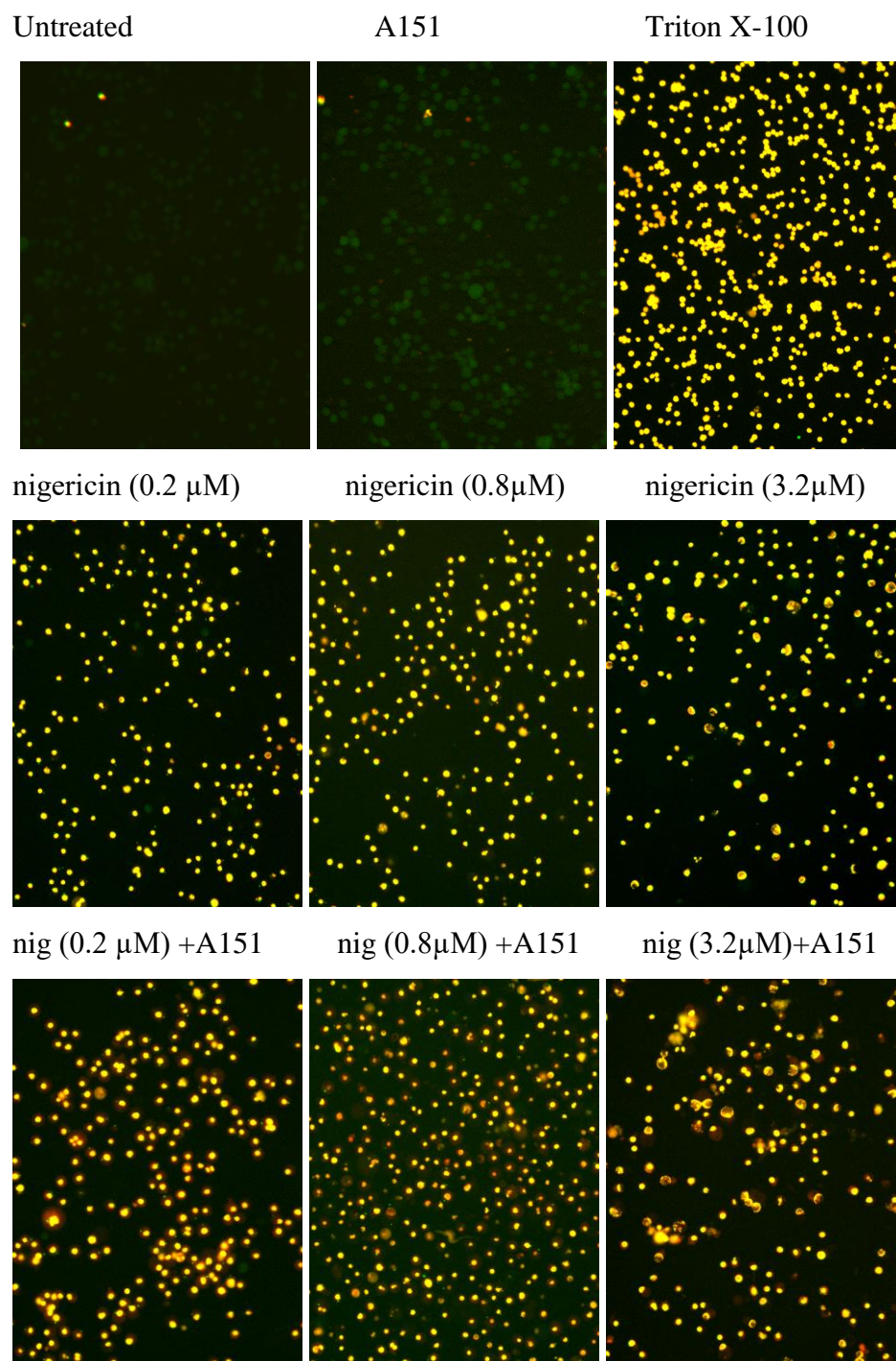
a.



b.



c.



d.

Figure 3.7 Fluorescence microscopy images of THP-1-ASC-GFP cells stained with cell impermeable nucleic acid dye SytoxOrange following dose dependent inflammasome activation of a) AIM2 with poly(dA:dT), b) NLRC4 with cytosolic flagelli, c) non-canonical with intracellular LPS, and d) nigericin induced NLRP3.

3.4 A151 ODN inhibits inflammasome activation by reducing mitochondrial stress

Mitochondrial stress has a critical role in inflammasome activation and propagation. In this context, several inflammasome activators were shown to generate mitochondrial reactive oxygen species (ROS) and mitochondrial damage (Nathan & Cunningham-Bussel, 2013). Based on this information, we wanted to assess whether A151 ODN interfered with inflammasome activation via a mitochondria-dependent mechanism. For this, primed BMDM's were primed with 1 μ g/ml LPS for 3 hours and subsequently stimulated for inflammasome activation. Three different ligand concentrations were used in order to see whether there was a dose-dependent effect on mitochondrial integrity. Mitochondrial health was monitored following staining of cells with JC-1, a lipophilic cationic dye that enters the mitochondria and changes its fluorescence emission depending on mitochondrial membrane potential. In healthy cells with high mitochondrial membrane potential, JC-1 forms aggregates that emit red fluorescence. In cells with low mitochondrial membrane potential (indicative of mitochondrial damage), the dye remains in its monomeric form and emits green fluorescence. Therefore, accumulation of green signal in cells serve as a readout of mitochondrial stress.

Stimulated and JC-1 treated cells were incubated for 15-30 minutes and imaged by fluorescent microscopy (Fig 3.8). Afterwards, attached BMDM's were washed with cold PBS and treated with 5mM EDTA and incubated at +4°C for 15 minutes. Detached cells were collected and analyzed via flow cytometry (Figure 3.9).

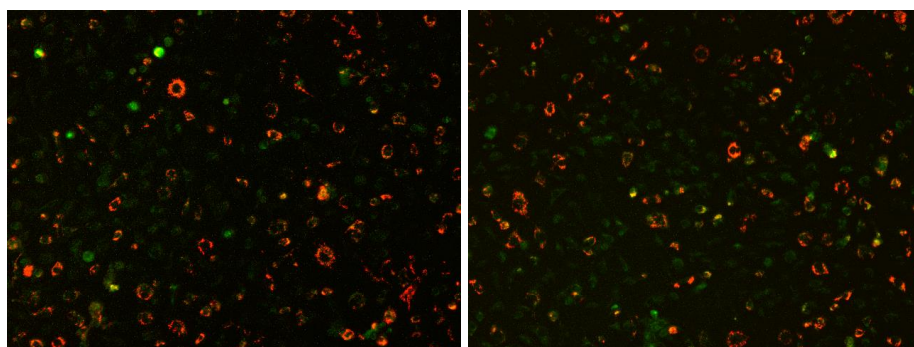
Results show that A151 ODN treatment decreased the accumulation of the green fluorescence, indicating that fewer monomers were present and JC-1 was able to form aggregates. This in turn can be interpreted as reduced mitochondrial stress in A151 ODN treated samples for the AIM2, NLRC4, and cytosolic LPS activated non-canonical inflammasomes (Fig 3.9 a,b,c,e). Consistent with previous observations, A151 ODN was ineffective in suppressing nigericin-mediated mitochondrial damage (Fig 3.9 d,e). Furthermore, A151 ODN failed to inhibit mitochondrial stress when highest doses of AIM2, NLRC4, and non-canonical inflammasome ligands were

employed. This makes sense in a way that stimuli overdose might have led to another cytotoxic pathway in addition to inflammasome activation.

Furthermore, we tried to explore the relationship between ROS production and inflammasome activation using mitochondria and cytoplasm specific redox probes MitoSOX Red and DHR (dihydrorhodamine 123), respectively. MitoSOX Red is a mitochondria targeted and fluorogenic dye that emits red fluorescence upon oxidation by superoxides. DHR 123 is also a fluorogenic ROS indicator that emits green fluorescence following oxidation. We observed that these cationic dyes bind to A151 ODN and emit fluorescence, generating a false positive signal. Therefore, we could not reliably measure the effect of A151 ODN on inflammasome ligand-mediated ROS production and discontinued these experiments.

Untreated

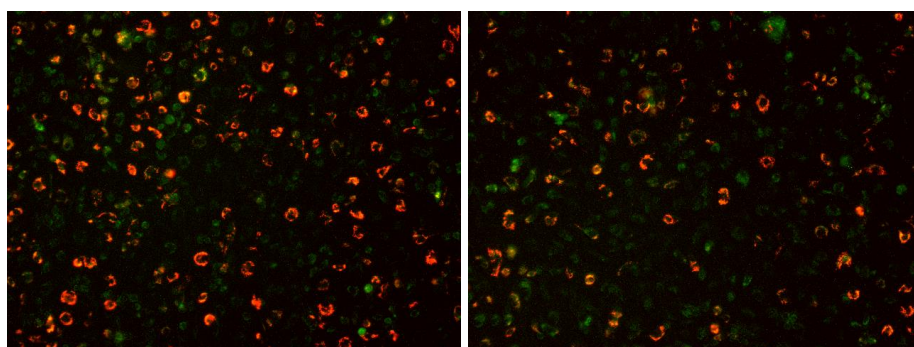
A151



a.

poly(dA:dT)

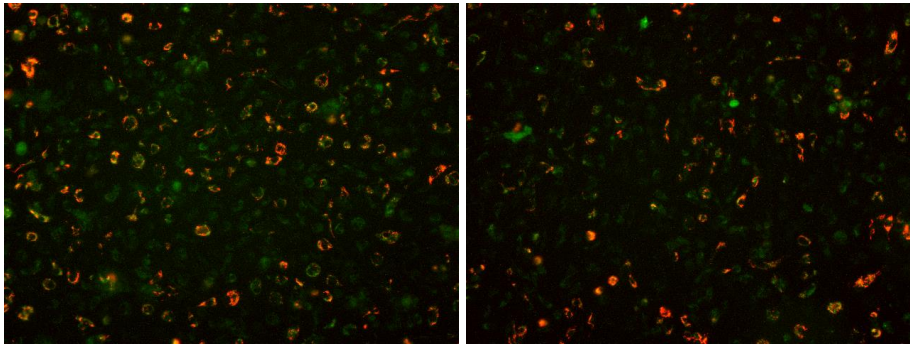
poly(dA:dT) +A151



b.

flagellin

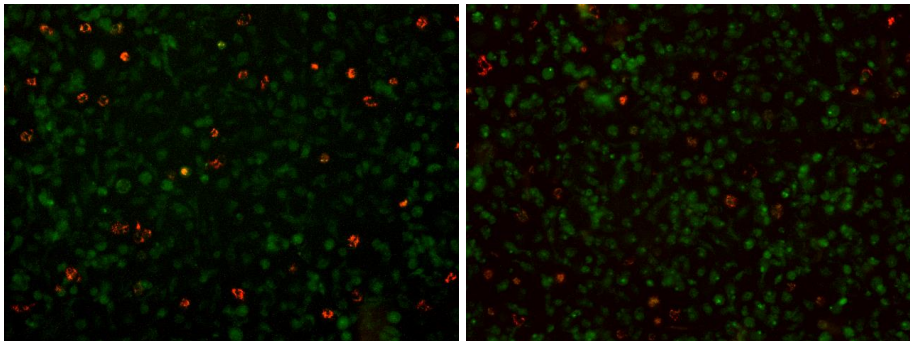
flagellin +A151



c.

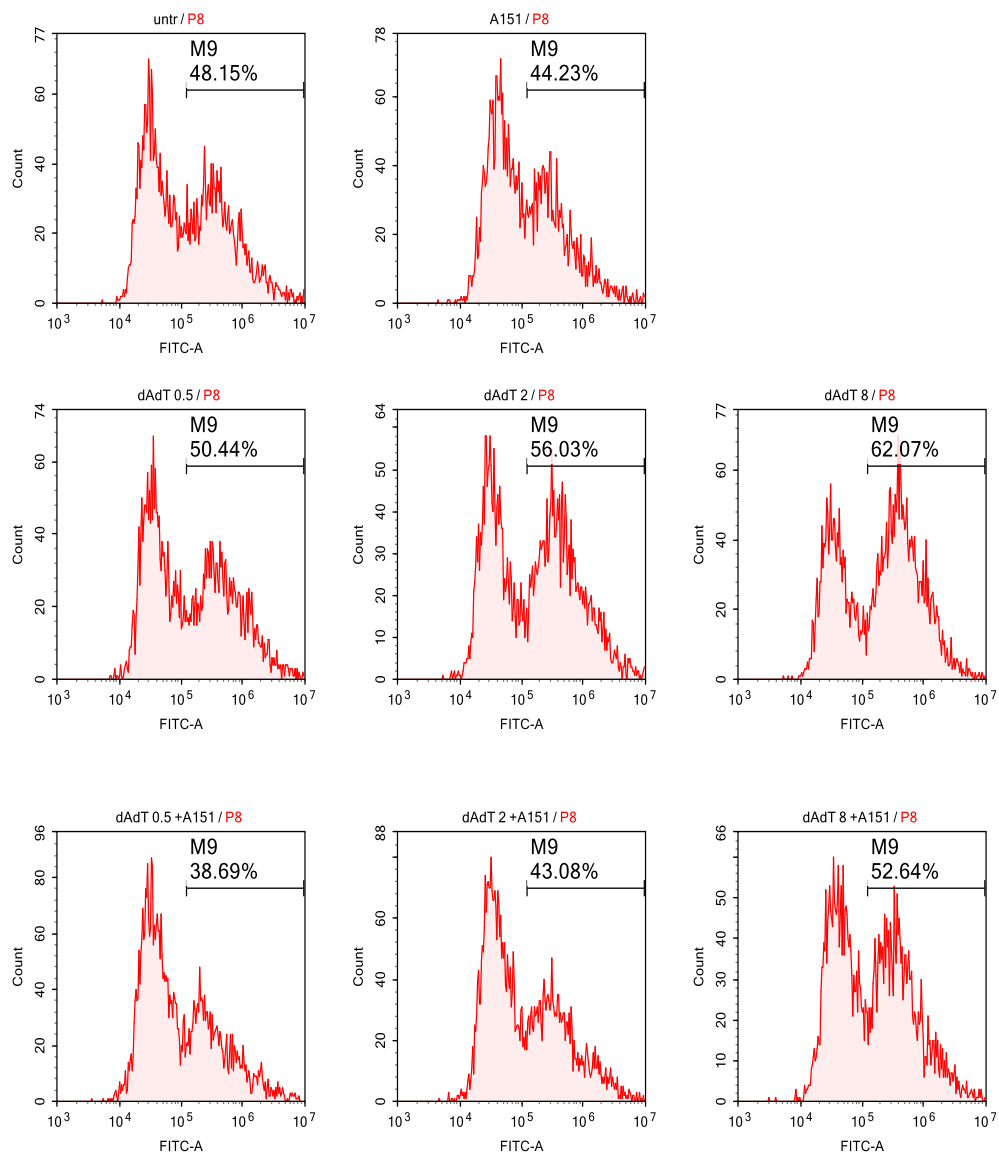
nigericin

nigericin+A151

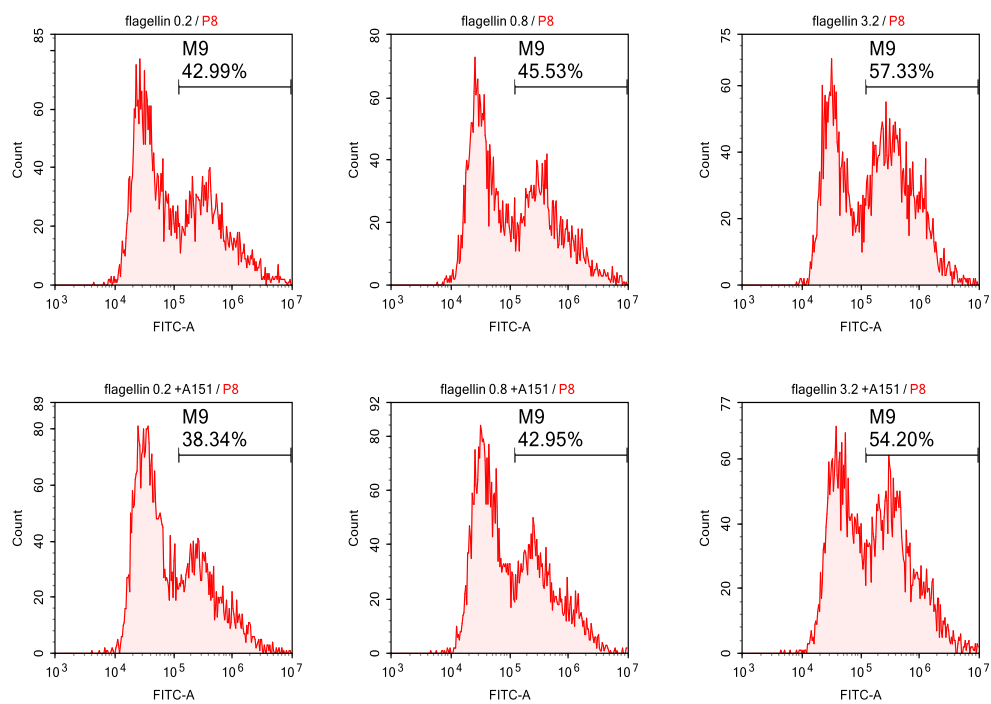


d.

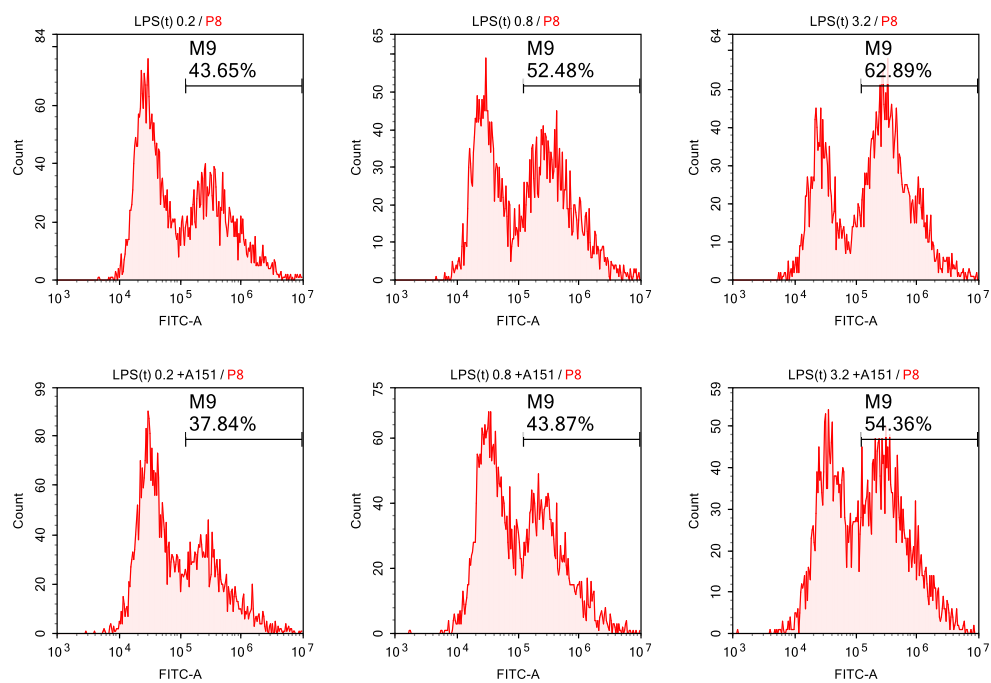
Figure 3.8 Fluorescence microscopy images of JC-1 treated BMDM's following inflammasome activation. Cells were primed with 1 μ g/ml LPS for 3hours and subsequently stimulated. Stimulation groups are a) untreated, b) poly(dA:dT) for AIM2, c) flagellin for NLRC4, and d) NLRP3 with nigericin.



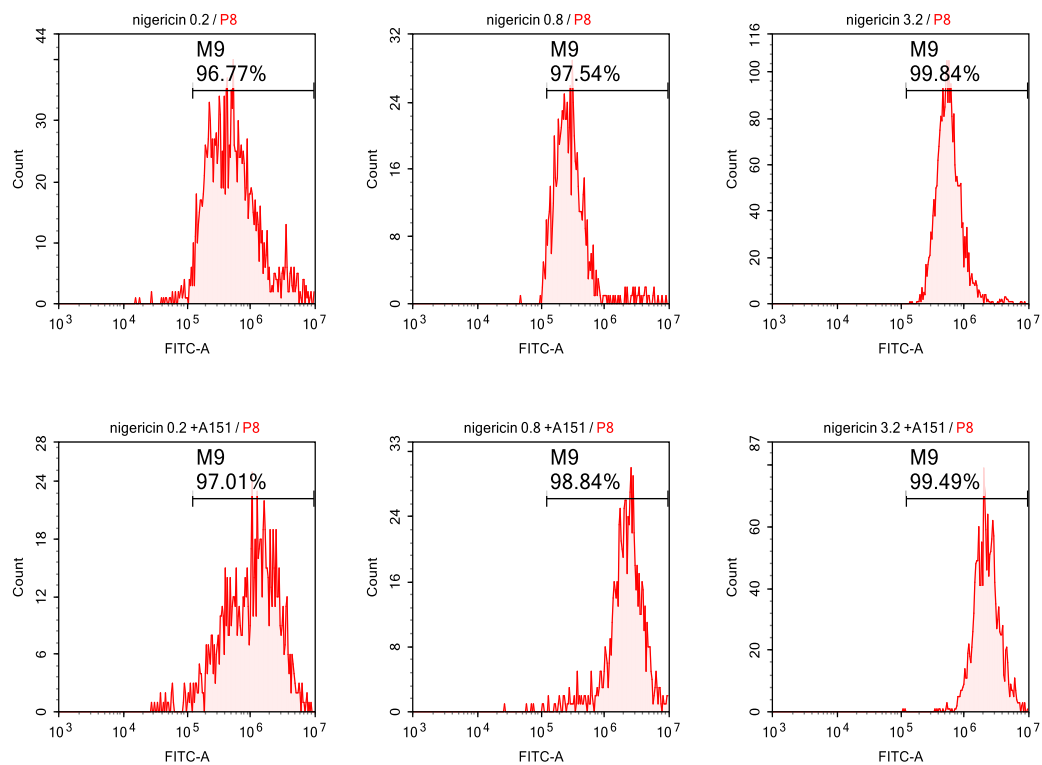
a.



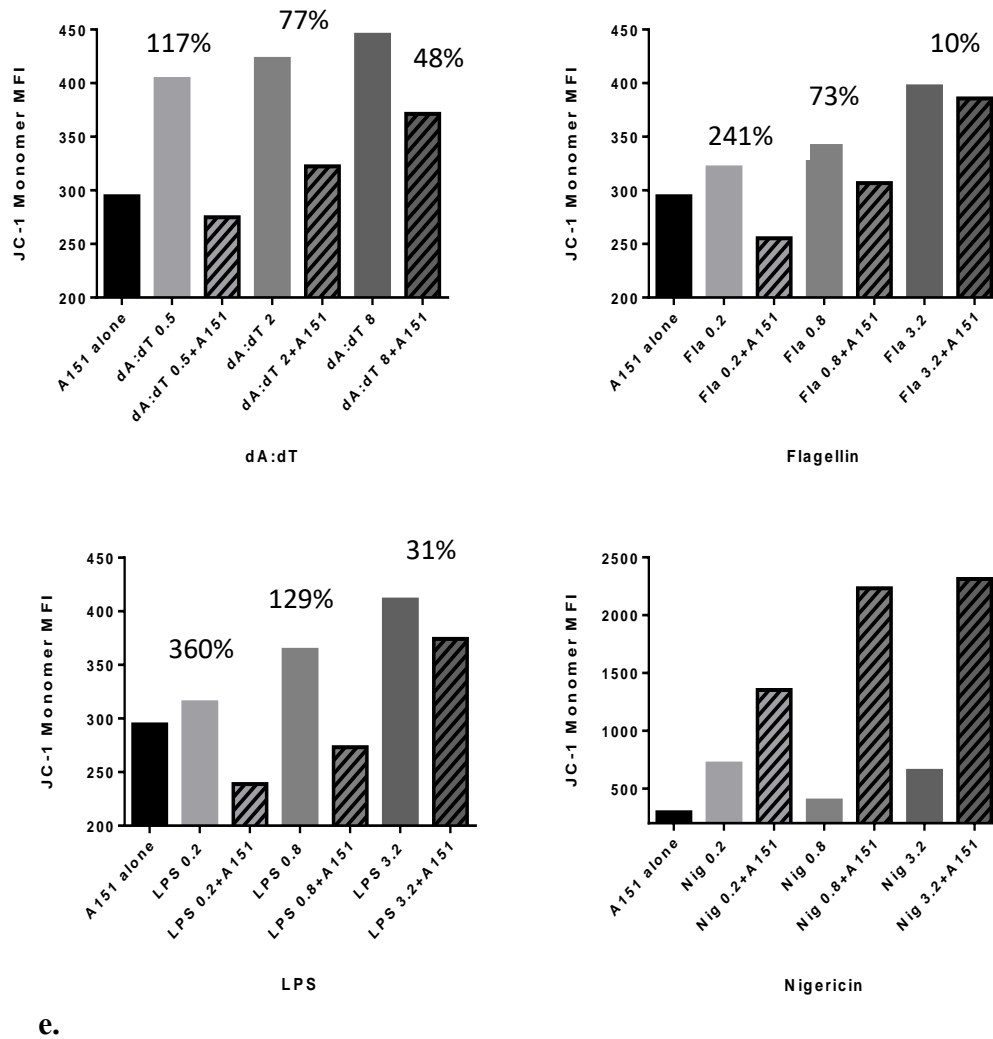
b.



c.



d.



e.

Figure 3.9 Flow cytometric analysis of mitochondrial stress assessed by JC-1 staining of BMDM's stimulated with 3 different doses of various inflammasome activators. BMDM's (4×10^5 cells/ml) were primed with $1\mu\text{g/ml}$ LPS for 3 hours. Cells were washed with wash medium and stimulated with indicated ligands. Histograms show green fluorescence intensity comparisons for (a) AIM2, (b)NLRC4, (c) non-canonical activated, and (d) nigericin induced NLRP3 inflammasomes. (e) Fluorescence intensity results of a,b,c,d plotted as bar graphs. Inhibition percentage is indicated on bar graphs.

3.5 A151 ODN inhibits inflammasome activation dependent IL-1 β secretion from hPBMC

We observed the suppressive effect of A151 ODN on inflammasome activation in THP-1 cell lines and BMDM cells. However, cell lines that display ideal properties and BMDM's derived from mice of identical genetic backgrounds is not sufficient to conclude that the effect of A151 ODN on inflammasome complexes is inhibitory. Therefore, we extended our research to human peripheral blood mononuclear cells and confirmed that A151 also suppressed IL-1 β secretion from two unrelated healthy donor cells. Of note, monocytes that are present in the hPBMC constitutively express inflammasome components and caspase-1. Hence, contrary to THP-1 cells, they do not require a previous priming step before inflammasome activation.

Similar to data obtained with THP-1 cells, A151 ODN effectively suppressed AIM2, poly(I:C)-dependent NLRP3 and NLRC4 inflammasome pathways (Fig. 3.10). The non-canonical inflammasome pathway was moderately suppressed in one donor but not in the second donor. A151 had no suppressive effect on nigericin-induced NLRP3 inflammasome formation.

Collectively, these results suggest that A151 ODN could be employed as a therapeutic agent in pathological conditions associated with excessive inflammasome activation.

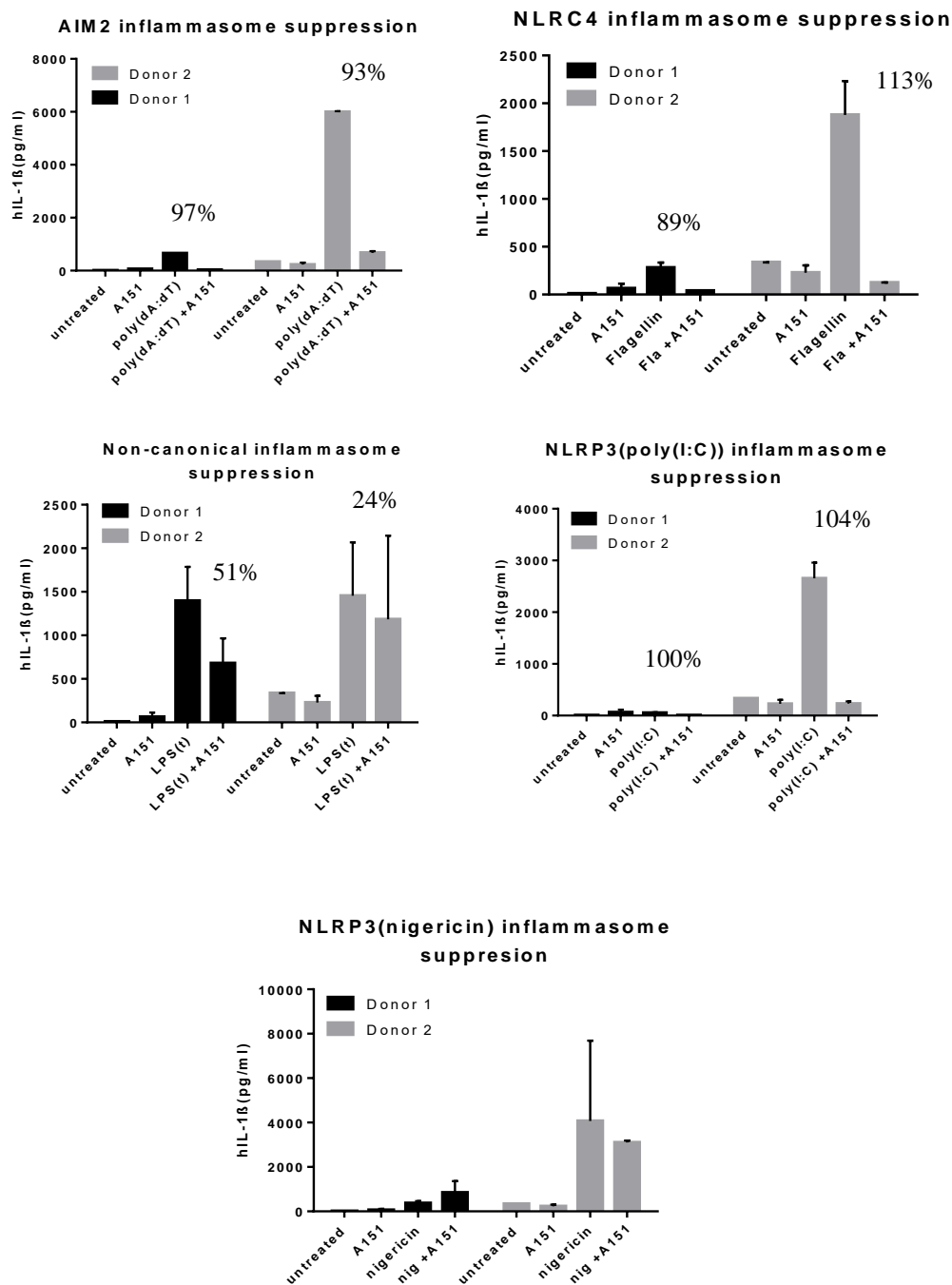


Figure 3.10 ELISA results for IL-1 β response of inflammasome activated hPBMC. Cells were stimulated with indicated ligands for 24hours at 37°C and IL-1 β accumulation in culture supernatants was assessed by ELISA. Inhibition percentage is indicated on bar graphs.

3.6 Histiocytosis and lymphadenopathy syndrome (H Syndrome)

The autosomal recessive disorder H syndrome is caused by mutations in the gene (SLC29A3) that encodes the nucleoside transporter hENT3 (human equilibrative nucleoside transporter) (Molho-pessach et al., 2008). hENT3 was shown to localize partially in late endosomes/lysosomes and mitochondria (Govindarajan et al., 2009). The transporter was demonstrated to salvage encapsulated pathogen or host derived nucleosides from late endosomes/lysosomes (Bissa, Beedle, & Govindarajan, 2016) and carry nucleosides into the mitochondria (Govindarajan et al., 2009). Patients with mutated SLC29A3 present with a variety of autoinflammatory manifestations characterized by recurrent febrile attacks, hyperpigmentation caused by massive histiocyte infiltration, deafness, skeletal and cardiac abnormalities, diabetes, short stature and uveitis (Morgan et al., 2010). The mechanism behind this autoinflammation is currently unknown.

In light of these reports, we reasoned that the mutations leading to the wide-ranging pathology in H Syndrome might be caused by a functional defect in hENT3, resulting in release of lysosomal cargo into the cytosol, thereby activating inflammasome pathway(s).

In order to test this hypothesis and determine which cytokines could be dysregulated in this rare disease, we analyzed IL-1 β , IL-29, and IFN α (pan-specific) responses of an H-syndrome patient with ELISA (Figure 3.6) in comparison to a healthy control and performed a fluorogenic bead based interferon panel (LegendPlex) that includes IFN α 2, IFN β , IFN γ , IFN λ 1 (IL-29), IFN λ 2/3 (IL-28A/B) (Figure 3.7).

Our results show that the patient had decreased response to stimulation with cytosolic viral DNA motif (HSV60; derived from the genome of herpes simplex virus 1). A lack of nucleoside transportation capacity could potentially decrease the possibility of the ligand to meet its cytosolic sensor. However, the five-fold increase of IL-1 β in response to cytosolic poly(I:C), the synthetic dsRNA analog, suggests that involvement of NLRP3 inflammasome overactivation could be plausible mechanism in which an over-active inflammasome pathway down-modulates and interferes with interferon production.

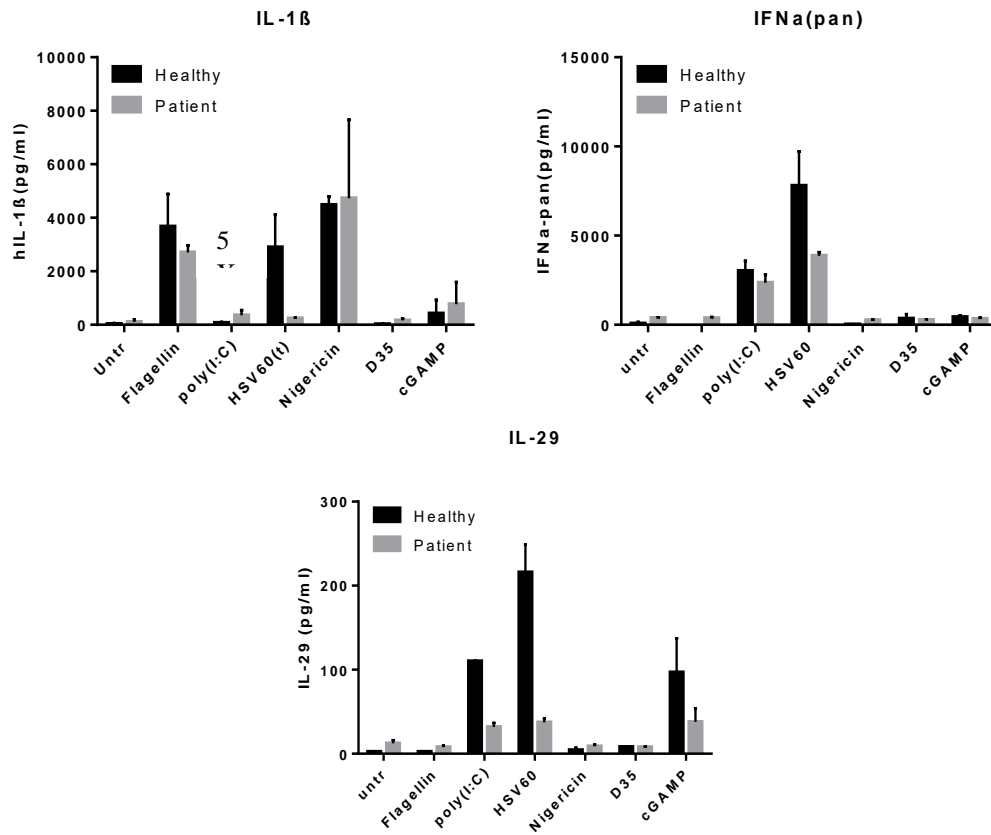


Figure 3.11 IL-1 β , IFN α (pan-specific), and IL-29 (IFN λ 1) ELISA results of PBMC isolated from one H Syndrome patient and one healthy donor. Cells were stimulated with indicated ligands. Cell culture media was collected after 24hour incubation. (5X) indicates the fold change between healthy and patient in response to poly(I:C) stimulation.

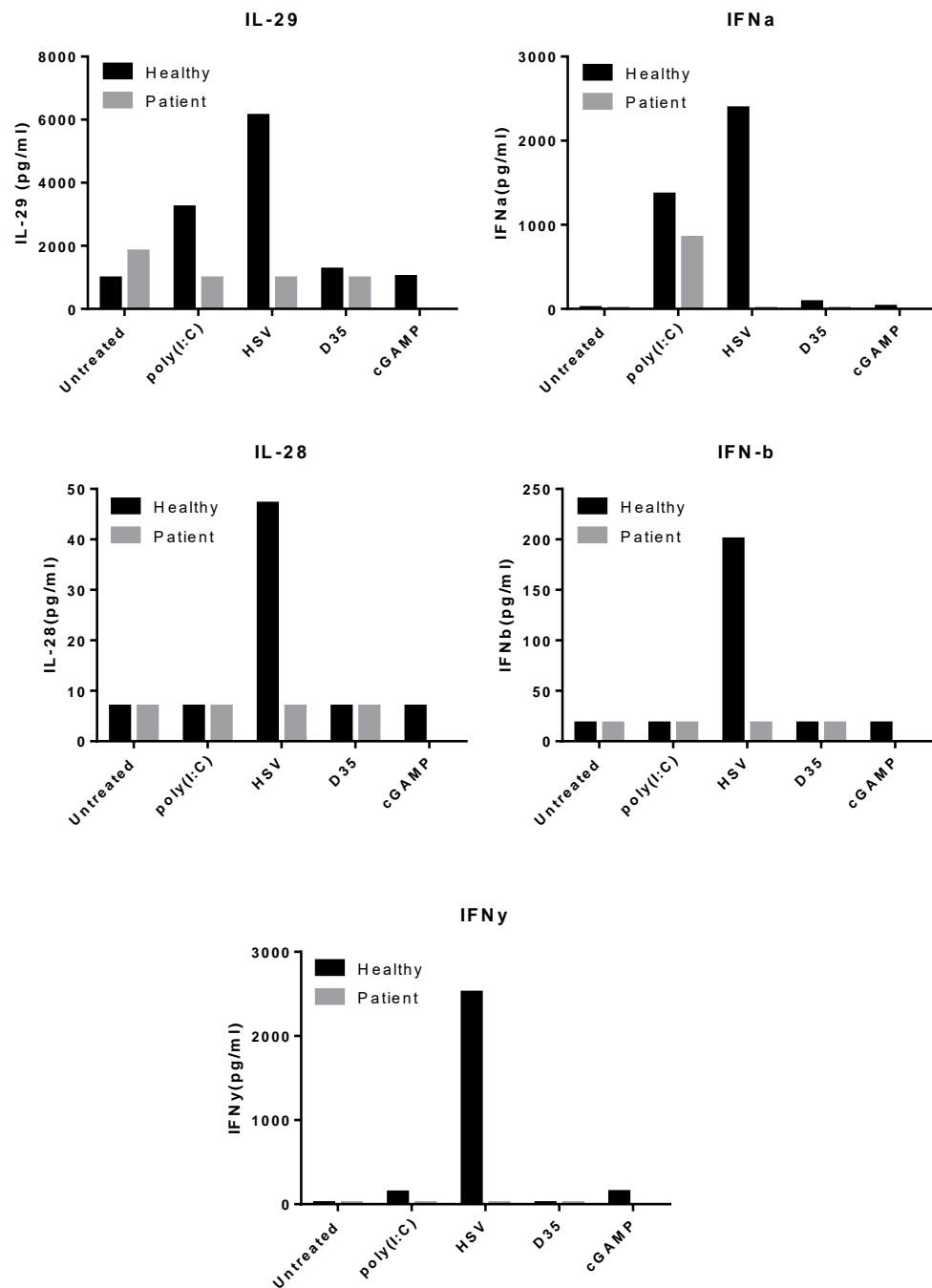
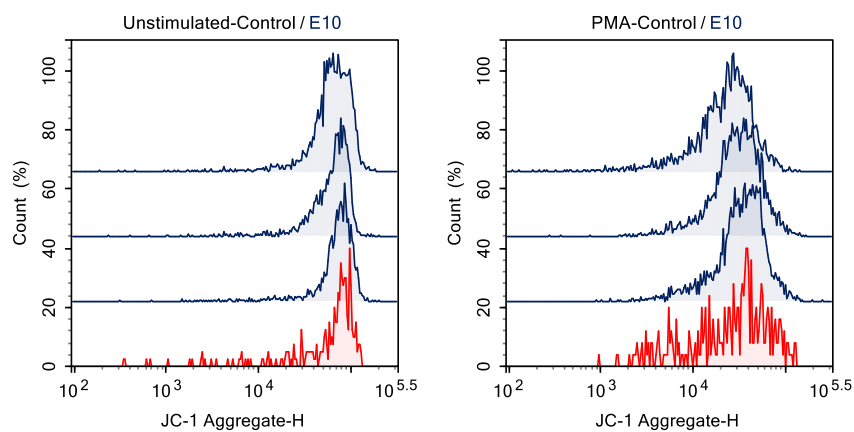
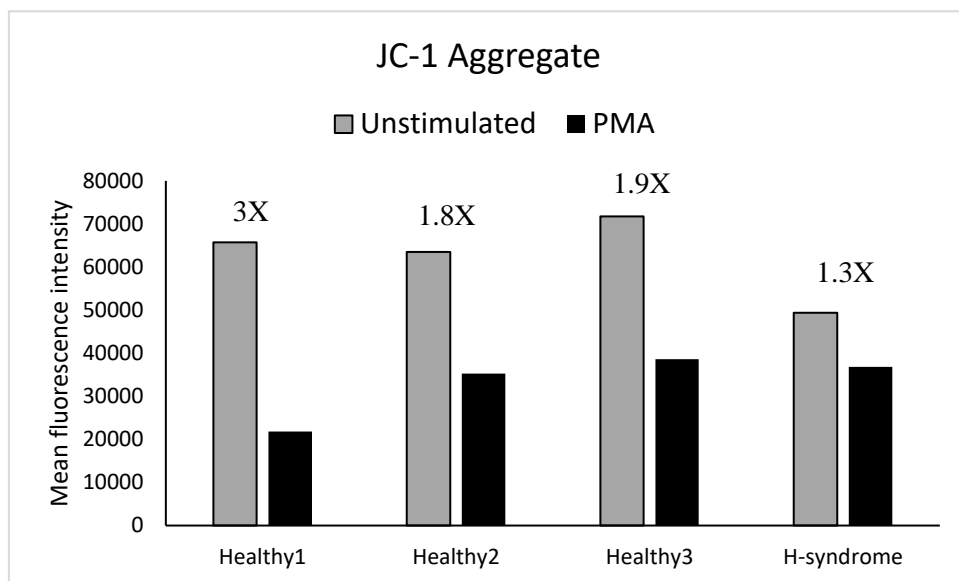


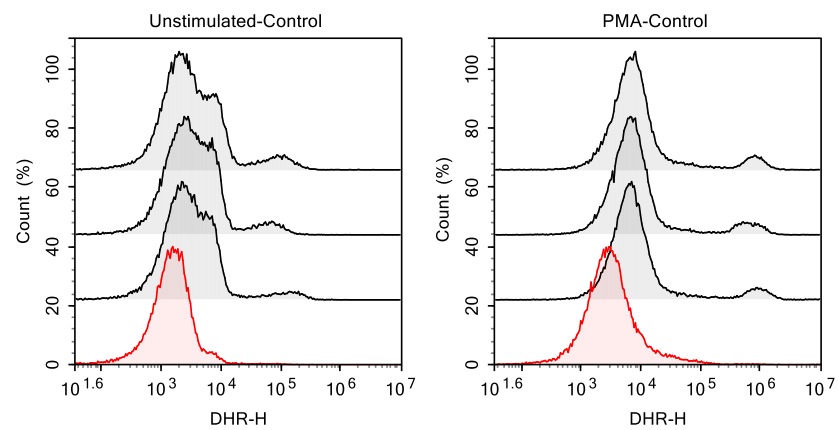
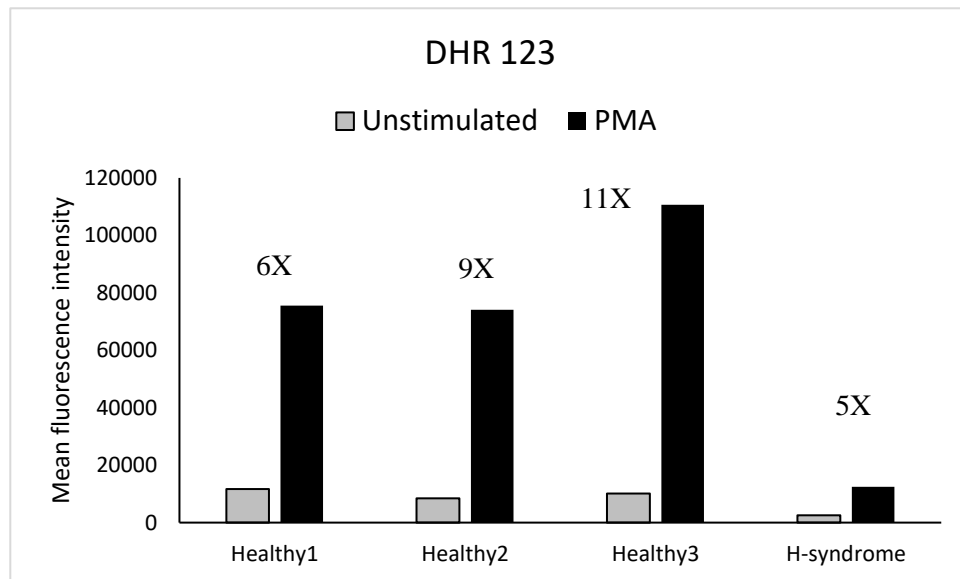
Figure 3.12 Flow cytometry results for the fluorogenic bead based interferon panel (LegendPlex) of PBMC isolated from one H Syndrome patient and one healthy donor. Cells were stimulated with indicated ligands. Cell culture media was collected after 24hour incubation and analyzed for IFN sub-type expression using the LegendPlex beads.

The above preliminary results suggest that an over-active inflammasome pathway could be involved in the pathogenesis of H-syndrome. Since mitochondrial stress and ROS production are important inflammasome triggers, we decided to investigate the mitochondrial stress/ROS production in H Syndrome pathology and used the fluorogenic dyes JC-1, DHR 123 and MitoSOX Red. Our results show that the patient had compromised mitochondrial membrane potential compared to three unrelated healthy controls (Fig. 3.13 a). Moreover, the patient's response to cytosolic ROS inducer PMA and the mitochondrial superoxide inducer ionomycin was substantially lower than healthy controls (Fig 3.13 b and 3.13 c, respectively). These results suggest that mitochondrial dysfunction might stem from the absence of hENT3 on mitochondrial membrane and a decrease in transportation of nucleosides from and into mitochondria could trigger stress-induced inflammasome activation.

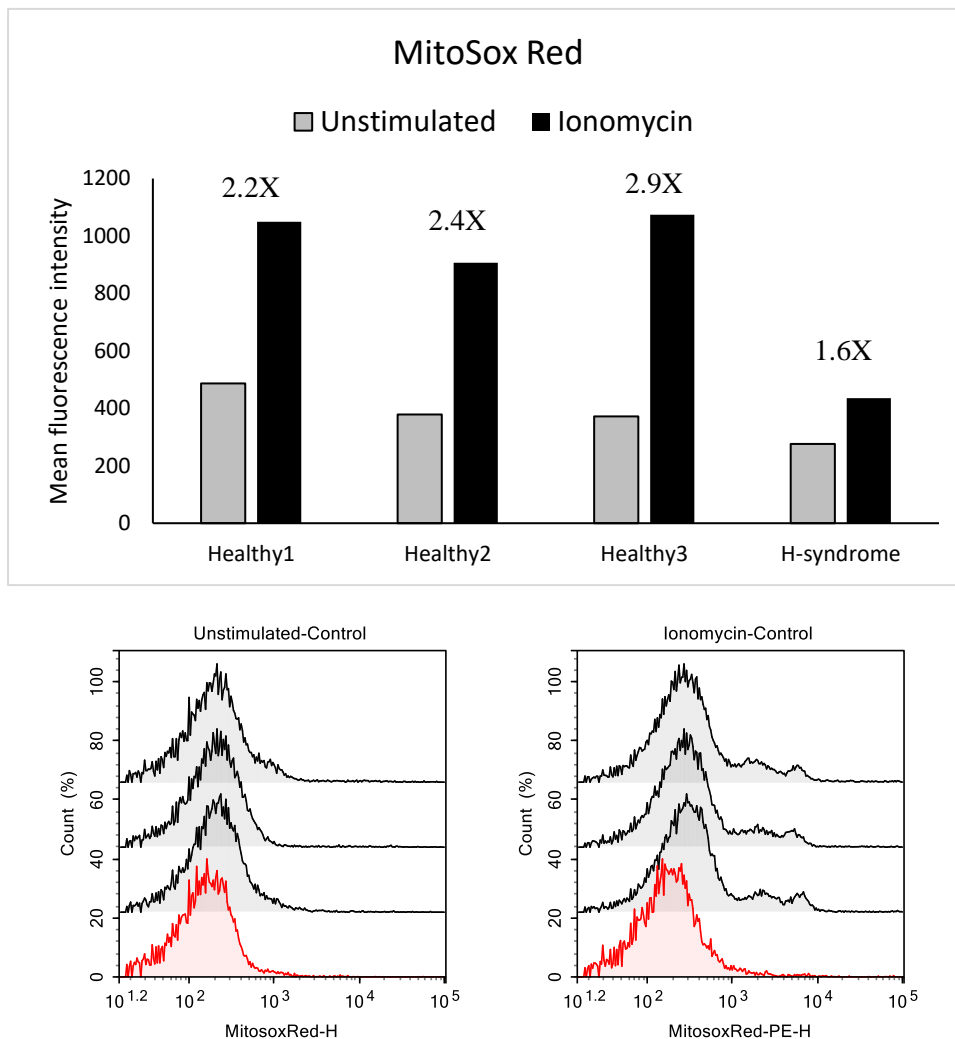
In summary, our results demonstrate that the H Syndrome patient has difficulty in generating a response to cytosolic viral DNA as well as ROS inducers. In addition, the mitochondrial integrity in PBMC seems to be compromised. Moreover, the five-fold increase in IL-1 β in response to cytosolic dsRNA analog poly(I:C) might imply a role of NLRP3 inflammasome overactivation contributing to disease pathology. Also, the inefficiency of IL-1 β production in response to HSV60 could suggest that the transportation defect of hENT3 hinders its recognition by a sensor of the inflammasome pathway. However, HSV60 is a very potent type-1 interferon inducer through the STING-TBK-IRF3 signaling pathway and it was shown in previous reports that the inflammasome and type-1 interferon pathways counter-regulate one another (van Kempen, Wenink, Leijten, Radstake, & Boes, 2015). Since we see IFN- α release in response to HSV60 stimulation, it may be the case that the type-1 interferon pathway dominates over the inflammasome pathway and diminishes IL-1 β secretion. Therefore, the precise reason for decreased IL-1 β in response to HSV60 remains unclear.



a.



b.



c.

Figure 3.13 Flow cytometry analysis of mitochondrial stress in PBMC isolated from one H Syndrome patient and three unrelated healthy donors. PBMC were stimulated with PMA for JC-1 and DHR 123 or ionomycin for MitoSOX Red as a positive control for mitochondrial superoxide production. Cells were incubated for 30 minutes following stimulation at 37°C. Bar graphs show mean fluorescence intensity for (a) JC-1 aggregate, (b) DHR 123, (c) MitoSOX Red stains. Fold changes of treated samples compared to untreated ones are shown on bar graphs as treated/untreated for DHR 123 and MitoSOX Red; 1 over treated/untreated for JC-1.

CHAPTER 4

CONCLUSION

This thesis intended to test the immunomodulatory potential of suppressive oligodeoxynucleotide (ODN) A151 on diverse inflammasome complexes and to explore its therapeutic capacity against diseases related to inflammasome overactivation. For this purpose; human monocytic cell line, human peripheral blood mononucleated cells (hPBMC), bone marrow derived macrophages (BMDM) were primed and/or stimulated with AIM2, NLRC4, non-canonical, and several NLRP3 inflammasome activating ligands and subsequently treated with A151-ODN. Repeated experiments for the quantification of IL-1 β , the primary readout for inflammasome activation from cell culture media via ELISA revealed a significant reduction in the secretion of IL-1 β . In addition, LDH assays for cytotoxicity measurement as an indication for pyroptosis demonstrated significant decrease in cell death in A151-ODN treated samples. Since IL-1 β secretion occurs through the pore formation and plasma membrane destabilization following pyroptosis initiation, these findings implied that A151-ODN was acting at an upstream event of pyroptosis (Shi et al., 2015). However, the inflammasome activation pathways have several known and still unidentified steps at which A151-ODN might show its immunomodulatory activity. In fact, Kaminski et al. showed in 2013 that A151-ODN competes with immune stimulatory DNA and binds AIM2, thereby inhibiting inflammasome activation. In addition to these findings, our results also demonstrate for the first time that A151-ODN abrogates ASC speck formation and mitochondrial stress in NLRC4 inflammasome activation. Since these are upstream events in NLRC4 inflammasome formation, it is probable that A151-ODN intervenes at an earlier event. This might be at the level of ligand recognition, NAIP-NLRC4 oligomerization, or at another yet undefined phase of the activation pathway. Another important finding is that A151-ODN inhibits the non-canonical inflammasome activation at least at the level of ASC speck formation and prevents

mitochondrial membrane destabilization. Alternatively, A151-ODN might intervene at the level of ligand recognition by caspase-11/4-5. This is important because non-canonical inflammasome activation is one of the least understood inflammasome pathways. Therefore, by the estimation of the involvement of A151-ODN mechanistically, another upstream event and/or component of non-canonical inflammasome activation could be identified. In the case of NLRP3, there are several stimulants that were investigated. The dsRNA analog poly(I:C) induced inflammasome activation seems to be abrogated in the presence of A151-ODN at a downstream event of ASC speck formation since ASC speck reduction was not as efficient as IL-1 β and cell death inhibition. This might suggest that A151-ODN might interfere at caspase-1 recruitment. Another ligand for NLRP3 was alum. Aluminum hydroxide and potassium salts are commonly used as vaccine adjuvants. However, the mechanism of how it acquires its adjuvanticity is unknown. There are reports suggesting that the means of alum crystals generating an immune response is through the initiation of the NLRP3 inflammasome complex. We observed inhibition of IL-1 β and cell death following treatment with A151-ODN, whereas ASC speck release was not reduced as efficiently. This could suggest a similar mechanistic method of inhibition as in the case of poly(I:C) induced NLRP3. Nigericin induced NLRP3 activation, on the other hand, could not be suppressed with A151-ODN. We reasoned that since nigericin is an extracellular ligand, it affects the cells externally whereas A151-ODN enters the cell and cannot act upon the downstream events. Also, nigericin is a very potent and fast-acting ligand so it should be hard to intervene with its effect. Our results regarding the effect of A151 ODN on investigated inflammasome activation pathways are summarized in **Table 4.1**.

As inflammasome overactivation was correlated with certain disease pathogenesis, IL-1 β inhibitors were effectively used in the treatment of these disorders. However, these inhibitors can only act extracellularly and the damage will be done to the cells which undergo pyroptosis. Even though IL-1 β is neutralized by the inhibitors, remaining cell content that is leaked due to pyroptosis will be taken up by circulating macrophages and immune activation will continue. Therefore; although IL-1 β inhibitors effectively

lower the degree of symptoms, therapeutics that could act before the cell undergoes pyroptosis might be even more successful in diminishing disease symptoms.

Collectively, our results reveal that the potential of A151-ODN to be utilized as a therapeutic agent against inflammasome overactivation is worth exploring. Unquestionably, there are many more experiments to be performed, mainly regarding the mechanism of action for A151-ODN.

Table 4.1 Summary of the effect of A151 ODN on investigated inflammasome pathways.

INVESTIGATED PATHWAYS	A151 ODN MEDIATED SUPPRESSION							
	IL-1 β secretion		Pyroptosis		ASC speck release		Mitochondrial damage	
AIM2	YES		YES		YES		YES	
NLRC4	YES		YES		YES		YES	
Non-canonical	YES		YES		YES		YES	
NLRP3 (poly(I:C))	YES		YES			NO		ND
NLRP3(alum)	YES		YES			NO		ND
NLRP3(nigericin)		NO		NO		NO		NO

Our results conducted with PBMC of an H syndrome patient show that cells secrete more IL-1 β in response to dsRNA analog compared to healthy control. Moreover, experiments carried out to determine the mitochondrial stress and integrity levels demonstrate that the patient has more unstable mitochondria in contrast to healthy control. When put together, these findings might point to a case of overactivation of the NLRP3 inflammasome. Another link to inflammasome overactivation is that the disorder shares symptoms like fever, deafness, and hepatosplenomegaly with the NLRC4 linked macrophage activation syndrome (MAS) or the NLRP3 related cryopyrin associated periodic syndromes (CAPS). More research has to be conducted

with a broader patient sample size in order to clarify whether there is in fact a relation between inflammasome overactivation and the presenting symptoms.

REFERENCES

- Allen, I. C., Scull, M. A., Moore, C. B., Holl, E. K., McElvania-TeKippe, E., Taxman, D. J., ... Ting, J. P. Y. (2009). The NLRP3 Inflammasome Mediates In Vivo Innate Immunity to Influenza A Virus through Recognition of Viral RNA. *Immunity*, 30(4), 556–565. <https://doi.org/10.1016/j.immuni.2009.02.005>
- Bissa, B., Beedle, A. M., & Govindarajan, R. (2016). Lysosomal solute carrier transporters gain momentum in research. *Clinical Pharmacology and Therapeutics*, 100(5), 431–436. <https://doi.org/10.1002/cpt.450>
- Broz, P., & Dixit, V. M. (2016). Inflammasomes: mechanism of assembly, regulation and signalling. *Nature Reviews Immunology*, 16(7), 407–420. <https://doi.org/10.1038/nri.2016.58>
- Broz, P., Moltke, J. Von, Jones, J. W., Vance, R. E., & Monack, D. M. (2010). Article Differential Requirement for Caspase-1 Autoproteolysis in Pathogen-Induced Cell Death and Cytokine Processing. *Cell Host and Microbe*, 8(6), 471–483. <https://doi.org/10.1016/j.chom.2010.11.007>
- Broz, P., & Monack, D. M. (2013). Newly described pattern recognition receptors team up against intracellular pathogens. *Nature Reviews Immunology*, 13(8), 551–65. <https://doi.org/10.1038/nri3479>
- Canna, S. W., de Jesus, A. A., Gouni, S., Brooks, S. R., Marrero, B., Liu, Y., ... Goldbach-Mansky, R. (2014). An activating NLRC4 inflammasome mutation causes autoinflammation with recurrent macrophage activation syndrome. *Nature Genetics*, 46(10), 1140–6. <https://doi.org/10.1038/ng.3089>
- Franchi, L., & Núñez, G. (2009). NIH Public Access, 38(8), 2085–2089. <https://doi.org/10.1002/eji.200838549>.The
- Franklin, B. S., Bossaller, L., De Nardo, D., Ratter, J. M., Stutz, A., Engels, G., ... Latz, E. (2014). The adaptor ASC has extracellular and “prionoid” activities that propagate inflammation. *Nature Immunology*, 15(8), 727–737.

<https://doi.org/10.1038/ni.2913> \rhttp://www.nature.com/ni/journal/v15/n8/abs/ni.2913.html#supplementary-information

Geijtenbeek, T. B. H., & Gringhuis, S. I. (2009). receptors: shaping immune responses. *Nature Publishing Group*, 9(7), 465–479. <https://doi.org/10.1038/nri2569>

Govindarajan, R., Leung, G. P. H., Zhou, M., Tse, C.-M., Wang, J., & Unadkat, J. D. (2009). Facilitated mitochondrial import of antiviral and anticancer nucleoside drugs by human equilibrative nucleoside transporter-3. *American Journal of Physiology. Gastrointestinal and Liver Physiology*, 296(4), G910–G922. <https://doi.org/10.1152/ajpgi.90672.2008>

Guo, H., Callaway, J. B., & Ting, J. P.-Y. (2015). Inflammasomes: mechanism of action, role in disease, and therapeutics. *Nature Medicine*, 21(7), 677–687. <https://doi.org/10.1038/nm.3893>

Gursel, I., Gursel, M., Yamada, H., Ishii, K. J., Takeshita, F., & Klinman, D. M. (2003). Repetitive elements in mammalian telomeres suppress bacterial DNA-induced immune activation. *J Immunol*, 171(3), 1393–1400. <https://doi.org/10.4049/JIMMUNOL.171.3.1393>

He, Y., Zeng, M., Yang, D., Motro, B., Nlrp, T., Nlrp, C., ... Fig, E. D. (2016). NEK7 is an essential mediator of NLRP3 activation downstream of potassium efflux. *Nature*, 530, 354–357. <https://doi.org/10.1038/nature16959>

Hornung, V., Roers, A., Carus, G., & Universita, T. (2016). Review Recognition of Endogenous Nucleic Acids by the Innate Immune System. <https://doi.org/10.1016/j.immuni.2016.04.002>

Janeway, C. A., & Medzhitov, R. (2002). Nnate mmune ecognition, (2), 197–216. <https://doi.org/10.1146/annurev.immunol.20.083001.084359>

Kaminski, J. J., Schattgen, S. A., Tzeng, T.-C., Bode, C., Klinman, D. M., & Fitzgerald, K. A. (2013). Synthetic oligodeoxynucleotides containing suppressive

TTAGGG motifs inhibit AIM2 inflammasome activation. *Journal of Immunology* (Baltimore, Md.: 1950), 191(7), 3876–83. <https://doi.org/10.4049/jimmunol.1300530>

Kang, N., Jun, A. H., Bhutia, Y. D., Kannan, N., Unadkat, J. D., & Govindarajan, R. (2010). Human equilibrative nucleoside transporter-3 (hENT3) spectrum disorder mutations impair nucleoside transport, protein localization, and stability. *Journal of Biological Chemistry*, 285(36), 28343–28352. <https://doi.org/10.1074/jbc.M110.109199>

Kawai, T., & Akira, S. (2010). The role of pattern-recognition receptors in innate immunity: update on Toll-like receptors. *Nature Publishing Group*, 11(5), 373–384. <https://doi.org/10.1038/ni.1863>

Kayagaki, N., Stowe, I. B., Lee, B. L., Rourke, K. O., Anderson, K., Warming, S., ... Dixit, V. M. (2015). Caspase-11 cleaves gasdermin D for non-canonical inflammasome signaling. <https://doi.org/10.1038/nature15541>

Lamkanfi, M., & Dixit, V. M. (2014). Mechanisms and functions of inflammasomes. *Cell*, 157(5), 1013–1022. <https://doi.org/10.1016/j.cell.2014.04.007>

Man, S. M., Karki, R., Malireddi, R. K. S., Neale, G., Vogel, P., Yamamoto, M., ... Kanneganti, T. (2015). The transcription factor IRF1 and guanylate-binding proteins target activation of the AIM2 inflammasome by Francisella infection. *Nature Immunology*, 16(November 2014), 1–11. <https://doi.org/10.1038/ni.3118>

Manthiram, K., Zhou, Q., Aksentijevich, I., & Kastner, D. L. (2017). The monogenic autoinflammatory diseases define new pathways in human innate immunity and inflammation. *Nature Immunology*, 18(8), 832–842. <https://doi.org/10.1038/ni.3777>

Mitoma, H., Hanabuchi, S., Kim, T., Bao, M., Zhang, Z., & Sugimoto, N. (2013). The DHX33 RNA Helicase Senses Cytosolic RNA and Activates the NLRP3 Inflammasome. *Immunity*, 39(1), 123–135. <https://doi.org/10.1016/j.immuni.2013.07.001>

Molho-pessach, V., Lerer, I., Abeliovich, D., Agha, Z., Libdeh, A. A., Broshtilova, V., ... Zlotogorski, A. (2008). The H Syndrome Is Caused by Mutations in the Nucleoside Transporter hENT3, 529–534. <https://doi.org/10.1016/j.ajhg.2008.09.013>.

Morgan, N. V, Morris, M. R., Cangul, H., Gleeson, D., Straatman-iwanowska, A., Davies, N., ... Trembath, R. C. (2010). Mutations in SLC29A3, Encoding an Equilibrative Nucleoside Transporter ENT3, Cause a Familial Histiocytosis Syndrome (Faisalabad Histiocytosis) and Familial Rosai-Dorfman Disease, 6(2). <https://doi.org/10.1371/journal.pgen.1000833>

Nathan, C., & Cunningham-Bussel, A. (2013). Beyond oxidative stress: an immunologist's guide to reactive oxygen species. *Nature Reviews. Immunology*, 13(5), 349–61. <https://doi.org/10.1038/nri3423>

Opdenbosch, N. Van, Gurung, P., Walle, L. Vande, Fossoul, A., Kanneganti, T., & Lamkanfi, M. (2014). Activation of the NLRP1b inflammasome independently of ASC-mediated caspase-1 autoproteolysis and speck formation. *Nature Communications*, 5, 1–14. <https://doi.org/10.1038/ncomms4209>

Rathinam, V. A. K., & Fitzgerald, K. A. (2016). Inflammasome Complexes: Emerging Mechanisms and Effector Functions. *Cell*, 165(4), 792–800. <https://doi.org/10.1016/j.cell.2016.03.046>

Reikine, S., Nguyen, J. B., & Modis, Y. (2014). Pattern recognition and signaling mechanisms of RIG-I and MDA5. *Frontiers in Immunology*, 5(JUL), 1–7. <https://doi.org/10.3389/fimmu.2014.00342>

Sawhney, S., Woo, P., & Murray, K. J. (2001). Macrophage activation syndrome: a potentially fatal complication of rheumatic disorders, 421–426.

Schattgen, S. A., Fitzgerald, K. A., & Fitzgerald, K. A. (2011). The PYHIN protein family as mediators of host defenses, 243, 109–118.

- Schlee, M., & Hartmann, G. (2016). in nucleic acid sensing. Nature Publishing Group. <https://doi.org/10.1038/nri.2016.78>
- Shi, J., Zhao, Y., Wang, K., Shi, X., Wang, Y., Huang, H., ... Shao, F. (2015). Cleavage of GSDMD by inflammatory caspases determines pyroptotic cell death. *Nature*, 526(7575), 660–665. <https://doi.org/10.1038/nature15514>
- Shinkai, K., Mccalmont, T. H., & Leslie, K. S. (2007). Cryopyrin-associated periodic syndromes and autoinflammation, (II), 1–9. <https://doi.org/10.1111/j.1365-2230.2007.02540.x>
- Shirota, H., Gursel, I., Gursel, M., Klinman, M., Shock, E., Shirota, H., ... Klinman, D. M. (2017). Suppressive Oligodeoxynucleotides Protect Mice from Lethal. <https://doi.org/10.4049/jimmunol.174.8.4579>
- Shu, C., Li, X., & Li, P. (2014). The mechanism of double-stranded DNA sensing through the cGAS-STING pathway. *Cytokine and Growth Factor Reviews*, 25(6), 641–648. <https://doi.org/10.1016/j.cytogfr.2014.06.006>
- Takeuchi, O., & Akira, S. (2010). Review Pattern Recognition Receptors and Inflammation. *Cell*, 140(6), 805–820. <https://doi.org/10.1016/j.cell.2010.01.022>
- Vanaja, S. K., Rathinam, V. A. K., & Fitzgerald, K. A. (2015). Mechanisms of inflammasome activation: Recent advances and novel insights. *Trends in Cell Biology*, 25(5), 308–315. <https://doi.org/10.1016/j.tcb.2014.12.009>
- van Kempen, T. S., Wenink, M. H., Leijten, E. F. a., Radstake, T. R. D. J., & Boes, M. (2015). Perception of self: distinguishing autoimmunity from autoinflammation. *Nature Reviews. Rheumatology*, advance on (8), 1–10. <https://doi.org/10.1038/nrrheum.2015.60>
- Yamada, H., Gursel, I., Takeshita, F., Ishii, K. J., Gursel, M., Takeshita, S., ... Klinman, D. M. (2002). Effect of Suppressive DNA on CpG-Induced ImmuneActivation. <https://doi.org/10.4049/jimmunol.169.10.5590>

APPENDIX A

BUFFERS, SOLUTIONS AND CULTURE MEDIA

RPMI-1640 (Gibco) supplemented with L-Glutamine

2 % :10 ml FBS (FBS is inactivated at 55°C)

5 %: 5 ml FBS

10 %: 50 ml FBS

5 ml Penicillin/Streptomycin (50µg/ml final concentration from 10 mg/ml stock)

5 ml HEPES (Biological Industries), (10mM final concentration from 1 M stock)

5 ml Na Pyruvate, (0,11 mg/ml final concentration from 100mM, 11 mg/ml stock)

5 ml Non-Essential Amino Acids Solution, (diluted into 1x from 100x concentrate stock)

Blocking Buffer (ELISA)

500ml 1x PBS

25 grams BSA (5%)

250µl Tween20 (0,025%)

Crystal particles of BSA should be dissolved very well, with magnetic-heating stirrer for 20-30 min. The buffer should be stored at -20°C.

PBS (Phosphate Buffered Saline) [10x]

80 grams NaCl

2 grams KCl

8,01 grams $\text{Na}_2\text{HPO}_4 \cdot 2\text{H}_2\text{O}$

2 grams KH_2PO_4

Complete to 1lt with ddH₂O (pH 6,8).

For 1X PBS, pH should be \approx 7,2-7,4 and autoclaved prior to use.

BS-BSA-Na azide (FACS Buffer)

500 ml 1x PBS

5g BSA (1%)

125mg (0,25%)

T-cell Buffer [ELISA]

500 ml 1x PBS

25 ml FBS (5%)

250µl Tween20 (0,025%)

The buffer should be stored at -20°C.

Wash Buffer [ELISA]

500 ml 10x PBS

2,5 ml Tween20

4,5lt ddH₂O

APPENDIX B

PERMISSION TO THE COPYRIGHTED MATERIAL

13.09.2017

Copyright Clearance Center



Note: Copyright.com supplies permissions but not the copyrighted content itself.

1
PAYMENT

2
REVIEW

3
CONFIRMATION

Step 3: Order Confirmation

Thank you for your order! A confirmation for your order will be sent to your account email address. If you have questions about your order, you can call us 24 hrs/day, M-F at +1.855.239.3415 Toll Free, or write to us at info@copyright.com. This is not an invoice.

Confirmation Number: 11669845
Order Date: 09/13/2017

If you paid by credit card, your order will be finalized and your card will be charged within 24 hours. If you choose to be invoiced, you can change or cancel your order until the invoice is generated.

Payment Information

Naz Sürücü
nazsrc@gmail.com
+90 (539)2127539
Payment Method: n/a

Order Details

Nature Reviews Immunology

Order detail ID: 70671531
Order License Id: 4187220691046
ISSN: 1474-1733
Publication Type: Journal
Volume:
Issue:
Start page:
Publisher: NATURE PUBLISHING GROUP

Permission Status: **Granted**

Permission type: Republish or display content
Type of use: Thesis/Dissertation

Requestor type: Academic institution

Format: Print, Electronic

Portion: chart/graph/table/figure

Number of charts/graphs/tables/figures: 1

Title or numeric reference of the portion(s): Figure 4

Title of the article or chapter the portion is from: Discriminating self from non-self in nucleic acid sensing

Editor of portion(s): N/A

Author of portion(s): N/A

Volume of serial or monograph: N/A

Page range of portion: 9

<https://www.copyright.com/printCoiConfirmPurchase.do?operation=defaultOperation&confirmNum=11669845&showTCCitation=TRUE>

1/6



Note: Copyright.com supplies permissions but not the copyrighted content itself.

1
PAYMENT

2
REVIEW

3
CONFIRMATION

Step 3: Order Confirmation

Thank you for your order! A confirmation for your order will be sent to your account email address. If you have questions about your order, you can call us 24 hrs/day, M-F at +1.855.239.3415 Toll Free, or write to us at info@copyright.com. This is not an invoice.

Confirmation Number: 11669854
Order Date: 09/13/2017

If you paid by credit card, your order will be finalized and your card will be charged within 24 hours. If you choose to be invoiced, you can change or cancel your order until the invoice is generated.

Payment Information

Naz Sürücü
nazsrc@gmail.com
+90 (539)2127539
Payment Method: n/a

Order Details

Cell

Order detail ID: 70671546
Order License Id: 4187230192323
ISSN: 0092-8674
Publication Type: Journal
Volume:
Issue:
Start page:
Publisher: CELL PRESS

Permission Status: **Granted**

Permission type: Republish or display content
Type of use: Thesis/Dissertation

Requestor type: Academic institution

Format: Print, Electronic

Portion: chart/graph/table/figure

Number of charts/graphs/tables/figures: 1

Title or numeric reference of the portion(s): Figure 1

Title of the article or chapter the portion is from: Mechanisms and Functions of Inflammasomes

Editor of portion(s): N/A

Author of portion(s): N/A

Volume of serial or monograph: N/A

Page range of portion: 1014

<https://www.copyright.com/printCoiConfirmPurchase.do?operation=defaultOperation&confirmNum=11669854&showTCCitation=TRUE>



Note: Copyright.com supplies permissions but not the copyrighted content itself.

1
PAYMENT

2
REVIEW

3
CONFIRMATION

Step 3: Order Confirmation

Thank you for your order! A confirmation for your order will be sent to your account email address. If you have questions about your order, you can call us 24 hrs/day, M-F at +1.855.239.3415 Toll Free, or write to us at info@copyright.com. This is not an invoice.

Confirmation Number: 11669854
Order Date: 09/13/2017

If you paid by credit card, your order will be finalized and your card will be charged within 24 hours. If you choose to be invoiced, you can change or cancel your order until the invoice is generated.

Payment Information

Naz Sürücü
nazsrc@gmail.com
+90 (539)2127539
Payment Method: n/a

Order Details

Cell

Order detail ID: 70671546
Order License Id: 4187230192323
ISSN: 0092-8674
Publication Type: Journal
Volume:
Issue:
Start page:
Publisher: CELL PRESS

Permission Status: **Granted**

Permission type: Republish or display content
Type of use: Thesis/Dissertation

Requestor type Academic institution

Format Print, Electronic

Portion chart/graph/table/figure

Number of charts/graphs/tables/figures 1

Title or numeric reference of the portion(s) Figure 1

Title of the article or chapter the portion is from Mechanisms and Functions of Inflammasomes

Editor of portion(s) N/A

Author of portion(s) N/A

Volume of serial or monograph N/A

Page range of portion 1014



Note: Copyright.com supplies permissions but not the copyrighted content itself.

1
PAYMENT

2
REVIEW

3
CONFIRMATION

Step 3: Order Confirmation

Thank you for your order! A confirmation for your order will be sent to your account email address. If you have questions about your order, you can call us 24 hrs/day, M-F at +1.855.239.3415 Toll Free, or write to us at info@copyright.com. This is not an invoice.

Confirmation Number: 11669864
Order Date: 09/13/2017

If you paid by credit card, your order will be finalized and your card will be charged within 24 hours. If you choose to be invoiced, you can change or cancel your order until the invoice is generated.

Payment Information

Naz Sürücü
nazsrc@gmail.com
+90 (539)2127539
Payment Method: n/a

Order Details

Trends in cell biology

Order detail ID: 70671563
Order License Id: 4187231376299
ISSN: 0962-8924
Publication Type: Journal
Volume:
Issue:
Start page:
Publisher: TRENDS JOURNALS

Permission Status: **Granted**

Permission type: Republish or display content
Type of use: Thesis/Dissertation

Requestor type Academic institution

Format Print, Electronic

Portion chart/graph/table/figure

Number of charts/graphs/tables/figures 1

Title or numeric reference of the portion(s) Figure 1

Title of the article or chapter the portion is from Mechanisms of inflammasome activation: recent advances and novel insights

Editor of portion(s) N/A


Author of portion(s) N/A

Volume of serial or monograph N/A

Page range of portion 1

Nature immunology

Order detail ID: 70671574
Order License Id: 4187231378893
ISSN: 1529-2908
Publication Type: Journal
Volume:

Permission Status:  **Granted**

Permission type: Republish or display content
Type of use: Thesis/Dissertation

Issue:
Start page:
Publisher: NATURE PUBLISHING GROUP

Requestor type	Academic institution
Format	Print, Electronic
Portion	chart/graph/table/figure
Number of charts/graphs/tables/figures	1
Title or numeric reference of the portion(s)	Figure 1
Title of the article or chapter the portion is from	The monogenic autoinflammatory diseases define new pathways in human innate immunity and inflammation
Editor of portion(s)	N/A
Author of portion(s)	N/A
Volume of serial or monograph	N/A
Page range of portion	833



Note: Copyright.com supplies permissions but not the copyrighted content itself.

1
PAYMENT

2
REVIEW

3
CONFIRMATION

Step 3: Order Confirmation

Thank you for your order! A confirmation for your order will be sent to your account email address. If you have questions about your order, you can call us 24 hrs/day, M-F at +1.855.239.3415 Toll Free, or write to us at info@copyright.com. This is not an invoice.

Confirmation Number: 11669867
Order Date: 09/13/2017

If you paid by credit card, your order will be finalized and your card will be charged within 24 hours. If you choose to be invoiced, you can change or cancel your order until the invoice is generated.

Payment Information

Naz Sürücü
nazsrc@gmail.com
+90 (539)2127539
Payment Method: n/a

Order Details

Cell

Order detail ID: 70671579
Order License Id: 4187240149573
ISSN: 0092-8674
Publication Type: Journal
Volume:
Issue:
Start page:
Publisher: CELL PRESS

Permission Status: **Granted**

Permission type: Republish or display content
Type of use: Thesis/Dissertation

Requestor type: Academic institution

Format: Print, Electronic

Portion: chart/graph/table/figure

Number of charts/graphs/tables/figures: 1

Title or numeric reference of the portion(s): Figure 1

Title of the article or chapter the portion is from: Inflammasome Complexes: Emerging Mechanisms and Effector Functions

Editor of portion(s): N/A

Author of portion(s): N/A

Volume of serial or monograph: N/A

Page range of portion: 794